International Association for Gondwana Research

2023 Convention and 20th International Conference on Gondwana to Asia

Abstract Volume

Editors

P G Athira[1], M Satish-Kumar[1] and M Santosh[2]

[1]Department of Geology, Faculty of Science, Niigata University, Ikarashi Niigata 950-2181, Japan

[2]School of Earth Sciences and Resources, China University of Geosciences Beijing, 29 Xueyuan Road, Beijing 100083, China

Organized by

Niigata University, Niigata and Fossa Magna Museum, Itoigawa

October 07th to 12th 2023, Niigata.

International Association for Gondwana Research

2023 Convention and 20th International Conference on Gondwana to Asia

Abstract Volume

Editors

P G Athira, M Satish-Kumar, and M Santosh

Published by the International Association for Gondwana Research
Headquarters: China University of Geosciences Beijing,
No.29 Xueyuan Road, Haidian, Beijing 100083, China
Pages: 114

Contents

International Association for Gondwana Research 2023 Convention and
20th International Conference on Gondwana to Asia
Niigata, Japan, October 2023
Abstract Volume

Indian Tsunami Early Warning System (ITEWS)

Harsh K Gupta

CSIR-National Geophysical Research Institute
E-mail: harshg123@gmail.com

Among the natural disasters, the Tsunamis are one of the worst. In the first 22 years of the present century, we already had two disastrous tsunamis, namely the 26 December 2024 Sumatra Mw 9.2 earthquake generated tsunami and the 11 March 2011 Tohoku Mw 9.0 earthquake generated tsunami. The Sumatra Tsunami claimed over a quarter million human lives in south and southeast Asia becoming one of the worst natural disasters. The Tohoku earthquake tsunami claimed some 20,000 human lives and caused a nuclear emergency (Gupta and Gahalaut, 2013).

'Tsunami' is a Japanese word that means 'harbor waves.' Tsunamis have a small amplitude in the open oceans and did not get noticed by the fishermen while in the open- ocean, away from the shore. When they returned, they found that the whole village has been washed away. The almost invisible tsunami waves in the open ocean had gained height once they entered the shallow water in the harbors and hence the name.

The undersea earthquakes occurring in a favorable geological condition are primarily responsible for the generation of Tsunami. When the rupture by the earthquake propagates to the bottom of the sea and causes a vertical displacement of the ocean bed, the entire column of the water above it gets displaced, and a tsunami is created. In the open ocean tsunamis can travel with velocities of up to 1000 km/h. However, as they approach shallow waters near the coast, the velocity decreases, and the amplitude increases (Gupta and Gahalaut, 2013).

Global distribution of earthquakes and major plate boundaries are shown in Figure 1. Earthquakes occurring in the Circum-Pacific belt account for almost 75% of the total seismic energy released by the earthquakes. The Alpine-Himalayan belt is the second most seismic active belt accounting for ~ 20% seismic energy release, and the remaining 5% seismic energy being released through the mid-oceanic ridges and other Stable Continental Region earthquakes. Most of the tsunamis are caused by the earthquakes occurring in the Circum-Pacific belt. 800 small and large tsunamis occurred in the 20th century with the source earthquakes in the Circum-Pacific belt. While only 3 tsunamis occurred in the Indian Ocean caused by the earthquakes in Alpine-Himalayan belt. There was no tsunami warning facility in the Indian Ocean when the 26 December 2004 Mw 9.2 earthquake occurred. Tsunami alerts issued by the Pacific Tsunami Warning Center and the Japan Meteorological Agency were used. There were several false alarms causing a lot of inconvenience to a large population residing along the east coast of India. This issue was underlined in the International Coordination Meeting during 3-8 March 2005 for the Development of an Indian Ocean Tsunami Warning and Mitigation System organized by the Inter-Governmental Commission on Oceanography at Paris. The issue was accepted as the following Communiqué (www.ioc-tsunami.org).

"Noting it is important to improve the science of issuing tsunami warnings to reduce false alarms given the inordinate inconvenience and disruptions to normal life caused by false alarms, especially given the high population densities and intensive operations in coastal areas in the Indian Ocean, and also to continuously improve forecasting".

The Indian delegate stated that there are only two geographical areas that can host tsunamigenic earthquakes in the Indian Ocean (Gupta, 2008). These are from Sumatra to Andaman Islands, a stretch of some 4000 km, and an area of about 500 km radius off Makaran Coast of Pakistan in the Arabian Sea (shown by a blue ellipse and circle in Figure1). There was quite a bit of a debate on this issue. Finally, it was accepted in the 2nd International Coordination Meeting during 14-16 April 2005 for the Development of an Indian Ocean Tsunami Warning and Mitigation System, held at Grand Baie, Mauritius, with the following declaration (www.ioc-tsunami.org):

Mauritius Declaration

"Recognize the unique tectonic plate structure of the Indian Ocean, and that there are primarily two tsunamigenic sources that could affect the coastlines of the Indian Ocean, namely the Indonesian seismic zone and its extensions, about 4000 km in length, and the Makaran source".

This provided the foundation of setting up of the Indian Tsunami Early Warning System. Global network of seismic stations permits determination of the location and the magnitude of the earthquake within a few minutes or so of its occurrence. If this earthquake has a magnitude ≥ 7 and if it is located within the ellipse and circle in blue color shown in Figure 1, there are chances of generation of tsunami (Gupta, 2008). However, whether a tsunami has been really generated and what is its magnitude cannot be determined, which is necessary to issue appropriate advisories. This issue can be resolved by placing ocean bottom pressure recorders in the immediate vicinity of the two regions capable of hosting a tsunamigenic earthquake. In the open ocean there are waves all the time. However, their amplitude decays

exponentially with depth. At ocean depths of a kilometer or so it is very quiet. Unlike the normal ocean waves, in the case of a tsunami, the entire column of water is moving. So, an ocean bottom pressure recorder placed in the vicinity would detect the tsunami and its amplitude. This is what has been done by planting ocean bottom pressure recorders in the immediate vicinity of the two -tsunamigenic zones in the Indian Ocean (Srinivasa et al., 2013; Nayak et al., 2021).

India undertook a very ambitious project to set up a state of art Tsunami warning capability in a short time of 30 months. This was achieved by end of August 2007, and tested by the 12 September 2007 Mw 7.8 earthquake. Over the past 16 years the system has worked very efficiently. It is now assessed as among the best in the world (Hébert et al., 2020; Nayak et al., 2021).

References

Gupta, H. (2008). India's Initiative in Mitigating Tsunami and Storm Surge Hazard. Journal of Earthquake and Tsunami, 2(04), 287-295.

Gupta, H.K. and Vineet K. Gahalaut (2013). Three Great Tsunamis: Lisbon (1755), Sumatra-Andaman (2004) and Japan (2011), Springer Briefs in Earth Sciences, Springer, ISBN: 978-94-007-6575-7, IX, pp. 1-89.

Srinivasa Kumar, T., Shailesh Nayak and Harsh K Gupta (2013). India's Tsunami Early Warning System, Extreme Natural Hazards, Disaster Risks and Societal Implications, Cambridge University, pp. 322-330.

Nayak, Shailesh, Srinivas Kumar T., and Pattabhi Rama Rao E (2021). Tsunami Watch and Warning Centers, Encyclopedia of Solid Earth Geophysics, Ed. Harsh K. Gupta, 2nd Edition, pp. 1868-1879.

Hébert, H., Occhipinti, G., Schindelé, F., Gailler, A., Pinel-Puysségur, B., Gupta, H. K., ... & Reymond, D. (2020). Contributions of Space Missions to Better Tsunami Science: Observations, Models and Warnings. Surveys in Geophysics, 41, 1535-1581. https://doi.org/10.1007/s10712-020-09616-2

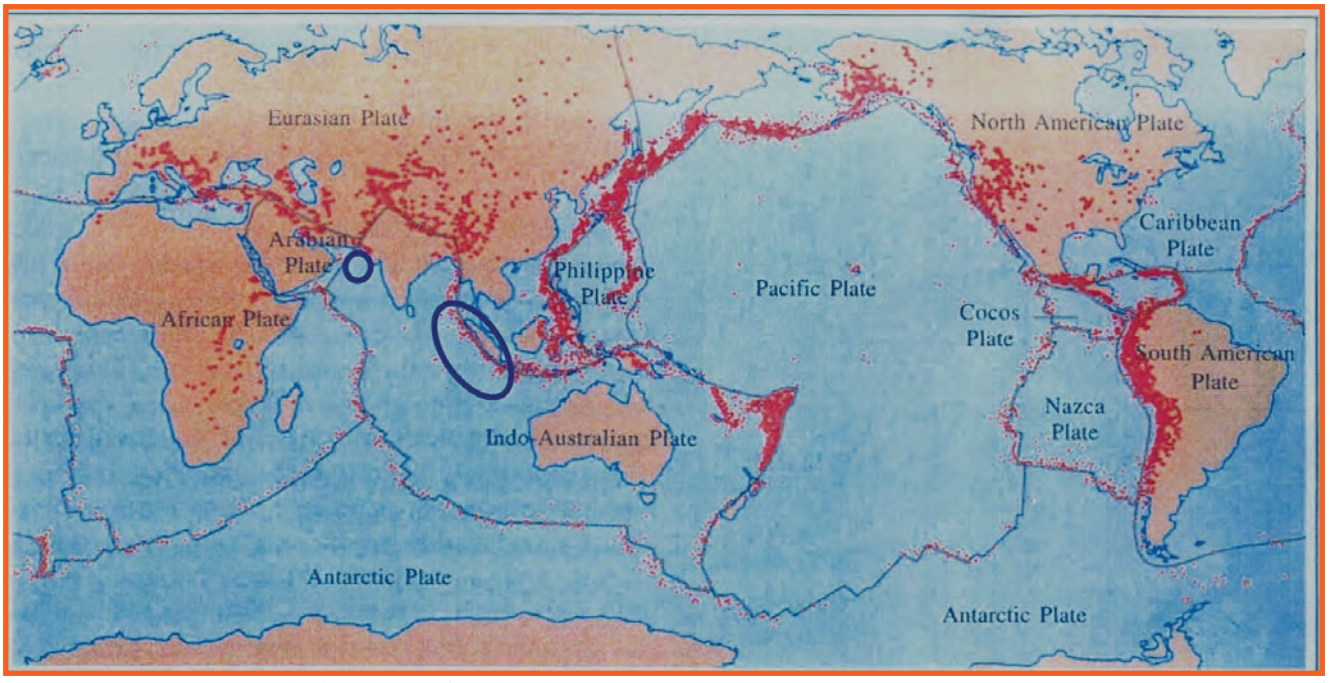

Figure 1: Diagram showing the distribution of earthquakes and major plate boundaries. It may be noted that globally, more than 75% of earthquake energy is released in the Circum-Pacific belt, about 20% in the Alpine-Himalayan belt, and remaining 5% through the mid-oceanic ridges and other Stable Continental Region earthquakes. For a tsunami to hit Indian coast, it is necessary that a tsunamigenic earthquake occurs and its magnitude should be larger than M 7, and the possible locations of such events are enclosed in blue circle and ellipse (Gupta, 2008).

Long-term Phanerozoic global mean sea level: Insights from strontium isotope variations and estimates of continental glaciation

Douwe G. van der Meer[1,2,*], Christopher R. Scotese[3], Benjamin J.W. Mills[4], Appy Sluijs[1], Aart-Peter van den Berg van Saparoea[5], Ruben M.B. van de Weg[2]

[1]Department of Earth Sciences, Utrecht University, 3584 CB Utrecht, the Netherlands
[2]CNOOC International, 90 Oxford Road, Uxbridge UB8 1LU, United Kingdom
[3]Department of Earth and Planetary Sciences, Northwestern University, Evanston, IL 60208, United States
[4]School of Earth and Environment, University of Leeds, Leeds LS2 9JT, United Kingdom
[5]Kallisto Geoscience, De Groene Haven 182, Delft, the Netherlands
[*]E-mail: douwevdm@gmail.com

Global mean sea level is a key component within the fields of climate and oceanographic modelling in the Anthropocene. Hence, an improved understanding of eustatic sea level in deep time aids in our understanding of Earth's paleoclimate and may help predict future climatological and sea level changes.

However, long-term eustatic sea level reconstructions are hampered because of ambiguity in stratigraphic interpretations of the rock record and limitations in plate tectonic modelling. Hence the amplitude and timescales of Phanerozoic eustasy remains poorly constrained. A novel, independent method from stratigraphic or plate modelling methods, based on estimating the effect of plate tectonics (i.e., mid-ocean ridge spreading) from the 87Sr/86Sr record led to a long-term eustatic sea level curve, but did not include glacio-eustatic drivers. Here, we incorporate changes in sea level resulting from variations in seawater volume from continental glaciations at time steps of 1 Myr. Based on a recent compilation of global average paleotemperature derived from δ18O data, paleo-Köppen zones and paleogeographic reconstructions, we estimate ice distribution on land and continental shelf margins. Ice thickness is calibrated with a recent paleoclimate model for the late Cenozoic icehouse, yielding an average ~1.4 km thickness for land ice, ultimately providing global ice volume estimates. Eustatic sea level variations associated with long-term glaciations (>1 Myr) reach up to ~90 m, similar to, and is at times dominant in amplitude over plate tectonic-derived eustasy. We superimpose the long-term sea level effects of land ice on the plate tectonically driven sea level record. This results in a Tectono-Glacio-Eustatic (TGE) curve for which we describe the main long-term (>50 Myr) and residual trends in detail.

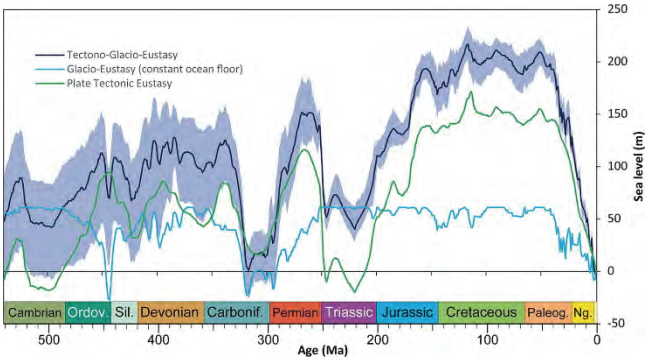

Figure: Tectono-Glacio-Eustatic (TGE) curve for the Phanerozoic.

International Association for Gondwana Research 2023 Convention and
20th International Conference on Gondwana to Asia
Niigata, Japan, October 2023
Abstract Volume

Rainfall-driven volcanic hazards in a changing climate

Jamie Farquharson

Research Institute for Natural Hazards and Disaster Recovery, Niigata University, Niigata 950-2181, Japan
E-mail: jfarquharson@gs.niigata-u.ac.jp

Many eruptive and non-eruptive volcanic hazards can be triggered or worsened by meteorological conditions (e.g., Farquharson and Amelung, 2020). For example, heavy rainfall can drive dome explosions, cause remobilisation of volcanogenic deposits in the form of lahars, induce seismicity, and initiate flank collapse: all of which can constitute substantial hazards in volcanic areas. Rainfall-triggered volcanism is often violently explosive (Mastin, 1994), and multiple direct fatalities have been recorded as a result, including at Karkar, Papua New Guinea (McKee et al., 1981), Guagua Pichincha, Ecuador (Global Volcanism Program, 1993), and Karangetang, Indonesia (Global Volcanism Program, 2011) volcanoes.

This is an especially pressing topic given recent trends in climate change–induced weather patterns (Aubry et al., 2022), in particular the projected increase in extreme rainfall events resulting from global warming. To investigate the propensity for heavy rainfall to increase in volcanic regions the future due to ongoing climate change, this study comprises a comparative analysis of nine general circulation models (ensemble global climate models)—GCMs. From these, the forced model response (FMR) is calculated: a metric which describes the percentage change of heavy precipitation for a given unit of global warming, serving as a proxy for the likelihood of extreme rainfall events in the future (e.g. Fischer et al., 2014). A positive FMR signifies a projected increase in heavy rainfall with increased warming, whereas a negative FMR indicates a decrease in extreme rainfall with increased warming. We show that heavy rainfall is projected to increase with continued global warming (i.e. FMR > 0) throughout the remainder of the twenty-first century in most or all subaerial volcanic regions, based on GCM projections from 2006–2100 CE. In turn, this implies an increase in the potential for rainfall-induced volcanic hazards. This result persists across a broad range of spatial scales, from countries and volcanic arcs down to individual volcanic systems. Key examples include Guagua Pichincha and Soufrière Hills Volcano (Montserrat): systems where observational and statistical evidence has previously revealed the importance of heavy rainfall events in initiating hazardous volcanic phenomena.

The analysis (Farquharson and Amelung, 2022) indicates that heavy precipitation will increase at more than 700 (Holocene-)active volcanoes over the next 80 years (approximately 60% of subaerial active volcanoes). Less than 10% of the studied catalogue are in regions projected to experience less heavy precipitation in 2100 CE relative to the start of this century (FMR < 0). These results imply a set of natural hazards linked to global climate change that is significant, geographically extensive, and increasing over time.

References

Aubry, T.J., Farquharson, J.I., Rowell, C.R., Watt, S.F.L., Pinel, V., Beckett, F., Fasullo, J., Hopcroft, P.O., Pyle, D.M., Schmidt, A., Sykes, J.S., 2022. Impact of climate change on volcanic processes: current understanding and future challenges. Bull Volcanol 84, 58. https://doi.org/10.1007/s00445-022-01562-8

Farquharson, J.I., Amelung, F., 2022. Volcanic hazard exacerbated by future global warming-driven increase in heavy rainfall. R. Soc. open sci. 9, 220275. https://doi.org/10.1098/rsos.220275

Farquharson, J.I., Amelung, F., 2020. Extreme rainfall triggered the 2018 rift eruption at Kīlauea Volcano. Nature 580, 491–495. https://doi.org/10.1038/s41586-020-2172-5

Fischer, E.M., Sedláček, J., Hawkins, E., Knutti, R., 2014. Models agree on forced response pattern of precipitation and temperature extremes. Geophysical Research Letters 41, 8554–8562. https://doi.org/10.1002/2014GL062018

Global Volcanism Program, 2011. Report on Karangetang [Api Siau] (Indonesia). Bulletin of the Global Volcanism Network 36. https://doi.org/10.5479/si.GVP.BGVN201102-267020

Global Volcanism Program, 1993. Report on Guagua Pichincha (Ecuador). Bulletin of the Global Volcanism Network 18. https://doi.org/10.5479/si.GVP.BGVN199302-352020

Mastin, L.G., 1994. Explosive tephra emissions at Mount St. Helens, 1989-1991: The violent escape of magmatic gas following storms? GSA Bulletin 106, 175–185. https://doi.org/10.1130/0016-7606(1994)106<0175:ETEAMS>2.3.CO;2

McKee, C.O., Wallace, D.A., Almond, R.A., Talai, B., 1981. Fatal hydro-eruption of Karkar volcano in 1979: Development of a maar-like crater. Cooke-Ravian Volume of Volcanological Papers, Geological Survey of Papua New Guinea 10, 63–84.

International Association for Gondwana Research 2023 Convention and
20th International Conference on Gondwana to Asia
Niigata, Japan, October 2023
Abstract Volume

Crisis hazard assessment for lahars at snow-covered volcanoes in Japan: Examples from the most recent phreatic eruptions at Mts. Ontake and Kusatsu-Shirane

Kyoko Kataoka[1, *], Takane Matsumoto[1], Kae Tsunematsu[2], and Katsuhisa Kawashima[1]

[1]Research Institute for Natural Hazards and Disaster Recovery, Niigata University, Niigata 950-2181, Japan
[2]Faculty of Science, Yamagata University, Yamagata, 990-8560, Japan
[*]E-mail: kataoka@gs.niigata-u.ac.jp

Two-thirds of the 111 active volcanoes in Japan are snow covered during winter having high risk potential to cause snow-related lahars during and after an eruption. Here we present two case studies (Kataoka et al., 2018; 2021) on crisis (i.e., short-term) hazard assessments for snow-associated lahars immediately after a sudden eruption onset at Mt. Ontake in 2014 and Mt. Kusatsu-Shirane in 2018; the former has a high peak at 3,067 m above sea level (a.s.l.), and the latter had a new-vent eruption in the middle of the ski field.

After the September 2014 phreatic eruption at Ontake, assuming future snowmelt lahar generation, we deployed a meteorological station at high altitude on the southeastern slope, 2190 m a.s.l. to obtain rainfall data and snowmelt rate during the winters of 2014/2015 and 2015/2016. Also, a tentative river monitoring system consisting of a pressure stage gauge, an interval camera, and water quality measuring instruments (turbidity and electric conductivity) was installed to record sediment supply and lahar events in the Akagawa River.

At least three rain-on-snow (ROS) events during the snow-melting season were recognized by the meteorological observation and river stage changes captured in the Akagawa River. Among the three events, a lahar was generated in the river on April 20, 2015. The ROS event caused the snowmelt of 120 mm water equivalent, and the total water input (rainwater+meltwater) was 398 mm. The ROS lahar was erosive in upstream and left clay-poor hyperconcentrated flow deposits in downstream.

After the phreatic eruption (23 January 2018) at the snow-clad Kusatsu-Shirane volcano, forecasting of future snow-related lahars and crisis hazards zonation of populated downslope areas need to be prepared. We carried out a timely approach, which consists of 1) characterization of eruption deposits, 2) meteorological observations and snow surveys, 3) lahar flow simulations by numerical models, and 4) real-time river monitoring.

The snow survey for snow water equivalent at different elevations around the volcano immediately after the eruption and post-eruption period was useful to estimate snow volumes around the new vents, which eventually was helpful for lahar flow simulation assuming snow-associated lahars such as snowmelt lahar, ice slurry lahar and rain-on-snow lahar.

Three scenarios (rain-on-snow triggered, ice/snow slurry, and full snowmelt triggered by a new eruption) were examined, and lahar flow simulations identified potential high-risk areas.

In Japan, risk assessments and hazard maps of lahars at such snow-clad volcanoes tend to focus only on the assumption of full snowmelt lahar caused by a direct pyroclastic (magmatic) eruption. However, lahar type and its trigger can vary by volcano-snow intereations. Therefore, several scenarios for and functions controlling lahars should be considered for lahar hazard assessments at snow-clad volcanoes in Japan (Kataoka et al., 2018, 2021). Also, studies on lahar deposits in historical and geological records are important (e.g., Kataoka et al., 2023) for calibration of numerical flow simulations for lahars to estimate flow travel distances and inundation areas.

References

Kataoka, K.S., Matsumoto, T., Saito, T., Kawashima, K., Nagahashi, Y., Iyobe, T., Sasaki, A., Suzuki, K. (2018) Lahar characteristics as a function of triggering mechanism at a seasonally snow-clad volcano: Contrasting lahars following the 2014 phreatic eruption of Ontake Volcano, Japan. Earth, Planets and Space, 70, 113 (28 pages), DOI: 10.1186/s40623-018-0873-x

Kataoka, K.S., Tsunematsu, K., Matsumoto, T., Urabe, A., Kawashima, K. (2021) Crisis hazard assessment for snow-related lahars from an unforeseen new vent eruption: the 2018 eruption of Kusatsu-Shirane volcano, Japan. Earth, Planets and Space, 73, 220 (22 pages), DOI: 10.1186/s40623-021-01522-0

Kataoka, K.S. (2023) From ‘source to sink’ to ‘sink to source’: a review of volcanic fluvial and lacustrine successions in Japan. In: Di Capua, A. et al. (eds.) Volcanic processes in the sedimentary record: When volcanoes meet the environment. Geological Society, London, Special Publication, 520, 393–416, DOI: 10.1144/SP520-2022-171.

Upper versus Lower Plate Ore Deposits and Hydrocarbon Endowments: A case study from the Canadian Cordillera

Stephen T Johnston

Department of Earth & Atmospheric Sciences, University of Alberta, Edmonton AB T6G 2E3, Canada

E-mail: stjohnst@ualberta.ca

The mid-Cretaceous (120 to 90 Ma, hereafter mK) period presents us with an economically and tectonically significant puzzle when it comes to understanding the tectonic setting of the Cordilleran Orogen of western North America. It was during this time period that the bulk of Canada's oil and gas reserves were produced and sequestered, including the massive oil sand deposits of northern Alberta. The mK also saw the deposition of much of the coal-bearing strata of BC and Alberta; the development of an enormous gold endowment in BC, Yukon and Alaska, including the Tintina Gold Belt; formation of the massive Cantung and MacTung tungsten deposits that lie along the Yukon-NWT border, and the related emplacement of the world-class Keno Hill silver vein deposit; emplacement of gem-quality emerald deposits in the eastern Cordillera of Yukon and northern BC; the development and remobilization of Mississippi Valley Pb-Zn deposits including the Pine Point body and the eruption of a series of diamondiferous kimberlite pipes that together define a 4000 km long, N-S striking kimberlite corridor that runs down the very centre of the continent. The development of such a 'Bonanza' of mineral deposits and energy reserves begs the question "Is there an underlying process or tectonic setting that explains the coeval development of so many important ore deposits and energy reserves?

The development of the kimberlite corridor points to E-W extension and lithospheric thinning of the continent. An overall extensional setting for the continent is consistent with the mK opening of the N Atlantic and the Canada Basin, all as part of the coeval acceleration of Pangea breakup. However, explaining the mK Bonanza as a product of continental extension is in direct conflict with our understanding of the Cordilleran Orogen. mK fold & thrust belts, including the Brooks Range of Alaska; the Selwyn-Columbian of Yukon-BC-Alberta; and the Sevier of the conterminous US, characterize the orogen and point to an overall compressional tectonic regime. mK contraction is commonly explained as a result of an increase in the relative rate of convergence between North America and the Panthalassan oceanic slabs inferred to have been subducting beneath the continent's west margin. In this 'Accretionary' model, mK strata of the Western Canadian Sedimentary Basin (WCSB) east of the Rocky Mountains are interpreted as a retro-arc foreland basin deposits developed in response to compressive loading of the continental lithosphere by crustal thickening within the Cordilleran Orogen. How then to reconcile the record of compressive tectonic setting of the Cordilleran orogen with the otherwise widespread expressions of extension found to the east of the orogen?

An alternative 'Westward Subduction' model may provide for reconciliation of the conflicting states of Cordilleran versus Continental strain, and explain the coeval development of the many significant ore deposits and hydrocarbon reserves. The Westward Subduction model entails west-dipping subduction of North American oceanic lithosphere that lay west of but which was continuous with continental North America. Subduction of N American lithosphere beneath the east (not west) side of the Cordillera, places the Cordillera in the upper plate and North America in the lower plate. While there may have been a landward (east) dipping Panthalassan subduction zone to the west of the Cordillera, its location relative to the eastern margin of the Cordilleran remains unclear and is not further considered here. The east-verging mk thrust belts develop along the eastern margin of the Cordillera and record the entry of continental North America into the Cordilleran trench. The bonanza of Au, Ag and Sn-W deposits all occur within and are characteristic of Cordilleran upper plate, and represent a

typical suite of arc and arc-continent collisional ore deposits. Cratonic Laurentia, forming the lower plate, thins due to slab pull and is characterised by a 'lower plate' hydrocarbon and ore deposit bonanza of, in order of increasing distance from the trench, coal, oil and gas, oil sands, Pb-Zn deposits, and diamondiferous kimberlite pipes. Entry of continental N America into the trench was immediately followed by slab break-off, limiting the effects of arc-continent collision, and shutting down the ore- and hydrocarbon reserve-forming processes.

The Westward Subduction model requires 1) an upper plate mK Cordilleran magmatic arc, 2) a suture that lies east of, and which separates the cratonic lower plate from the upper plate arc, and 3) a coeval foredeep, rather than a foreland, basinal sequence deposited on the cratonic lower plate during its entry into the trench. Satisfying all three of these predictions requires significant reinterpretation of existing Cordilleran and cratonic geological features.

Physics-informed and data-driven for landslide warning

Songlin Liu[1], Wengang Zhang [1,2,3,4,*]

[1]School of Civil Engineering, Chongqing University, Chongqing 400045, China
[2]Key Laboratory of New Technology for Construction of Cities in Mountain Area, Chongqing University, Ministry of Education, Chongqing 400045, China;
[3]National Joint Engineering Research Center of Geohazards Prevention in the Reservoir Areas, Chongqing University, Chongqing 400045, China;
[4]Chongqing Field Scientific Observation Station for Landslide Hazards in Three Gorges Reservoir Area, Chongqing University, Chongqing 400045, China
[*]Email: zhangwg@cqu.edu.cn

Landslides present considerable risks to human lives and infrastructure. Consequently, an effective and precise landslide warning system is indispensable for ensuring safety. Recent research has predominantly focused on displacement-prediction-centric warning methods that leverage data-driven approaches, with a particular emphasis on machine learning models. However, these techniques frequently neglect qualitative analysis, which can limit interpretability and lead to inaccuracies in real-world engineering contexts. This study introduces a physics-informed, data-driven methodology for landslide warnings. Polynomial regression is employed to discern the trend component of historical displacement records, while the periodic trend is modeled using long-short term memory networks (LSTM). This model is then supplemented with the corresponding trend term to produce a data-driven displacement prediction. Concurrently, Flac3D is utilized to conduct a qualitative displacement analysis based on shear strength parameters obtained from site investigations. The qualitative and quantitative outcomes for each time step are integrated and serve as input for an artificial neural network, which then forecasts the actual displacement. The improved tangent angle is subsequently used to determine the threshold for warning levels based on the predicted displacement. This approach ensures that both physics-informed insights and data-driven predictions are incorporated into the final analysis, thereby optimizing the efficacy and efficiency of the warning system.

Rheology and seismic anisotropy of continental lithosphere

Shengsi Sun

State Key Laboratory of Continental Dynamics, Department of Geology, Northwest University, Xi'an 710069, China
E-mail: shsun@nwu.edu.cn

Rheology of rocks controls the deformation of Solid Earth at multiple space-time scales, which is crucial to understand the tectonic evolution of continental lithosphere. The research of rock rheology is mainly conducted by high-pressure and temperature rheology experiments and multi-scale observation and measurement of naturally deformed rocks. At present, a large number of data have been accumulated. This contribution provides an up-to-date comprehensive complication of the rheological mechanism, fabric types and seismic properties of the main rock-forming minerals at different depths of lithosphere, including olivine, orthopyroxene, clinopyroxene, amphibole, plagioclase, quartz and mica. The high-pressure and temperature experimental results and natural deformation observations of peridotite, eclogite, mafic granulite, amphibolite and felsic rocks are introduced, including the progress on rheology strength and behavior, seismic velocity and anisotropy. Taking the Tibetan Plateau as an example, the application of rock rheology in quantitative interpretation of seismic anisotropy data is discussed. The combination of mineral deformation fabric and seismic anisotropy is expected to make an important breakthrough in rheology mechanism and structure of continental lithosphere.

International Association for Gondwana Research 2023 Convention and
20th International Conference on Gondwana to Asia
Niigata, Japan, October 2023
Abstract Volume

Groundwater quality of India: a status review

E. Shaji[1,*], M. Santosh[2,3]

[1]Department of Geology, University of Kerala, Kariavattom Campus, Thiruvananthapuram, Kerala, 695581, India
[2]School of Earth Sciences and Resources, China University of Geosciences (Beijing), 29 Xueyuan Road, Beijing 100083, China
[3]Department of Earth Science, University of Adelaide, Adelaide, SA 5005, Australia
[*]Email: shajigeology@keralauniversity.ac.in

India is the world's largest user of groundwater and still Indian aquifers can be considered one of the best groundwater reservoirs in the world. More than 60 percent of irrigated agriculture and 85 percent of drinking water depend on the groundwater resource of the country. The Indian Sub- Continent is endowed with diverse geological formations from the oldest Achaeans to Recent alluviums and characterized by varying climatic conditions in different parts of the country. The quality of groundwater is influenced by the depth of the soils, sub-surface geological formations, and primary and secondary porosity of aquifer units through which groundwater flows. In general, in the larger part of the country, groundwater is of good quality and suitable for drinking, agricultural and industrial purposes. The groundwater in shallow aquifers is generally of calcium bicarbonate and mixed type and the deep aquifers show mixed type and sodium-chloride type water. However, the quality of groundwater in shallow and deeper aquifers varies from place to place depending on climate, geology, and recharge and draft. This paper addresses the major quality issues pertaining to the groundwater resources of India. Central Ground Water Board, Govt of India is the authority to monitor and document the quality issues of groundwater resources of India. The major quality issues reported are salinity problems, and high incidence of fluoride, arsenic, iron, manganese, heavy metals, and pesticides from different geographical locations with varied hydrogeological settings.

Inland salinity in groundwater is common in the arid and semi-arid regions of Rajasthan, Haryana, Punjab, Gujarat, Uttar Pradesh, Delhi, Andhra Pradesh, Maharashtra, Karnataka, and Tamil Nadu. In some parts of Rajasthan and Gujarat, groundwater salinity is too high that the well water is directly used for salt manufacturing by solar evaporation. Inland salinity is also noticed in some canal command areas. The coastal salinity is widespread in the dynamic coastline of India. The western coast is characterized by a wide continental shelf and is marked by backwaters and mud flats while the eastern coast has a narrow continental shelf and is characterized by deltaic and estuarine landforms. The quality of groundwater in coastal aquifers varies considerably depending upon climate change, disposition of fresh and saline water interface in multi-aquifer systems, groundwater development scenario, and coastal geomorphology and dynamics. Salinity issues are more predominant along the eastern coastal tract when compared with its western counterpart.

Fluoride contamination in groundwater is one of the most widespread quality issues in India It is widely prevalent in different parts of India, particularly in the state of Andhra Pradesh, Tamil Nadu, Uttar Pradesh, Gujarat, and Rajasthan. As per an estimate about 66 million people in India are consuming water with fluoride levels beyond the permissible limit. The next important contamination is arsenic in terms of its carcinogenic nature and the number of persons affected. In India, 20 states and 4 Union Territories have so far been affected by arsenic contamination in groundwater. An attempt to evaluate the correlation between arsenic poisoning and aquifer type shows that the groundwater extracted from unconsolidated sedimentary aquifers, particularly those which are located within the younger orogenic belts of the world, are the worst affected. More than 90% of arsenic pollution is inferred to be geogenic. We infer that alluvial sediments derived from the Himalayas are the major source of arsenic contamination in groundwater and we postulate a strong relation with plate tectonic processes, mountain building, erosion, and sedimentation.

Problems related to iron and manganese in groundwater are found in widely distributed geographical areas. Elevated iron has been reported from almost all states, covering almost all major aquifer systems. Elevated levels of Mn are sporadic in nature in comparison to Fe. An elevated level of Mn has been reported mainly from West Bengal, Tamil Nadu, Orissa, UP, and Bihar.

Uranium, radon, and strontium contamination in groundwater are also reported from many parts of India. The uranium and radon are limited in aerial extent and confined to Andhra Pradesh, Himachal Pradesh, Chhattisgarh, Madhya Pradesh, Karnataka, Rajasthan, and Punjab. Strontium has been reported from Ranga Reddy district of Andhra Pradesh. Chromium has been reported from different parts of India. Selenium in groundwater is highly localized in distribution and has been reported as patches in Himachal Pradesh and Punjab. Similarly, nitrate problems in groundwater are widespread in India. Of late heavy contamination in groundwater (Lead (above 0.01 mg/l) Cadmium (above 0.003 mg/l) Chromium (above 0.05 mg/l)

are also on the rise.

Though all these quality issues of groundwater prevail, still India has a good potential for groundwater development, provided it is sustainably exploited. We need to focus on the protection of the aquifers of India. Access to safe water is the most basic human need for health and well-being. Demand for groundwater is rising owing to rapid population growth, urbanization, and increasing water needs from agriculture, industry, and energy sectors. Therefore, we need to work in line with UN Sustainable Development Goals (SDG-6) to protect the productive aquifer units of India.

Source: reports of CGWB.
https://cgwb.gov.in/wqreports.html

Vaguely right or exactly wrong: some thoughts on complex zircon and the handling of isotopic age data from microbeam analysis

Daniel J. Dunkley

Department of Polar and Marine Research, Institute of Geophysics, Polish Academy of Sciences ul. Księcia Janusza 64 Warsaw PL-01452 POLAND
E-mail: daniel.dunkley@igf.edu.pl

In high-grade gneissic terranes, much of the interpretation of geological history is made from the isotopic dating of zircon by microbeam analysis, especially where it is the only mineral that survives multiple insults of metamorphism and deformation. Careful analysis linked with interpretation of structure in zircon can 'see through' metamorphism to identify protolith ages and multiple tectonometamorphic events. But in common enough situations where isotopically concordant age data scatter continuously beyond analytical precision, the interplay between data interpretation and inference of geological boundary values is problematic. This is because, although analytical scatter can be reasonably assumed to obey classical statistical distributions, such assumptions cannot be made for actual geological events and processes. Examples include metamorphic zircon growth over periods longer than the precision of measurement; isotopically disturbed arrays, (especially where the disturbance is ancient) and in zircon from mixed sources, such as detritus in sediments. Nevertheless, measured age continua still incorporate analytical precision, so that statistical equivalence must always be taken into account when considering the minima and maxima of such ranges. Here some case studies will be presented where neglect of this issue can lead us down some false paths. Examples include: the extraction of minimum ages for the protoliths of gneisses; confusion between xenocrystic and magmatic zircon populations in metaigneous rocks; constraining the duration of metamorphic zircon growth, and the definition of Maximum Deposition Age (MDA) for sedimentary rocks.

Funding: OPUS grant UMO-2021/43/B/ST10/03161 "ANTARCHEA" to D. J. Dunkley from the National Science Center (NCN), Poland.

International Association for Gondwana Research 2023 Convention and
20th International Conference on Gondwana to Asia
Niigata, Japan, October 2023
Abstract Volume

Complex polymetamorphic and magmatic history in Napier Mountains, East Antarctica revealed by zircon

Piotr Król[1, *], Monika A. Kusiak[1], Daniel J. Dunkley[1], Martin J. Whitehouse[2], Simon A. Wilde[3], Lars E. Augland[4]

[1] Institute of Geophysics, Polish Academy of Sciences, Warsaw 01-452, Poland
[2] Department of Geosciences, Swedish Museum of Natural History, Stockholm 114 18, Sweden
[3] School of Earth and Planetary Sciences, Curtin University, Perth 6845, Australia
[4] Department of Geosciences, Oslo University, Oslo 0371, Norway
[*]Email: piotr.krol@igf.edu.pl

The Napier Complex in Enderby Land and western Kemp Land is one of the least studied regions where early Earth rocks have been preserved. It is a unique component of the East Antarctic Shield because it archives a timeline of crustal growth from the Eo- to Neoarchean, with protoliths dating back to 3.75 Ga at locations such as Mount Sones, Gage Ridge, (Kusiak et al., 2013; Guitreau et al., 2019), Budd Peak, Mount Jewell (Król et al., 2020) and Aker Peaks (Kusiak et al., 2021). It is predominantly composed of enderbitic and charnockitic gneisses and granulites that underwent metamorphism at ca. 2.5 Ga, and locally at ca. 2.8 Ga, under high- to ultra-high-temperature conditions (Harley et al., 2019). Putatively, the complex is composed of different crustal domains with independent geological histories, but this hypothesis needs to be tested by further constraining the magmatic and metamorphic events.

To gain deeper insights into the crustal evolution of the Napier Complex, samples from the Napier Mountains were selected for zircon imaging and U-Pb dating by Secondary Ion Mass Spectrometry. They record metamorphic growth, modification of zircon and recrystallization at 2800-2770, 2740-2720 Ma and 2490-2460 Ma. The ca. 2800 metamorphic event is recorded in zircon grains from Grimsley Peaks with ages as young as 2770 Ga, thus extending the duration of the event by 20 Myr when compared to the earlier date of 2790 Ma proposed by Hokada et al. (2003). For the first time in the Napier Complex, evidence of fluid-related alteration at around 2730 Ma has been observed in a granitic gneiss from Grimsley Peaks. At the similar time, dioritic gneiss was formed at Mount Marr. Furthermore, protolith crystallization ages of around 3210 and 2825 Ma, were determined for tonalitic and granitic gneisses from Grimsley Peaks, respectively. The generation of granitic gneiss was coeval with ~2.8 Ga metamorphism in the area. All the samples show significant zircon modification due to the 2490-2460 Ma metamorphism. Research conducted within a grant UMO2019/34/H/ST10/00619 to MAK

References

Harley, S.L., Kelly, N.M., Kusiak, M.A. (2019) Chapter 35 - Ancient Antarctica: The Archean of the East Antarctic Shield, in: Kranendonk, M.J.V., Bennett, V.C., Hoffmann, J.E. (Eds.), Earth's Oldest Rocks (Second Edition). Elsevier. 856-897

Hokada, T., Misawa, K., Shiraishi, K., Suzuki, S. (2003) Mid to late Archaean (3.3-2.5 Ga) tonalitic crustal formation and high-grade metamorphism at Mt. Riiser-Larsen, Napier Complex, East Antarctica. Precambrian Research 127, 215-228.

Król, P., Kusiak, M.A., Dunkley, D.J., Wilde, S.A., et al. (2020) Diversity of Archean crust in the eastern Tula Mountains, Napier Complex, East Antarctica. Gondwana Research 82, 151-170.

Kusiak, M.A., Dunkley, D.J., Wilde, S.A., Whitehouse, M.J., Kemp, A.I.S. (2021) Eoarchean crust in East Antarctica: Extension from Enderby Land into Kemp Land. Gondwana Research, 1-16.

Kusiak, M.A., Whitehouse, M.J., Wilde, S.A., Dunkley, D.J., et al. (2013) Changes in zircon chemistry during Archean UHT metamorphism in the Napier Complex, Antarctica. American Journal of Science 313, 933-967.

International Association for Gondwana Research 2023 Convention and
20th International Conference on Gondwana to Asia
Niigata, Japan, October 2023
Abstract Volume

Genesis of Olivine-charnockite and its Gondwana connections

K. Sajeev[1, *], P. Rajkumar[2], Durgalakshmi[3], M. Satish-Kumar[4], Sayantani Chatterjee[4,5], Ian S. Williams[3], Eiichi Takazawa[4]

[1]Centre for Earth Sciences, Indian Institute of Science, Bengaluru 560 012, India.
[2] Advanced Facility for Microscopy and Microanalysis, Indian Institute of Science, Bengaluru 560 012, India.
[3]Research School of Earth Sciences, Australian National University, Canberra 2601, Australia
[4]Department of Geology, Faculty of Science, Niigata University, Niigata 950-2181, Japan
[5]Earthquake Research Institute, The University of Tokyo, Tokyo113-0032, Japan
[*]Email: sajeev@iisc.ac.in

Olivine (fayalite)-bearing granitic rocks are not common. Oyawoye (1964) reported a rare fayalite-orthopyroxene-bearing quartz monzonite from Nigeria named Bauchite. Subsequently fayalite-bearing, felsic plutonic rocks are occasionally reported worldwide. Frost and Frost (2008) and Touret and Huizenga (2012) mentioned the rare occurrence of olivine-bearing charnockite. The present study identified a peculiar fayalite-bearing charnockite from the south-eastern Madurai Block, India. The primary rock type in the region is hornblende-rich charnockite, intercalated with thin, disrupted layers of pyroxenite and garnet-rich felsic rocks. Fayalite-bearing charnockite is exposed in a rock quarry at Paneerkulam village and nearby areas, hosted within hornblende-rich charnockite. Geochemically, olivine-bearing charnockite and surrounding rocks have a similar bulk chemical composition (slightly low SiO_2 content).

The prominent reaction texture is coarse-grained fayalite and clinopyroxene rimmed by orthopyroxene coronas. The clinopyroxene grains have crisscrossing exsolution lamellae of orthopyroxene oriented in at least three directions, a texture indicating that the primary clinopyroxene was pigeonite. In a few domains, fayalite is associated with magnetite and minor quartz. The matrix assemblage is mostly plagioclase, mesoperthite and minor quartz. Zircon is associated with both the mafic and felsic matrix mineral assemblages. Zircon grains associated with olivine or clinopyroxene are rounded, with a concentrically zoned CL-bright core rimmed by a CL-dark mantle overprinted by a thin grey rim. Zircon grains associated with mesoperthite and plagioclase are more elongate, with a similar zoning pattern but a thick outer rim. Temperature estimates based on the composition of clinopyroxene and integrated mesoperthite are *ca*. 850–890°C. Based on *P-T* estimates from an isochemical phase diagram, the primary minerals were formed at high-temperature (*ca.* 850°C) at a pressure of *ca.* 7.5 kbar. These mineral assemblages were later overprinted by orthopyroxene at a similar temperature (*ca.* 800°C) but lower pressure (*ca*. 6 kbar).

Zircon U-Pb dating gave a mean core age of *ca*. 800 Ma and a rim age of *ca*. 520 Ma. There is a small cluster of analyses (n = 4) at *ca*. 670 Ma. Based on the textural relations and dating, the primary magma was emplaced at *ca.* 800 Ma, possibly in connection with the break-up of the Rodinia supercontinent. Primary zircon was later overgrown by *ca*. 520 Ma rims during metamorphism and orthopyroxene formation associated with the amalgamation of Gondwana. The significantly negative $\varepsilon Nd^{(t)}$ and the 1000 to 1800 Ma TDM model ages suggest that the melting of a depleted contaminated mantle source could have formed these rocks. The primary crystallization of fayalite, along with clinopyroxene, falls below the fayalite-magnetite-quartz buffer, indicating low activity of oxygen and volatiles such as H_2O. This conclusion is supported by the absence of hydrous phases such as hornblende or biotite in any of the observed fayalite-bearing charnockite samples. These results indicate that during Rodinia break-up, the lower crust of south-eastern India was subject to a high-temperature heat pulse under highly reducing conditions.

References

Frost, B.R. and Frost, C.D. (2008) On charnockites Gondwana Research 13, 30–44.

Oyawoye, M.O. (1964) Bauchite: A New Variety in the Quartz Monzonitic Series. Nature, P689.

Touret, J.L.R. and Huizenga, J. M. (2012) Charnockite microstructures: From magmatic to metamorphic. Geoscience Frontiers 3, 745-753.

'Selective' UHT metamorphism in the deep crust

Sanjeewa P.K. Malaviarachchi

Department of Geology, Faculty of Science, University of Peradeniya, Sri Lanka
E-mail: malavi@sci.pdn.ac.lk

Conventionally, ultra-high temperature (UHT) metamorphism demarcates >900 °C crustal temperatures, texturally controlled by diagnostic mineral assemblages. Instead of this critical temperature, lately, thermobaric ratio (dT/dP) > 75 □C kbar-1 is in-use to designate regions of ultra-hot crust that undergo UHT metamorphism (UHT thermal envelope). A P-T diagram plotted with curves of thermobaric ratios of deep crustal rocks using the published data shows that in addition to UHT granulites, a vast proportion of ordinary-granulites (for example, typical high temperature metamorphic rocks with peak T> 750 °C) also encompass within the above-defined characteristic UHT thermal-envelope. Despite the fact that these ordinary-granulites well exceed the critical thermobaric ratio of 75 °C kbar-1 they hardly reach UHT metamorphism, even after long-lived stay in the ultra-hot crust, as evidenced by natural examples. This denotes a 'selective' UHT metamorphism in the deep crust, despite the rocks inside the UHT thermal envelope are theoretically qualified for UHT metamorphism, such as having appropriate bulk chemical composition, thermobaric ratio and sufficient heat production rates ('UHT eligible' crust). We suggest that this selective UHT metamorphism alerts of a 'thermobaric barrier' persistent at least in some regimes of this thermally matured hot/ultra-hot crust that may resist developing UHT mineral assemblages. As observable from global examples, fragments of UHT-eligible crust do relate tectonically with collisional orogens or accretionary (arc-back arc) settings, evidencing sufficient thermal energy existed to reach UHT conditions, but they do not. Hence, I open an avenue here for discussion on the 'UHT-eligible crust' i.e., ultra-hot crust that survive UHT metamorphism.

International Association for Gondwana Research 2023 Convention and
20th International Conference on Gondwana to Asia
Niigata, Japan, October 2023
Abstract Volume

Early Cambrian high pressure/low temperature metamorphism in the southeastern Tarim craton associated with cold subduction along circum-Gondwana

Qian Liu[1,*], Toshiaki Tsunogae[2,3], Guochun Zhao[4,1], Sam Uthup[2], Kazuki Takahashi[2], Jinlong Yao[1], Yu Wu[5], Yigui Han[1], Kei Ikehata[2]

[1] State Key Laboratory of Continental Dynamics, Department of Geology, Northwest University, Xi'an 710069, China
[2] Faculty of Life and Environmental Sciences, The University of Tsukuba, Ibaraki 305-8572, Japan
[3] Department of Geology, University of Johannesburg, Auckland Park 2006, South Africa
[4] Department of Earth Sciences, The University of Hong Kong, Pokfulam Road, Hong Kong
[5] Beijing Research Institute of Uranium Geology, Beijing100029, China
[*]E-mail: liuqian@nwu.edu.cn

The early Cambrian subduction along circum-Gondwana has been considered to reflect the establishment of modern plate tectonics in response to global plate re-organization due to the final assembly of Gondwana. Indicators for the circum-Gondwana subduction in the modern plate tectonic regime are primarily Mariana-type ophiolites and trench-arc assemblages. Metamorphic rocks, especially blueschist and low temperature (LT) eclogite that form under high pressure (HP)/LT conditions with low thermobaric (T/P) ratios, as a hallmark of cold subduction in the modern tectonic regime have not been well investigated. The early Paleozoic HP/LT metamorphic rocks in the Altyn Tagh, the southeastern Tarim craton, record the initial subduction along the northern margin of Gondwana. They are key to understanding the subduction processes along the Gondwana's margins and to testing the possible link between the circum-Gondwana subduction and the emergence of the modern plate tectonics.

This study integrated field investigation, petrography, mineral chemistry, phase equilibrium modelling, quartz-in-garnet Raman elastic geobarometry, and Ar-Ar geochronology. The HP/LT metamorphic rocks in the Altyn Tagh occur as a tectonic sliver associated with early Paleozoic volcanosedimentary sequences. Zoisite blueschist is enclosed by or intercalated with glaucophane (Gln)-bearing quartz schist, both of which constitute a lens of a 2 m width surrounded by muscovite quartz schist. Mineral assemblage and chemistry indicate that the zoisite blueschist and Gln-bearing quartz schist samples have blueschist-facies mineral assemblages of garnet (outer domains) + glaucophane + zoisite + rutile + quartz + chlorite and garnet + phengite + glaucophane + zoisite + rutile + quartz + chlorite, respectively.

Phase equilibrium modelling and quartz-in-garnet Raman elastic geobarometry reveal that the studied samples experienced lawsonite to epidote blueschist-facies metamorphism at 520-545 °C and 16-19 kbar, representing HP/LT metamorphism with low T/P ratios of <300 °C/GPa. These blueschist-facies metamorphic rocks underwent rapid

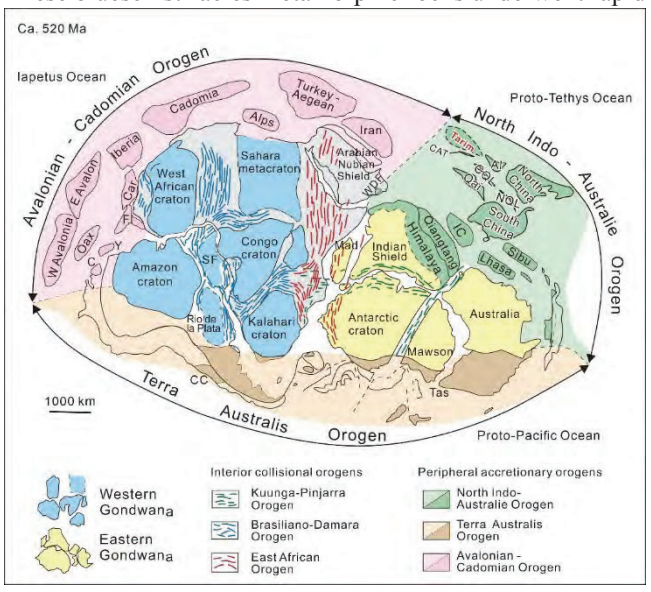

Figure 1: Reconstruction of Gondwana at ca. 520 Ma (modified after Cawood et al., 2021; Liu et al., 2021). Abbreviations: CAT— Central Altyn Tagh, Al— Alxa, CQL— Central Qilian, Qai— Qaidam, NOL— North Qinling, IC— Indochina, Sibu— Sibumasu, WDF— Western Deformational Front, Oax— Oaxaquia, C— Cortis, Y— Yucatan, Fl— Florida, Car— Carolina, CC— Cuyania and Chilenia, SF— San Francisco, Mad— Madagascar, and Tas— Tasmania.

decompression due to exhumation starting at P-T conditions of <495 °C and <9.6 kbar. Ar-Ar geochronological results record paragonite Ar-Ar plateau ages of 520-506 Ma for the zoisite blueschist samples and phengite Ar-Ar plateau ages of 522-516 Ma for the Gln-bearing quartz schist samples. It is suggested that the peak HP/LT metamorphism occurred

prior to ca. 522 Ma. Combined new results with available data from the major Gondwana blocks, cold subduction is considered to have initiated by the early Cambrian along circum-Gondwana after the amalgamation of Gondwana (Figure. 1). The intense circum-Gondwana subduction probably represents the earliest global, cold subduction in Earth's history indicative of the establishment of the modern plate tectonics, as supported by the studied early Cambrian HP/LT metamorphic rocks and a dramatic drop in the mean T/P of metamorphism since the early Paleozoic.

This study was financially supported by a National Natural Science Foundation of China Project (41730213) and a Grant-in-Aid for Scientific Research from Japan Society for the Promotion of Science (JSPS) to Prof. Toshiaki Tsunogae (18H01300).

References

Cawood, P.A., Martin, E.L., Murphy, J. B., Pisarevsky, S.A., 2021. Gondwana's interlinked peripheral orogens. Earth and Planetary Science Letters 568, 117057.

Liu, Q., Zhao, G.C., Li, J.H., Yao, J.L., Han, Y.G., Wang, P., Tsunogae, T., 2021b. Provenance of early Paleozoic sedimentary rocks in the Altyn Tagh orogen: Insights into the paleoposition of the Tarim craton in northern Gondwana associated with final closure of the Proto–Tethys Ocean. Geological Society of America Bulletin 133(3-4), 505-522.

Miocene-Pliocene UHT metamorphism in Western Sulawesi, Indonesia

Juiyen Hsia[1], Jian Zhang[1,2,*], Guochun Zhao[2], Jiahui Qian[1], Jin Liu[3], Min Sun[2], Changqing Yin[1], Peng Gao[1], Welson Weisheng Xian[4], Minjie Guo[1]

[1]School of Earth Sciences and Engineering, Sun Yat-sen University, Guangzhou, China
[2]Department of Earth Sciences, University of Hong Kong, Pokfulam Road, Hong Kong SAR
[3]College of Earth Sciences, Jilin university, Changchun, China
[4] Pt. Enersteel, Jl.Pejaten Barat II No. 20 Kav. C, South Jakarta 12510, Indonesia
[*]E-mail: zhangjian@mail.sysu.edu.cn

Ultrahigh-temperature (UHT) metamorphism represents an extreme crustal thermal event with peak conditions exceeding 900 C at 7–13 kbar. In the modern-style plate tectonic system, records of UHT metamorphism are relatively rare due to the secular cooling of Earth. In the Palu region of Western Sulawesi, we newly discovered a series of HT-UHT metamorphic rocks including amphibolite, granulite, eclogites and gneiss. Of them, two granulite samples (18CS14-2, 18CS14-4) with high garnet content (>50 mol%) are chosen for petrographic observation, phase equilibrium modelling, and zircon U-Pb dating. These rocks are characterized by a relic M_1 assemblage of Grt + Ky + Bt + Rt and a M_2 assemblage of Grt + Sil + Pl + Spl + Crd ± Qtz + Ilm + melt. Phase equilibrium modelling based on effective bulk compositions yields UHT conditions of 7.2–8.5 kbar/940–1080 °C (18CS14-2) and 7.0–7.3 kbar/1000–1040 °C (18CS14-4). U-Pb analysis reveals two generations of metamorphic zircon with evolving REE content that is intimately related to garnet growth and decomposition. Zircon age of 36–5.3 Ma is ascribed to syn- to post-M_1 metamorphism, whereas the young zircon age of 5.1–3.8 Ma is linked to syn- and post-M_2 stage. The UHT metamorphism was probably the consequence of the upwelling of asthenospheric mantle triggered by post-collisional delamination of lithosphere in the Miocene-Pliocene (ca. 5 Ma). It is one of the youngest known UHT metamorphism on Earth.

Acknowledgement

This work was financially supported by the National Natural Science Foundation of China [42025204 and 41890831]; Guangdong Province Introduced Innovative R&D Team of Geological Processes and Natural Disasters around the South China Sea [2016ZT06N331] and HKU Seed Fund for Basic Research [201811159089]. We are grateful to Mr. Norman Edward of the Pt. Enersteel, Indonesia, for his great help in geological collaboration and the field investigations.

Protolith and metamorphic ages of eclogites from the Eastern Alps: Implications for the Permian to Cretaceous Wilson cycle of the Austroalpine mega-unit

Ruihong Chang [1,*], Guochun Zhao [1], Franz Neubauer [2], Yongjiang Liu [3,4], Johann Genser [2], Sihua Yuan [5]

[1] Department of Earth Sciences, the University of Hong Kong, Pokfulam, Road, Hong Kong, China
[2] Department Geography and Geology, University of Salzburg, A-5020 Salzburg, Austria.
[3] Frontiers Science Center for Deep Ocean Multispheres and Earth System, Key Lab of Submarine Geoscience and Prospecting Techniques, College of Marine Geosciences, Ocean University of China, Qingdao 266100, China.
[4] Laboratory for Marine Mineral Resources, Qingdao National Laboratory for Marine Science and Technology, Qingdao 266237.
[5] China College of Earth Science, Institute of Disaster Prevention, Sanhe, 065201, Hebei Province, China.
[*]Email: ruihong_chang@163.com

The Austroalpine mega-unit contains the type locality of eclogites (Haüy, 1822) but their protolith age is largely unknown except that of the Permian Bärofen eclogite, for which three Sm-Nd ages between 275 ± 18 and 275 ± 18 Ma have been reported (Thöni and Jagoutz, 1993; Miller and Thöni, 1997). Therefore, we studied the non-gabbroic eclogites from the Saualpe-Koralpe and Sieggraben Complexes, which are considered to represent a previously coherent subducted and then exhumed fragment of a continental rift, which led to the formation of the late Middle Triassic Meliata oceanic basin. A combined zircon U–Pb and Hf isotopic study, whole rock geochemistry of two complexes revealed a protolith age of 242.3 ± 2.6 Ma (Middle Triassic) in the Sieggraben Complex, and 283 ± 5 Ma, 255 ± 3 Ma (Early and Late Permian), 251 ± 3 Ma, and 241 ± 3 Ma (Early to Middle Triassic) in the Saualpe-Koralpe Complex. Magmatic zircons from the Sieggraben eclogites have 176Hf/177Hf ratios of 0.283067–0.283174, εHf(t) values of +15.7 to +19.4, and that from Saualpe-Koralpe eclogite have 176Hf/177Hf ratios of εHf(t) 0.282935–0.283090, εHf(t) values of +10 to +17.4 showing their juvenile mantle source rather than significant crustal assimilation. In both complexes, N-MORB geochemical characteristics are established. Associated ultramafic rocks of Sieggraben eclogites as part of oceanic or Permian subcontinental mantle lithosphere suggest a depleted mantle source and a deep subduction environment. Two zircon grains of Sieggraben eclogites with low Th/U ratios yield ages of 113 ± 2 Ma and 86 ± 4 Ma and represent the approximate age of eclogite metamorphism during Cretaceous. A trondhjemite dike cutting through the eclogite gives a crystallization age of 82.19 ± 0.4 Ma and formed by partial melting of likely eclogite during decompression. The host metasedimentary rocks of Sieggraben and Saualpe-Koralpe Complexes are interpreted as old continental crust close to the margin of the Meliata basin and were affected by Permian migmatitic metamorphism. Metamorphic zircons of one eclogite from the Saualpe-Koralpe Complex gives an age of 87–93 Ma (peak at 91 ± 1.2 Ma). The results of this study combined with previous results are used to present a new model for the tectonic evolution of the distal Austroalpine unit associated with the Meliata Ocean in a Wilson cycle: The Austroalpine Sieggraben and Saualpe-Koralpe Complexes represent a location on the distal continental margin during Permian to Middle Triassic rifting. The mafic rocks are associated with numerous Permian and potential Triassic acidic pegmatites, whereas structurally separated thick Triassic sedimentary cover successions lack any magmatism, likely excluding the present-day eclogite-bearing units as Triassic basement of the sedimentary cover successions.

The now eclogite-bearing piece of continental crust adjacent to the Meliata oceanic lithosphere subducted during Early Cretaceous times to mantle depth. The subducted continental crust was then exhumed incorporating even ultramafic mantle rocks. During exhumation and decompression of mafic rocks, partial melting took place forming the trondhjemite dike in Late Cretaceous times. **Keyword**: In-situ trace elements; Elemental mapping; C-H-O isotopes; Mineralization processes; Baguamiao gold deposit; East Paleo-Tethys Ocean

References

Haüy, R. J. 1822, Trait & de mineralogie, 2nd, ed., Bachelier.

Thoni, M., Jagoutz, E. 1993. Isotopic constraints for Eo-alpine High-P metamorphism in the Austroalpine nappes of the Eastern Alps-bearing on alpine orogenesis. Schweizerische Mineralogische Und Petrographische Mitteilungen 73(2),177-189.

Miller, C., Thoni, M. 1997. Eo-Alpine eclogitisation of Permian MORB-type gabbros in the Koralpe (Eastern Alps, Austria): New geochronological, geochemical and petrological data. Chemical Geology 137(3-4), 283-310.

Correlation and comparison of Paleozoic oceans in NE and NW Gondwana

Wei Dan [1, 2,*], Qiang Wang [1, 2], Xiu-Zheng Zhang [1, 2], Gong-Jian Tang [1, 2]

[1]State Key Laboratory of Isotope Geochemistry, Guangzhou Institute of Geochemistry, Chinese Academy of Sciences, Guangzhou 510640, China
[2]CAS Center for Excellence in Deep Earth Science, Guangzhou, 510640, China
[*]E-mail: danwei@gig.ac.cn

Several Paleozoic oceans with local names in NW Gondwana and NE Gondwana complicate the correlation and comparison of these Paleozoic oceans, which have important implications for the Paleozoic tectonic evolution and paleogeography of northern Gondwana. The two major Paleozoic oceans in NW Gondwana are the Iapetus and Rheic oceans. The Iapetus Ocean opened by the separation of three large continents (Laurentia, Baltica and Gondwana) coincided with ca. 620-550 Ma large igneous province (LIP), and the Rheic Ocean initiated as a backarc basin by the subduction of the Iapetus Ocean beneath Gondwana at ca. 500-490 Ma. The Iapetus Ocean closed by the subduction of both margins, and as a result of the collision of the Larentia and Baltica and peri-Gondwana terranes during the Silurian. Closure of the Rheic Ocean occurred by northward subduction and by collision of Laurussia and Gondwana in the Carboniferous. In contrast, there are three major Paleozoic oceans (Proto-Tethys, Proto-Qiangtang and Paleo-Tethys) in NE Gondwana. The Proto-Tethys Ocean initiated by the separation of Tarim and North China from Gondwana in the late Neo-Proterozoic (ca. 630-580 Ma), and the recently identified Proto-Qiangtang Ocean formed probably as a backarc basin of the Proto-Tethys Ocean, combined with a ca. 510 mantle plume contribution, by the separation of peri-Gondwana terranes from Gondwana at ca. 510-500 Ma. The Proto-Tethys Ocean underwent both margins of subduction and closed by collision of the peri-Gondwana terranes with Tarim and North China in Silurian. The Proto-Qiangtang Ocean closed by northward subduction during the Late Ordovician-Silurian. The Paleo-Tethys Ocean initiated in the Silurian and has been opened in the Early Devonian from the Middle East to East Asia. It underwent northward subduction beginning in the Middle Devonian and closed by the accretion of Cimmerian terranes in the Late Triassic. Therefore, the remarkably analogous evolution of the Proto-Tethys Ocean with the Iapetus led to that them can be viewed as a unified ocean framing north Gondwana. The initiation of the Rheic and Proto-Qiangtang oceans is similar in both timing and geodynamics, thus, they can also be considered as a unified ocean. The western extension of the Paleo-Tethys in Europe is highly controversial but is likely a small ocean south of the Rheic Ocean. The latter two ocean systems closed in different times between NW Gondwana and NE Gondwana are likely due to different continent sizes north of the associated oceans, which would result in different geodynamics in different parts.

International Association for Gondwana Research 2023 Convention and
20th International Conference on Gondwana to Asia
Niigata, Japan, October 2023
Abstract Volume

Post-peak fluid-induced metamorphic microstructures and the P-T conditions from Perlebandet, Sør Rondane Mountains, East Antarctica

Fumiko Higashino[1,*], Tetsuo Kawakami[1], Tatsuro Adachi[2], Masaoki Uno[3]

[1] Department of Geology and Mineralogy, Graduate School of Science, Kyoto University, Kitashirakawa-Oiwake-cho, Sakyo-ku, Kyoto 606-8502, Japan
[2] Division of Earth Sciences, Faculty of Social and Cultural Studies, Kyushu University, Fukuoka 819-0395, Japan
[3] Graduate School of Environmental Studies, Tohoku University, Sendai 980-8579, Japan
[*]E-mail: higashino.fumiko.2m@kyoto-u.ac.jp

Introduction

The Sør Rondane Mountains (SRM), East Antarctica is located in a key area of Gondwana formation where the East African Orogen and the Kuunga Orogen cross (e.g., Satish-Kumar et al., 2013 and references therein). The East African Orogen and the Kuunga Orogen are respectively considered to be a collision of east-west Gondwana at ca. 750-620 Ma and north-south Gondwana at ca. 570-530 Ma (Meert, 2003). In contrast, there are previous studies suggesting that the younger event is also included in the East African-Antarctic Orogeny (e.g., Jacobs and Thomas, 2004; Jacobs et al., 2015; Fitzsimons, 2016).

The SRM is divided into the Northeastern-terrane (NE-terrane) and the Southwestern-terrane (SW-terrane) by a mylonite zone termed the Main Tectonic Boundary (MTB) that dips gently to the north and the northeast (Osanai et al., 2013). Osanai et al. (2013) interpreted that the timings of peak metamorphism (650-600 Ma) and retrograde metamorphism under andalusite-stability field (590-530 Ma) are the same in the NE- and SW-terranes. Most of the previous U-Pb zircon dating to determine the timing of metamorphism in the SRM used separated zircon grains, and therefore, in situ U-Pb zircon dating that takes microstructural context into account has been limited (e.g., Higashino et al., 2013, 2015, 2023a; Kawakami et al., 2017). Additionally, a petrochronological approach that takes into account the distribution of rare earth elements (REE) between zircon and garnet is rare in the SRM (e.g., Hokada et al., 2013; Higashino et al., 2023a). Recently, Higashino et al. (2023a) reported several different periods of garnet forming metamorphism at >600 Ma and <580 Ma both from the NE- and SW-terranes based on in situ U-Pb zircon dating and distribution of REE between zircon and garnet. Higashino et al. (2023a) implies that garnet grains overgrowing sillimanite from northern Perlebandet, which is ~ 10 km long nunataks in the western part of the SRM, do not have clear evidence that they were formed by regional metamorphism due to the lack of pressure shadows. This garnet is considered to have formed during prograde stage of counter-clockwise P-T path (Kawakami et al., 2017). Since igneous intrusion is not exposed in northern Perlebandet (Shiraishi et al., 1992), the effect of reheating by igneous intrusion has not been taken into account in previous studies in Perlebandet. In contrast, granodioritic bodies are widely distributed beneath the metamorphic rocks in southern Perlebandet (Shiraishi et al., 1992). Therefore, in order to evaluate the effect of igneous intrusion bodies, this study examines P-T path of pelitic gneiss and massive Hbl-Bt granodiorite from southern Perlebandet.

Sample description of pelitic gneiss

The studied sample is Grt-Sil-Bt gneiss whose gneissose structure is cut by ~ 1 mm-thick biotite-bearing selvage. The selvage is mainly composed of Cl-rich biotite (~ 0.7 wt% Cl) and andalusite is exclusively present within the selvage. In the wall rock, garnet is commonly rimmed by cordierite-biotite intergrowth at the margin. Cordierite is present in the intergrowth texture and multi solid inclusion in garnet which is characterized by decrepitated texture. The intergrowth is cut by the biotite-bearing selvage. Within the intergrowth, biotite has ~ 0.2-0.3 wt% Cl, and CO2 and H2O peaks were detected in cordierite by Raman spectroscopy. This suggests that CO2-Cl-H2O fluid infiltration caused the biotite-cordierite intergrowth formation. K-feldspar in the matrix partly has perthitic texture. Detailed descriptions are given in Higashino et al. (2023b).

P-T estimation

Peak P-T conditions of the pelitic gneiss were estimated to be ~800-900 °C, 0.8-1.1 GPa under the sillimanite stability field, using GASP geobarometer (Holdaway, 2001) and

ternary feldspar thermometry (Fuhrman and Lindsley, 1988; Kroll et al., 1993; Benisek et al., 2004, 2010). In order to estimate P-T conditions of the cordierite-biotite intergrowth formation following the peak P-T conditions, the garnet-biotite geothermometer (Holdaway, 2000), the GASP geobarometer (Holdaway, 2001) and the GBPQ geobarometer (Wu et al., 2004) were applied to the composition of garnet rim, biotite and plagioclase present in the intergrowth. This resulted in ~ 590-645 °C, ~ 0.24-0.35 GPa. In addition, biotite-bearing selvage-forming temperature was estimated to be ~ 490 °C under the pressure of andalusite stability field using two-feldspar thermometry (Benisek et al., 2004, 2010). This suggests that Cl-bearing aqueous fluid infiltrated through a thin crack at ~ 490 °C. These P-T conditions imply a clockwise P-T path, which is inconsistent with the one from northern Perlebandet (cf. Kawakami et al., 2017).

Solidification P-T conditions of massive Hbl-Bt granodiorite were estimated using the Al-in-hornblende geobarometer of Mutch et al. (2016) and amphibole-plagioclase geothermometer of Holland and Blundy (1994). This resulted in ~ 650-670 °C and ~ 0.34-0.43 GPa, plotted on the H_2O-saturated haplogranite solidus within error.

Discussion

The metamorphic P-T conditions recorded in the matrix mineral assemblage are similar to the peak P-T conditions reported from northern Perlebandet, whereas P-T conditions for garnet breakdown reaction are different (cf. Kawakami et al., 2017). Since the solidification P-T conditions are consistent with that of cordierite-biotite intergrowth formation, the garnet breakdown reaction was possibly triggered by the fluid infiltration originated from the intruded granodiorite. The inconsistence of cooling histories in southern and northern Perlebandet suggests the following two possibilities: (i) Existence of tectonic boundary between southern and northern Perlebandet or (ii) Contact metamorphism occurred following the counter-clockwise P-T path. There is little supporting evidence for the existence of a tectonic boundary between northern and southern nunataks so far. Therefore, the latter possibility would be preferred.

The solidification P-T conditions of the granodiorite were slightly lower than that of garnet formation in Kawakami et al. (2017). This does not support that the garnet was formed by contact metamorphism of hidden igneous body in northern Perlebandet. In order to understand the tectonic evolution at the final stage of Gondwana amalgamation, however, effect of hidden igneous rocks needs to be taken into consideration.

References

Benisek, A., Kroll, H. and Cemic, L. 2004. New developments in two-feldspar thermometry. American Mineralogist, 89, 1496-1504.

Benisek, A., Dachs, E. and Kroll, H. 2010. A ternary feldspar-mixing model based on calorimetric data: development and application. Contributions to Mineralogy and Petrology, 160, 327-337.

Fitzsimons, I. C., 2016. Pan–African granulites of Madagascar and southern India: Gondwana assembly and parallels with modern Tibet. Journal of Mineralogical and Petrological Sciences, 111(2), 73-88.

Fuhrman, M.L. and Lindsley, D.H. 1988. Ternary-feldspar modeling and thermometry. American Mineralogist, 73, 201-215.

Higashino, F., Kawakami, T., M. Satish-Kumar, Ishikawa, M., Maki, K., Tsuchiya, N., Grantham, G.H., Hirata, T., 2013. Chlorine-rich fluid or melt activity during granulite facies metamorphism in the Late Proterozoic to Cambrian continental collision zone- An example from the Sør Rondane Mountains, East Antarctica. Precambrian Research 234, 229-246.

Higashino, F., Kawakami, T., Tsuchiya, N., Satish-Kumar, M., Ishikawa, M., Grantham, G.H., Sakata, S., Hattori, K., Hirata, T., 2015. Geochemical behavior of zirconium during Cl-rich fluid or melt infiltration under upper amphibolite facies metamorphism – A case study from Brattnipene, Sør Rondane Mountains, East Antarctica. Journal of Mineralogical and Petrological Sciences 110, 166-178.

Higashino, F., Kawakami, T., Sakata, S., & Hirata, T. 2023a. Multiple timings of garnet-forming high-grade metamorphism in the Neoproterozoic continental collision zone revealed by petrochronology in the Sør Rondane Mountains, East Antarctica. Gondwana Research, 119, 204-226.

Higashino, F., Kawakami, T., Adachi, T., & Uno, M. 2023b. Multiple post-peak metamorphic fluid infiltrations in southern Perlebandet, Sør Rondane Mountains, East Antarctica. Journal of Mineralogical and Petrological Sciences, 118(ANTARCTICA), 230131a.

Hokada, T., Horie, K., Adachi, T., Osanai, Y., Nakano, N., Baba, S., Toyoshima, T., 2013. Unraveling the metamorphic history at the crossing of Neoproterozoic orogens, Sør Rondane Mountains, East Antarctica: Constraints from U-Th-Pb geochronology, petrography, and REE geochemistry. Precambrian Research 234, 183-209.

Holdaway, M.J. 2000. Application of new experimental and garnet Margules data to the garnet-biotite geothermometer. American mineralogist, 85, 881-892.

Holdaway, M.J. 2001. Recalibration of the GASP

geobarometer in light of recent garnet and plagioclase activity models and versions of the garnet-biotite geothermometer. American Mineralogist, 86, 1117-1129.

Holland, T. and Blundy, J. 1994. Non-ideal interactions in calcic amphiboles and their bearing on amphibole-plagioclase thermometry. Contributions to Mineralogy and Petrology, 116, 433–447.

Jacobs, J., Thomas, R. J., 2004. Himalayan-type indenter-escape tectonics model for the southern part of the late Neoproterozoic–early Paleozoic East African–Antarctic orogen. Geology, 32(8), 721-724.

Jacobs, J., Elburg, M., Läufer, A., Kleinhanns, I. C., Henjes-Kunst, F., Estrada, S., Ruppel, A. S., Damaske, D., Montero, P., Bea, F., 2015. Two distinct late Mesoproterozoic/early Neoproterozoic basement provinces in central/eastern Dronning Maud Land, East Antarctica: The missing link, 15–21 E. Precambrian Research, 265, 249-272.

Kawakami, T., Higashino, F., Skrzypek, E., Satish-Kumar, M., Grantham, G., Tsuchiya, N., Ishikawa, M., Sakata, S., Hirata, T., 2017. Prograde infiltration of Cl-rich fluid into the granulitic continental crust from a collision zone in East Antarctica (Perlebandet, Sør Rondane Mountains). Lithos 274-275, 73-92.

Kroll, H., Evangelakakis, C. and Voll, G. 1993. Two-feldspar geothermometry: a review and revision for slowly cooled rocks. Contributions to Mineralogy and petrology, 114, 510-518.

Meert, J., 2003. A synopsis of events related to the assembly of eastern Gondwana. Tectonophysics, 362, 1-40.

Mutch, E.J.F., Blundy, J.D., Tattitch, B.C., Cooper, F.J. and Brooker, R.A. 2016. An experimental study of amphibole stability in low-pressure granitic magmas and a revised Al-in-hornblende geobarometer. Contributions to Mineralogy and Petrology, 171, 1-27.

Osanai, Y., Nogi, Y., Baba, S., Nakano, N., Adachi, T., Hokada, T., Toyoshima, T., Owada, M., Satish-Kumar, M., Kamei, A., Kitano, I., 2013. Geologic evolution of the Sør Rondane Mountains, East Antarctica: Collision tectonics proposed based on metamorphic processes and magnetic anomalies. Precambrian Research, 234, 8-29.

Satish-Kumar, M., Hokada, T., Owada, M., Osanai, Y., Shiraishi, K., 2013. Neoproterozoic orogens amalgamating East Gondwana: Did they cross each other?. Precambrian Research 234, 1-7.

Shiraishi, K., Osanai, Y., Tainosho, Y., Takahashi, Y., Tsuchiya, N., Kojima, S., Yanai, K., Moriwaki, K. 1992. Geological map of Widerøefjellet. Antarctic Geological Map Series, sheet 32, scale 1:100,000, National Institute of Polar Research, Tokyo.

Wu, C.M., Zhang, J. and Ren, L.D. 2004. Empirical garnet–biotite–plagioclase–quartz (GBPQ) geobarometry in medium-to high-grade metapelites. Journal of Petrology, 45, 1907-1921.

Neoproterozoic to Cambrian granitoids of northern Mozambique and Dronning Maud Land Antarctica: Implications for the assembly of Gondwana

G.H. Grantham[1,2,*], P.H. Macey[2,3], M.P. Roberts[4], B.A. Ingram[2], R.A. Armstrong[5], K. Shiraishi[6], T. Hokada[6], B. Eglington[7], P. le Roux[3] and G. Cune[8]

[1]Department of Geology, University of Johannesburg, P.O. Box 524, Auckland Park 2006
[2]Council for Geoscience, South Africa
[3]Department of Geological Sciences, University of Cape Town, Rondebosch, South Africa, 7700.
[4]University of Western Australia, Perth, Western Australia, Australia.
[5]RSES, Australian National, University, Canberra, ACT, Australia
[6]NIPR, Tachikawa, Tokyo, Japan,
[7]University of Saskatchewan, Saskatoon, Canada.
[8]National Directorate of Geology, Tete, Mozambique
[*]E-mail: ghgrantham@uj.ac.za

The field relationships, petrography, whole rock major and trace element chemistry and radiogenic isotope chemistry and geochronology of Cambrian Granites from the Nampula Terrane (NT), northern Mozambique are reported. The whole rock major and trace element data are compared with published data from Neoproterozoic to Cambrian granites from Central Dronning Land (CDML). Age comparisons include data from CDML as well as the Cabo Delgado/Namuno Terrane of northern Mozambique (CDNMT).

Whereas there is significant overlap in the chemistry and ages of the granites from the Nampula Terrane compared to those from CDML and CDNMT, indicating their probable genesis within the same broad orogenic event, subtle differences in mineralogy, chemistry and age are seen. These differences include subsolvus peraluminous mica-dominated granites with ages <~530 Ma in all three areas but concentrated in the Nampula Terrane, in contrast to dominantly metaluminous hypersolvus charnockitic syenogranites with ages >~530 Ma in CDML and CDTNM but absent from the Nampula Terrane (Mozambique) and western Sverdrupfjella (western Dronning Maud Land, Antarctica).

The differences between the two granite varieties are inferred to reflect differences in tectonic setting during genesis with the marginally older CDML and CDTNM granites/charnockites resulting from decompression dehydration melting dominantly of amphibole in an extensional setting in the hanging wall of a mega-nappe. The timing and P-T genesis of the marginally older CDML and CDTNM granites/charnockites are consistant with isothermal decompression paths recognised in country rocks hosting the intrusions.

In contrast the marginally younger NT granites were generated from dehydration melting of mica in the footwall of the mega-nappe structure. The dehydration partial melting and metamorphism in the footwall requires rapid burial of the Nampula Terrane post deposition of the intra-orogenic Mecuburi Group at ca. 530 Ma.

Pseudosection modelling of the Murrupula Suite suggest P-T conditions of genesis of <6kb and temperatures of ~700 - 775oC, constrained by the absence of orthopyroxene. The presence of andalusite in one intrusion suggests pressures <2.5kb for that intrusion.

Pseudosection modelling of the CDML charnockites suggest P-T conditions of genesis of <8kb and temperatures of >825oC, constrained by the anhydrous charnockitic assemblages and the absence of garne

International Association for Gondwana Research 2023 Convention and
20th International Conference on Gondwana to Asia
Niigata, Japan, October 2023
Abstract Volume

Boron isotope compositions of coexisting kornerupine and tourmaline in high-grade metabasic rocks: an example from Akarui Point, Lützow-Holm Complex, East Antarctica

Tetsuo Kawakami[1,*], Simon Harley[2]

[1] Department of Geology and Mineralogy, Graduate School of Science, Kyoto University, Japan
[2] School of GeoSciences, The University of Edinburgh, UK
[*]E-mail: t-kawakami@kueps.kyoto-u.ac.jp

Boron is an incompatible element present in trace amount in mafic igneous rocks and altered oceanic crust (Leeman and Sisson, 1996). Unusual concentrations of B, such as tourmaline aggregates in metamorphic rocks, are therefore considered evidence for B–bearing fluid infiltration (e.g., Kawakami, 2001; Kawakami et al., 2008, 2019; Marschall et al., 2009). Tourmaline becomes unstable in granulite facies conditions depending on bulk composition of the host rock (Dutrow and Henry, 2011; Kawakami, 2001), and instead, kornerupine becomes stable in high–pressure (high–P) conditions above ~ 0.5 GPa (Grew, 1996; Robbins and Yoder, 1962; Werding and Schreyer, 1996). Accumulation of kornerupine can, therefore, be a tracer of B–bearing fluids under high–P conditions as well.

In this study, B isotope compositions were measured in kornerupine and tourmaline from lenses consisting primarily of kornerupine, plagioclase and corundum. The measurements were performed in situ by secondary ionization mass spectroscopy, and the results and discussions are briefly summarized below based on Kawakami and Harley (2023). The kornerupine-bearing lenses occur within hornblende–gneiss or along the boundary between this gneiss and an amphibolite lens at Akarui Point in the Lützow–Holm Complex, Prince Olav Coast, East Antarctica (Kawakami et al., 2008). The peak metamorphic conditions of the Akarui Point have been estimated to be ~ 800–900 °C and ~ 8–11 kbar (Iwamura et al., 2013; Kawakami et al., 2008; Nakamura et al., 2014; Suzuki and Kawakami, 2019). The δ11B compositions of kornerupine, which is interpreted to have been a stable phase at the metamorphic peak, are −11.6 ± 0.4 to −7.8 ± 0.5‰ and −9.8 ± 0.3 to −6.1 ± 0.2‰ in two different samples. Prograde tourmaline grains included in kornerupine and corundum yielded δ11B = −2.1 ± 0.3 to +0.6 ± 0.3‰, and the secondary tourmaline replacing kornerupine yielded δ11B = −4.6 ± 0.2 to −3.7 ± 0.2‰. Therefore, the isotopic fractionation between kornerupine and tourmaline, Δ11BTur–Krn (= δ11BTur − δ11BKrn), of the average prograde tourmaline and average host kornerupine is +6.7 ± 1.5‰. This value is interpreted to indicate isotopic equilibrium at the metamorphic peak on the basis of previous studies of isotope fractionation between tourmaline and minerals of the kornerupine–prismatine series (Kowalski and Jahn, 2011; Kowalski et al., 2013; MacGregor et al., 2013). The δ11B values obtained on prograde tourmaline are between whole rock δ11B of MORB and mantle rocks and of some sedimentary rocks, and are similar to the δ11B of blackwall tourmalines that crystallized during the decompression stage following high–pressure metamorphism (e.g., Kawakami and Harley, 2023; Marschall et al., 2009). Therefore, we infer that the syn–metamorphic B–bearing fluid present in the kornerupine–plagioclase–corundum lens is likely sourced from a mixture of sedimentary, mafic and ultramafic lithologies in a subduction setting. A boundary between positive and negative magnetic anomalies is indicated near Akarui Point in the reduced to the pole magnetic anomaly map of the LHC (Nogi et al., 2013), which would be consistent with the presence of small tectonic discontinuity. The metabasic and meta–ultramafic lenses found in Akarui Point could be interpreted as the remnant of mixing zone of Ediacaran to Cambrian subduction channel (Kawakami and Harley, 2023).

References

Dutrow, B. L., & Henry, D. J. (2011). Tourmaline: A geologic DVD. Elements, 7(5), 301–306. https://doi.org/10.2113/gselements.7.5.301

Grew, E.S. (1996) Borosilicates (exclusive of tourmaline) and Boron in rock–forming minerals in metamorphic environments. Reviews in Mineralogy, 33, 387–502. (Additions were made in 2002.)

Iwamura, S., Tsunogae, T., Kato, M., Koizumi, T., & Dunkley, D. J. (2013). Petrology and phase equilibrium modeling of spinel-sapphirine bearing mafic granulite from Akarui point, Lützow-Holm Complex, East Antarctica: Implications for the P-T path. Journal of Mineralogical and Petrological Sciences, 108(6), 345–350. https://doi.org/10.2465/jmps.130621a

Kawakami, T. (2001). Tourmaline breakdown in the migmatite zone of the Ryoke metamorphic belt, SW Japan. Journal of Metamorphic Geology, 19(1), 61–75.

https://doi.org/10.1046/j.0263-4929.2000.00298.x

Kawakami, T., Grew, E. S., Motoyoshi, Y., Shearer, C. K., Ikeda, T., Burger, P. V., & Kusachi, I. (2008). Kornerupine sensu stricto associated with mafic and ultramafic rocks in the Lützow-Holm Complex at Akarui Point, East Antarctica: What is the source of boron? In Geological Society Special Publication (Vol. 308). https://doi.org/10.1144/SP308.17

Kawakami, T., & Harley, S.L. (2023). Boron isotope compositions of coexisting kornerupine and tourmaline in high – grade metabasic rocks: an example from Akarui Point, Lützow – Holm Complex, East Antarctica. https://doi.org/10.2465/jmps.230131b

Kawakami, T., Sakai, H., & Sato, K. (2019). Syn-metamorphic B-bearing fluid infiltrations deduced from tourmaline in the Main Central Thrust zone, Eastern Nepal Himalayas. Lithos, 348–349, 105175. https://doi.org/10.1016/j.lithos.2019.105175

Kowalski, P.M. and Jahn, S. (2011) Prediction of equilibrium Li isotope fractionation between minerals and aqueous solutions at high P and T: an efficient ab initio approach. Geochimica et Cosmochimica Acta, 75, 6112–6123.

Kowalski, P.M., Wunder, B. and Jahn, S. (2013) Ab initio prediction of equilibrium boron isotope fractionation between minerals and aqueous fluids at high P and T. Geochimica et Cosmochimica Acta, 101, 285–301.

MacGregor, J. R., Grew, E. S., De Hoog, J. C. M., Harley, S. L., Kowalski, P. M., Yates, M. G., & Carson, C. J. (2013). Boron isotopic composition of tourmaline, prismatine, and grandidierite from granulite facies paragneisses in the Larsemann Hills, Prydz Bay, East Antarctica: Evidence for a non-marine evaporite source. Geochimica et Cosmochimica Acta, 123, 261–283. https://doi.org/10.1016/j.gca.2013.05.030

Marschall, H. R., Korsakov, A. V., Luvizotto, G. L., Nasdala, L., & Ludwig, T. (2009). On the occurrence and boron isotopic composition of tourmaline in (ultra)high-pressure metamorphic rocks. Journal of the Geological Society, 166(4), 811–823. https://doi.org/10.1144/0016-76492008-042

Nakamura, A., Kitamura, M., & Kawakami, T. (2014). Microstructural records of multiple retrograde local H2O supplement in the pelitic gneiss, Lützow-Holm Complex at Akarui Point, East Antarctica. Mineralogy and Petrology, 108(2), 177–186. https://doi.org/10.1007/s00710-013-0300-8

Nogi, Y., Jokat, W., Kitada, K., & Steinhage, D. (2013). Geological structures inferred from airborne geophysical surveys around Lützow-Holm Bay, East Antarctica. Precambrian Research, 234, 279–287. https://doi.org/10.1016/j.precamres.2013.02.008

Robbins, C.R. and Yoder, H.S. Jr. (1962) Stability relations of dravite, a tourmaline. Carnegie Institution Washington Yearbook, 61, 106–107.

Suzuki, K., & Kawakami, T. (2019). Metamorphic pressure-temperature conditions of the Lützow-Holm Complex of East Antarctica deduced from Zr-in-rutile geothermometer and Al2SiO5 minerals enclosed in garnet. Journal of Mineralogical and Petrological Sciences, 114(6), 267–279. https://doi.org/10.2465/jmps.190801

Werding, G. and Schreyer, W. (1996) Experimental studies on borosilicates and selected borates. In Boron: Mineralogy, Petrology and Geochemistry (Anovitz, L.M. and Grew, E.S. Eds.). Mineralogical Society of America, Reviews in Mineralogy, 33, 117–163.

Neoproterozoic tectonic evolution and proto-basin of the Yangtze Block, China

Yunpeng Dong[1,2,*], Bo Hui[1], Shengsi Sun[1], Dengfeng He[1], Jiaopeng Sun[1], Feifei Zhang[1], Chao Cheng[1], Zhao Yang[1], Xiaohui Shi[1], Rutao Zang[1], Xiaoping Long[1]

[1]State Key Laboratory of Continental Dynamics, Department of Geology, Northwest University, Northern Taibai Str. 229, Xi'an 710069, China
[2]Collaborative Innovation Centre of Continental Tectonics, Northwest University, Northern Taibai Str. 229, Xi'an 710069, China
[*]E-mail: dongyp@nwu.edu.cn

The Neoproterozoic assembly and break-up of the supercontinent Rodinia had significant impacts on the global tectonic framework, affecting the configuration of oceans and continents. These processes also led to active tectonic activities and basin fillings, ultimately influencing Earth's habitability. The Yangtze Block contains abundant Neoproterozoic magmatic rocks along its edges and sedimentary successions within its inner shield. These geological features provide valuable insights into the tectonic evolution of Rodinia. Based on available geological, geochemical, and geochronological data, it is suggested that during the late Mesoproterozoic (around 1.17–1.02 Ma), the landmasses of Rodinia were surrounded by the Pan-ocean on the exterior and separated by interior oceans. The Yangtze Block occupied the northwest edge of Rodinia, facing the exterior ocean to the north and west. It underwent a Neoproterozoic co-evolution characterized by the coupling of inner basins and the formation of three marginal orogens. The Jiangnan Orogen in the east formed through prolonged subduction-collision between the Yangtze and Cathaysia Blocks from approximately 1000 to 820 Ma. This orogen represents an interior orogenic event corresponding to the assembly of Rodinia. In comparison, the Longmen-Kangdian Orogen was an Andes-type subduction orogen along the western active continental margin during ca. 870–720 Ma, while the South Qinling Orogen was a wide accretionary orogen to the north of the nucleus of the Yangtze Block during ca. 880–720 Ma. Both the Longmen-Kangdian Orogen and the South Qinling Orogen were exterior orogens of Rodinia. Subductions along the outer edges of Rodinia, specifically along the western and northern parts of the Yangtze Block, occurred synchronously with the assembly of Rodinia from around 880 to 820 Ma. However, continuous exterior subductions during approximately 820–720 Ma might coincide with the breakup of Rodinia. These different spatiotemporal patterns of sedimentary fillings and the evolution of the inner Yangtze Basin were controlled by the Neoproterozoic tectonic processes of the three orogens. During ca. 1000–880 Ma, the exterior ocean underwent extension, resulting in passive continental marginal deposition. Simultaneously, the Paleo-South China interior oceanic slab subducted beneath the eastern part of the Yangtze Block, leading to the formation of an arc-related continental marginal basin. From approximately 880 to 820 Ma, the westward interior subduction-collision closed the Paleo-South China interior ocean, causing the collision between the Yangtze and Cathaysia Blocks around 820 Ma. Subsequently, the southward and eastward exterior subductions from around 820 to 720 Ma resulted in the formation of a wide accretionary continental marginal orogen in the South Qinling Belt, as well as an Andean-type active continental arc along the Longmen-Kangdian Belt. The continuous exterior subduction along the western and northern parts of the Yangtze Block, coupled with the collapse of the Jiangnan Orogen, led to interior rifting in the inner Yangtze Basin, which was subsequently filled with thick layers of rift-related sediments. Between ca. 720 and 635 Ma, the western part of the Yangtze Block transitioned into a westward-deepening passive continental margin, while the eastern part remained in rift basins. Most of the Yangtze Block then evolved into an extensional tectonic setting, characterized by widespread deposits from glacial and interglacial periods. Subsequently, the entire Yangtze Block transformed into a depressional basin filled with shallow marine or bathyal-abysmal facies clastic and carbonate successions during the Ediacaran and Cambrian

International Association for Gondwana Research 2023 Convention and
20th International Conference on Gondwana to Asia
Niigata, Japan, October 2023
Abstract Volume

India and South China in the Tonian: New Constraints from the Harohalli Alkaline Province

Joseph G Meert[1,*], S. Raghuvanshi[2], N.V. Chalapathi Rao[2], D. Talukdar[1,2], B. Belyatsky[3], P. Prabhat[4], W. Rahaman[4], B. Lehmann[5]

[1]Neil Opdyke Paleomagnetic Laboratory, Department of Geological Sciences, University of Florida, 241 Williamson Hall, Gainesville, FL 32611
[2]Mantle Petrology Laboratory, Department of Geology, Institute of Science, Banaras Hindu University, Varanasi 221005, India
[3]HR-SIMS Lab, 40 Dharitri Building. Geological Survey of India, Sector V, Salt Lake, Kolkata 700091
[4]National Centre for Polar and Ocean Research, Ministry of Earth Sciences, Headland Sada, Vasco da Gama, Goa 403804, India
[5]Mineral Resources, Technical University of Clausthal, Adolph-Roemer-Straße 2A, 38678, Clausthal-Zellerfeld, Germany
*E-mail: jmeert@ufl.edu

The position of India in the supercontinents of Rodinia and Columbia is enigmatic. Most models relegate Peninsular India to the margins of these supercontinents (Meert and Santosh, 2022). This is due, at least in part, to limited paleomagnetic data. For example, a recent compilation of reliable paleomagnetic data from India lists only two poles for the Columbia interval (~1.8-1.4 Ga) and single poles for the assembly of Rodinia (~1.1 Ga) and breakup (~770 Ma) (Meert et al., 2021). India has traditionally been placed at the margin of Rodinia. In many reconstructions, it remains linked to the East Antarctic craton and Australia in an East Gondwana configuration (Li et al., 2008). Links between India and South China in the Rodinia supercontinent were based on stratigraphic similarities and isotopic/detrital zircon studies (Jiang et al., 2003; Wang et al., 2017). Other reconstructions place India and South China in proximity although separated from one another by another craton or micro-continents (see Li et al., 2008; Chang et al., 2022, Li et al., 2023 for example). India's location in these reconstructions relied on the ~770 Ma MIS suite pole (Torsvik et al., 2001; Gregory et al., 2008; Meert et al.,2013).

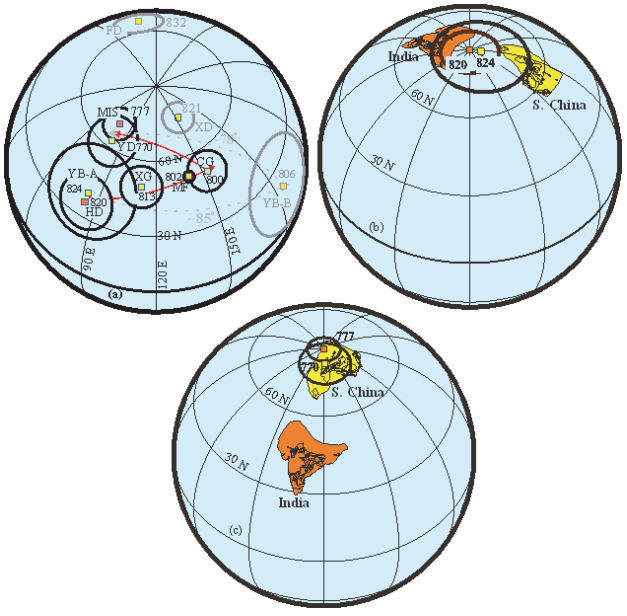

Figure 1: (a) Paleomagnetic poles from South China and India during the 824-770 Ma interval. (b) Reconstruction of India and South China at ~820 Ma; (c) Reconstruction of India and South China at ~770 Ma.

We recently reported a new U-Pb titanite age of 820 ± 15 Ma on a shoshonitic lamprophyre in the Harohalli alkaline province of the Dharwar craton (Raghuvanshi et al., 2023). This lamprophyre is part of a large region of alkaline intrusions which were previously studied for paleomagnetism (Dawson and Hargraves, 1994; Radhakrishna and Joseph, 1996; Pradhan et al., 2012). Rb-Sr and K-Ar ages were similar to our new U-Pb age, but Pradhan et al. (2012) obtained a much older U-Pb age from one of the dykes in this region. Because the dated dyke in the Pradhan et al. (2012) study did not yield paleomagnetic data, caution was urged in using the Harohalli dykes pole (HD) for reconstructions. We have reviewed the paleomagnetic data in those 3 studies and calculated an updated pole for the alkaline dykes at 36.1° N, 84.0° E (A95=11.3°, K=30). Coeval data from South China at 824 Ma (Yanbian Dykes-A=YA pole; Niu et al., 2016) and 770 Ma (Yangtze dykes=YD, Chang et al., 2022) can be used to reconstruct India and South China (Figure 1a-c). The fit between the two pairs of similar age poles from both cratons is excellent (HD-YA Bayes error=.482 and MIS-YD Bayes error=.384; Meert and Santosh, 2022).

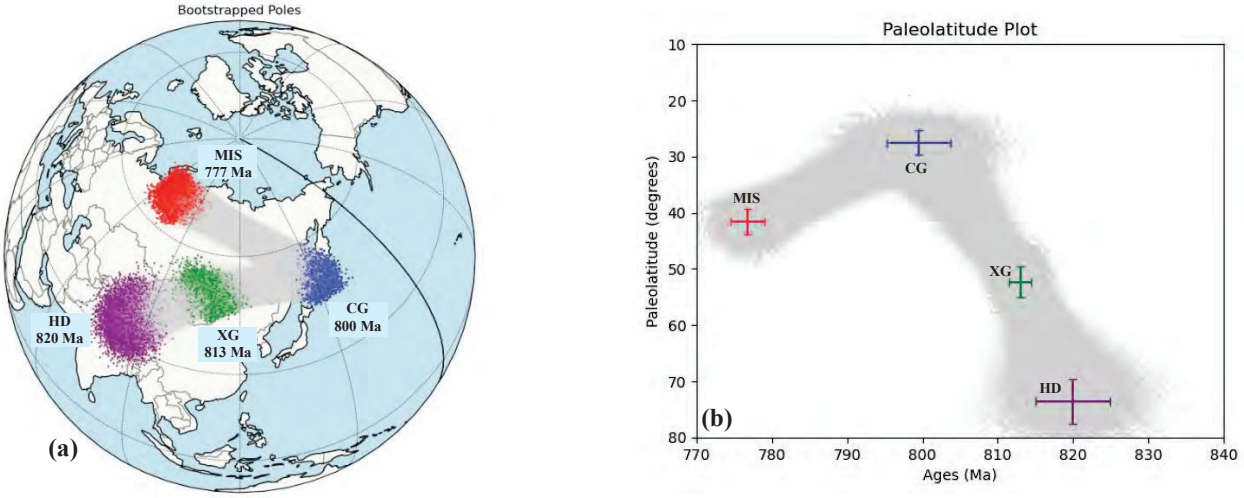

Figure 2: (a) Bootstrapped paleomagnetic mean poles for India and South China; (b) Paleolatitudinal plot based on bootstrapped mean poles.

If we assume that South China and India were fellow travelers during the 825-770 Ma, then we can use other poles from South China to evaluate the drift rate of both cratons.

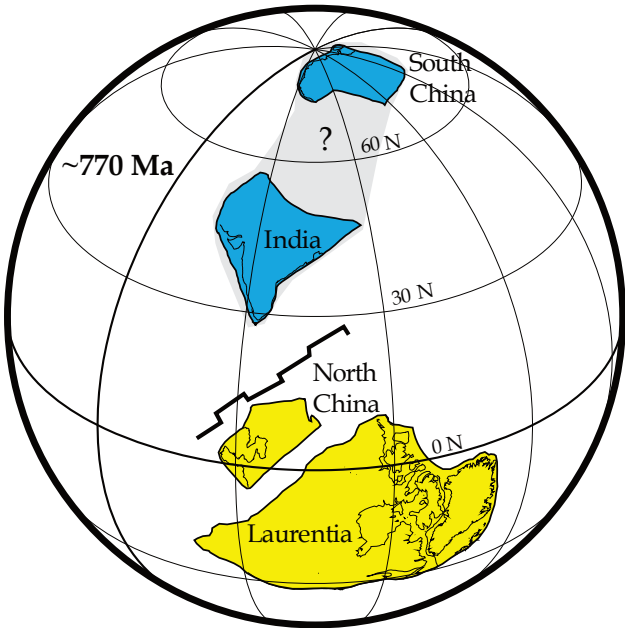

Figure 3: Reconstruction at 770 Ma based on paleomagnetic data from India, South China, North China and Laurentia.

We perform a bootstrap calculation for each of the poles and the calculated both apparent polar wander (APW) rates and latitudinal drift rates (Figures 2a-d). Rates of APW range from 20-36 cm/year indicating that true polar wander should be considered in addition to normal plate motion. We also examine paleomagnetic data from Laurentia during this same interval using data which would suggest a large separation between Laurentia and a combined India-South China and therefore disaggregation of Rodinia by 820 Ma (Figure 3).

References

Chang, L., Zhang, S., Li, H., Xian, H., Wu, H, Yang, T, 2022. New paleomagnetic insights into the Neoproterozoic connection between South China and India and their position in Rodinia, Geophysical Research Letters, 49, doi:101029/2022GL098348

Dawson, E.M. and Hargraves, R.B., 1994. Paleomagnetism of Precambrian dyke swarms in the Harohalli area, south of Bangalore, India. Precambrian Research, 69, 157-167.

Gregory, L.C., Meert, J.G., Bingen, B.H. Pandit, M.K. and Torsvik, T.H., 2009. Paleomagnetic and geochronologic study of Malani Igneous suite, NW India: implications for the configuration of Rodinia and the assembly of Gondwana, Precambrian Research, 170, 13-26.

Jiang, G., Sohl, L.E., Christie-Blick, N., 2003. Neoproterozoic stratigraphic comparison of the Lesser Himalaya (India) and the Yangtze Block (South China): paleogeographic implications, Geology, 31, 917-920.

Jing, X, Yang, Z., Evans, D.A.D, Tong, Y., Xu, Y., Wang, H., 2020. A pan-latitudinal Rodinia in the Tonian true polar wander frame, Earth and Planetary Science Letters, 530, doi:10.1016/j.epsl.2019.115880.

Li, Z-X, Zhang, L., Powell, C.McA., 1995. South China in Rodinia: part of the missing link between Australia-East Antarctica and Laurentia, Geology, 23, 407-410.

Li, Z.X., Bogdanova, S., Collins, A.S., Davidson, A., De

Waele, B., Ernst, R.E., Fitzsimons, I.C.W., Fuck, R.A., Gladkochub, D.P., Jacobs, J. and Karlstrom, K.E., 2008. Assembly, configuration, and break-up history of Rodinia: a synthesis. Precambrian research, 160, 179-210.

Li, Z.X., Liu, Y. and Ernst, R., 2023. A dynamic 2000–540 Ma Earth history: From cratonic amalgamation to the age of supercontinent cycle. Earth-Science Reviews, 238, doi:10.1016/j.earscirev.104336.

Maloof, A.C., Halverson, G.P., Kirschvink, J.L., Schrag, D.P., Weiss, B.P. and Hoffman, P.F., 2006. Combined paleomagnetic, isotopic, and stratigraphic evidence for true polar wander from the Neoproterozoic Akademikerbreen Group, Svalbard, Norway. Geological Society of America Bulletin, 118, 1099-1124.

Meert, J.G., 2014. Strange Attractors, Spiritual Interlopers and Lonely Wanderers: The Search for Pre-Pangæan Supercontinents. Geoscience Frontiers, 5, 155-166.

Meert, J.G., Pivarunas, A.K., Miller, S.R., Nutter, R.F., Pandit, M.K., Sinha, A.K., 2021. The Precambrian drift history and paleogeography of India, in: Pesonen et al.(eds) Ancient Supercontinent and the Paleogeography of the Earth, Elsevier, ISBN: 978-0-12-818533-9.

Meert, J.G., Pivarunas, A.F., Evans, D.A., Pisarevsky, S.A., Pesonen, L.J., Li, Z.X., Elming, S.Å., Miller, S.R., Zhang, S. and Salminen, J.M., 2020. The magnificent seven: a proposal for modest revision of the quality index. Tectonophysics, 790, doi:10.1016/j.tecto.2020.228549.

Niu, J., Li, Z-X., Zhu, W., 2016. Paleomagnetism and geochronology of mid-Neoproterozoic Yanbian dykes, South China: implications for a 820-800 Ma true polar wander event and the reconstruction of Rodinia, Geological Society of London Special Publication 424, doi:10,1144SP424.11.

Park, Y., Swanson-Hysell, N.L., Xian, H., Zhang, S., Condon, D.J., MacDonald, F., 2021. A consistently high-latitude South China from 820-780 Ma: Implications for exclusion from Rodinia and the feasibility of large scale true polar wander, Journal of Geophysical Research, 126, doi:10.1029/2020.JB021541.

Radhakrishna, T. and Mathew, J., 1996. Late Precambrian (850-800 Ma) paleomagnetic pole for the south Indian shield from Harohalli alkaline dykes: geotectonic implications for Gondwana reconstructions, Precambrian Research, 80, 77-87.

Torsvik, T.H., Carter, L.M., Ashwal, L.D., Bhushan, S.K., Pandit, M.K. and Jamtveit, B., 2001. Rodinia refined or obscured: palaeomagnetism of the Malani igneous suite (NW India). Precambrian Research, 108, 319-333.

Wang, W., Cawood, P.A., Zhou, M-F., Pandit, M.K., Xian, X-P, Zhao, J-H., 2017. Low δ18O rhyolites from the Malani igneous suite: A positive test for South China and NW India, Geophysical Research Letters, 44, 10,295-10,305.

Xian, H., Zhang, S., Li, H., Xian, H., Wu, H., Yang, J., 2020. Geochronological and paleomagnetic investigation of the Madiyi Formation, lower Banxi Group, South China: Implications for Rodinia reconstructions, Precambrian Research, 326, doi:10.1016/j.precamres.2019.105494.

International Association for Gondwana Research 2023 Convention and
20th International Conference on Gondwana to Asia
Niigata, Japan, October 2023
Abstract Volume

Intra-plate oceanic island basalts: from formation to accretion

Inna Safonova[1,*], M. Santosh[2]

[1]South-West Jiaotong University, FGEE, Chengdu 610031, Sichuan, China
[2] School of Earth Sciences and Resources, China University of Geosciences Beijing, China
E-mail: inna03-64@mail.ru

Oceanic islands/seamounts/plateaus form by dominantly basaltic magmatism in oceanic intra-plate environments and travel together with the subducting oceanic lithosphere towards the trench to be later accreted to Pacific-type (P-type) convergent margins, i.e., island arcs or active continental margins, and incorporated into accretionary complex (AC) or subducted into the mantle. Worldwide, oceanic rises occur as fragments within accretionary complexes that include oceanic lithosphere fragments, terrigeneous trench sediments, fore-arc flysch, oceanward olistostrome, and tectonic or serpentinite mélanges and record the history of former oceans (Safonova and Santosh, 2014). Magmatism producing oceanic islands is widely believed to be related to mantle plumes, which are imaged as columns of heated material ascending from the core-mantle boundary or mantle transition zone (e.g., Hofmann, 1997). Oceanic islands are parts of Oceanic Plate Stratigraphy or OPS (e.g., Kusky et al., 2013), which represents a regular succession of igneous and sedimentary rocks of the oceanic lithosphere. The OPS includes sedimentary and volcanic rocks that were deposited and erupted, respectively, on the igneous rocks of the underlying oceanic basement.

Oceanic intra-plate magmatism of oceanic islands, seamounts, and plateaus typically produce basaltic lavas characterized by increased TiO2, Nb, and LREE. Those are typically referred to as OIBs or OIB-type rocks when stressing both their intraplate origin and the specific composition. Recognizing OIB-type lavas as elements of OPS is important (i) for reconstructing the evolution of paleo-oceans and the formation of accretion or Pacific-type orogens, (ii) for geological mapping of structurally complicated orogenic belts and (iii) for petrogenetic implications (e.g., Safonova et al., 2009, 2011; Maruyama and Safonova, 2019). According to geochemical modeling made for OIB-type basalts from several accretionary complexes in central and east Asia (Safonova, 2020), the variations in the concentrations of REE and Nb in intraplate oceanic basalts are due to the changes of the composition and melting depths of mantle sources from spinel to garnet peridotites at decreasing degree of melting from 5-15 to 3-0.1%. The stable parameters of the genesis of OIB-type melts reflect similar PT-parameters and composition of the mantle during the late Precambrian - late Phanerozoic.

Oceanic OIB-type lavas are specified by variable compositions of both major oxides and incompatible elements, i.e., by different conditions of partial melting of the source mantle during generation of basaltic melts. The mantle plume columns beneath oceanic hot spots generating OIB-type basalts may be highly heterogeneous and consist of refractory upper mantle material depleted in incompatible elements and enriched segments, that not only have higher contents of incompatible elements, but are less refractory and thus melt easier/faster than the surrounding refractory mantle. Under young/thin oceanic lithosphere, the melting column is higher and consequently the degree of melting is higher, so that more refractory upper mantle material is involved into the melting. Under older/thick lithosphere, the melting column would be shorter, and a heterogeneous mantle source could produce basaltic melts more enriched in incompatible elements due to lower degree melting. Therefore, the geochemical variability of OIB-type lavas may be used a as a key for geological servey in poorly exposed regions at objective having highly complicated geological strictures, like accretionary complexes consisting of numerous tectonic sheets, piled over each other and commonly forming duplex structures, which all disturb or conceal the original succession of rock deposition and the relationships between rock units.

Recently, it has been found that oceanic island while approaching subduction zone actively interact with an active margin through destruction of accretionary prism (von Huene et al., 2000) and destruction of the hanging wall of subduction zone and thus enhancing subduction erosion (Safonova and Khanchuk, 2021). Evidence for the destruction of accretionary prism by subducting seamounts comes from bathymetry imagery and seismic survey showing, for example, the active interaction of seamounts and P-type convergent margin at the shoreline of central Costa-Rica (Martínez-Loriente et al., 2019). The physical kinematics of such interactions is a meter of future research and modelling.

Conclusively, pieces of oceanic island/seamounts/plateaus as parts of accretionary prisms or complexes, along with intra-oceanic island arcs and HP metamorphic belts represent is a key diagnostic feature of Pacific-type convergent margins and related orogenic belts. They contribute to the growth of continental crust through accretion and to its destruction through subduction and related tectonic erosion. Understanding of the balance

between all those processes would allow better reconstruction of the global cycles of the geological evolution of the Earth.

Acknowledgement

The work was supported by Fundamental Research Funds for the Central Universities (2682023CX016) and SWJTU startup funds (YH1100312372220 and YH1199911352302).

References

Hofmann A.W., 1997. Mantle geochemistry: the message from oceanic volcanism. Nature 385, 219–229.

Kusky T., Windley B., Safonova I., Wakita K., Wakabayashi J., Polat A., Santosh M., 2013. Recognition of Ocean Plate Stratigraphy in accretionary orogens through Earth history: A record of 3.8 billion years of sea floor spreading, subduction, and accretion. Gondwana Research 24, 501–547.

Martínez-Loriente S., Sallarès V., Ranero C.R., Ruh J.B., Barckhausen U., Grevemeyer I., Bangs N., 2019. Influence of incoming plate relief on overriding plate deformation and earthquake nucleation: Cocos Ridge subduction (Costa Rica). Tectonics 38, 4360–4377.

Maruyama S., Safonova I. Yu., 2019. Orogeny and mantle dynamics: role of tectonic erosion and second continent in the mantle transition zone. Novosibirsk: IPC NSU – 208 p.

Safonova I. Yu., 2020. Intraplate oceanic basalts from accretionary complexes of the Central Asian Orogenic belt and western Pacific. Doctor of science Thesis. Novosibirsk: IPC IGM SB RAS – 528 p.

Safonova I. Yu., Khanchuk A. I., 2021. Subduction Erosion at Pacific-Type Convergent Margins. Russian Journal of Pacific Geology 15 (6), 495-509.

Safonova I., Santosh M., 2014. Accretionary complexes in the Asia-Pacific region: tracing archives of ocean plate stratigraphy and tracking mantle plumes. Gondwana Research 25, 126–158.

Safonova I., Seltmann R., Kröner A., Gladkochub D., Schulmann K., Xiao W., Kim T., Komiya T., Sun M., 2011. A new concept of continental construction in the Central Asian Orogenic Belt (compared to actualistic examples from the Western Pacific). Episodes 34, 186–194.

Safonova I.Y., Utsunomiya A., Kojima S., Nakae S., Tomurtogoo O., Filippov A.N., Koizumi K., 2009. Pacific superplume-related oceanic basalts hosted by accretionary complexes of Central Asia, Russian Far East and Japan. Gondwana Research 16 (3–4), 587–608.

von Huene R., Ranero C.R., Weinrebe W., Hinz K., 2000. Quaternary convergent margin tectonics of Costa Rica, segmentation of the Cocos Plate, and Central American volcanism. Tectonics 19, 314–334.

International Association for Gondwana Research 2023 Convention and
20th International Conference on Gondwana to Asia
Niigata, Japan, October 2023
Abstract Volume

Significance of mélanges in the evolution of subduction complexes and orogenic belts

Andrea Festa[1, 2]

[1] Dipartimento di Scienze della Terra, Università di Torino, Via Valperga Caluso 35, 10125 Torino, Italy
[2] Istituto di Geoscienze e Georisorse, Consiglio Nazionale delle Ricerche, Via Valperga Caluso 35, 10125 Torino, Italy
E-mail: andrea.festa@unito.it

Most of mélanges and chaotic rock units occurring in exhumed subduction-accretion complexes and metamorphic orogenic belts are commonly interpreted as the product of tectonic processes (e.g., underplating and return flow) acting at intermediate to great depths. Field and analytical data outline two main clusters of depth at which mélange and tectonic slices/blocks are exhumed: at ~30-40 km (i.e., downdip of the seismogenic zone) and at ~ 80 km. This also suggests that the mélange rocks recovery is episodic, and the subducted material returns over relatively short-lived episodes, representing only a fraction of subduction lifetime.

In this complex scenario, the open question is whether the mélange record in subduction-accretion complexes and metamorphic orogenic belts reliably reflects depths of processes at which tectonic slices/blocks get scraped off or instead some other process, preventing the recovery of already detached material, or episodic switches between subduction accretion and erosion.

Field examples in non-metamorphic subduction-accretion complexes and orogenic belts around the world clearly show that the subduction of structural inheritances (e.g., ocean-continent transition zones, and ocean plate stratigraphy) may play a significant role in forming mélanges and broken formations already at very shallow depths (T<250°C). The subduction of these inheritances also controls the location of the plate interface and the dynamics of the wedge front (i.e., tectonic accretion vs. erosion). However, not all mélanges that formed at shallow structural levels can be subducted. As subducted, their fate could be very different if they become part of the plate interface or if they share the fate of the lower plate.

Evidence that a consistent part of mélanges form at shallow depths has significant implications for a better understanding of the tectonic evolution of Precambrian to Phanerozoic subduction complexes and metamorphic orogenic belts around the world.

International Association for Gondwana Research 2023 Convention and
20th International Conference on Gondwana to Asia
Niigata, Japan, October 2023
Abstract Volume

Redox state of upper mantle recorded in the mantle peridotites of Oman ophiolite

Eiichi Takazawa[1,*], Tani Masafumi[1], Nami Kanke[1], Ryutaro Murakami[1]

[1]Department of Geology, Faculty of Science, Niigata University, Niigata 950-2181, Japan
[*]E-mail: takazawa@geo.sc.niigata-u.ac.jp

Exploring the behavior of subducting oceanic crust-derived fluids and sediment-derived melts in the mantle wedge is important for understanding mass transport in subduction factories. In the Oman Ophiolite, it has been pointed out that a high-temperature subduction zone was formed by the contraction of the Neo Tethys Ocean at about 95 Ma. In this study, we attempted to explore the behavior of oxidizing fluids and reducing sedimentary melts using mantle peridotites of the northern Oman ophiolite as an analogue of mantle wedges and oxygen fugacities of peridotite as an indicator. The mantle section of the Oman ophiolite is in contact with a lower oceanic crust-derived metamorphic sole separated by a basal thrust, a rare example of a mantle wedge in direct contact with the upper surface of a subducting slab.

We calculated Δlog fO2 (FMQ) from the chemical composition of olivine and spinel in the mantle section olivine using the formula of Ballhaus et al. (1991). The ratio of Fe(II) to Fe(III) in spinel was determined assuming stoichiometry, but no significant difference was found between the two when compared with the results from Mössbauer analysis, and the influence of the ratio on the calculated Δlog fO2 (FMQ) was limited. When Δlog fO2 (FMQ) is plotted on the topographic map of the Fizh mantle section, it is found to be more oxidizing on the eastern Moho side and more reducing on the western basal thrust side. This indicates that the lowest part of the mantle section in contact with the subducting slab is the most reducing.

Next, we considered the V/Sc ratio as a proxy for oxygen fugacity and examined its relationship with Δlog fO2 (FMQ). A negative correlation between Δlog fO2 (FMQ) and V/Sc ratios of all peridotite rocks was confirmed, in which the V/Sc ratio increases as Δlog fO2 (FMQ) decreases. For vanadium, the partition coefficient between peridotite and melt is strongly affected by oxygen fugacity, and the more oxidized it becomes, the lower the partition coefficient becomes (Lee et al., 2005, J. Petrol.). On the other hand, the distribution coefficient of scandium is not affected by oxygen fugacity. The above results indicate that Δlog fO2 (FMQ) calculated using the formula of Ballhaus et al. (1991) is consistent with the redox trend recorded in Oman peridotite as V/Sc ratio.

A possible reason for the reductive nature of the lowermost part of the Fizh lithosphere mantle section is the reaction of mantle peridotite with reductive melts produced by melting of subducted reductive sediments. Samples with low Δlog fO2 (FMQ) values near the basal thrust tend to have relatively high Th/Ce ratios for both whole rock and clinopyroxene. The high Th/Ce ratio is one of the features that indicates the contribution of marine sediments and supports the possibility of reactions with reducing melts. In other words, the Oman ophiolite may have been infiltrated by reducing sediment-derived melts from beneath the mantle wedge during its thrusting, making the reacting peridotite more reductive. It is possible that the reaction of oceanic sediment-derived melts with peridotite could result in the formation of orthopyroxenite. Since orthopyroxene veins are relatively abundant in areas where peridotites with low Δlog fO2 (FMQ) values are distributed, the possibility of a reaction between sediment-derived melts and peridotites will be investigated in the future.

References

Ballhaus, C., Berry, R.F., Green, D.H., 1991. High pressure experimental calibration of the olivine-orthopyroxene-spinel oxygen geo- barometer: implications for the oxidation state of the upper mantle. Contrib. Mineral. Petrol., 107, 27-40.

Lee, C.-T.A., Leeman, W.P., Canil, D., Li, Z.-X.A., 2005. Similar V/Sc Systematics in MORB and arc basalts: Implications for the oxygen fugacities of their mantle source regions. Jour. Petrol., 46, 2313-2336. doi:10.1093/petrology/egi056

Apparent standstill of the Mongolia block in the Carboniferous: decelerated plate motion in a true polar wander frame

Donghai Zhang [1,*], Guochun Zhao [1,3], Baochun Huang [2], Qian Zhao [2], Hai Zhou [4], Enkh-Orshikh Orsoo [5]

[1]State Key Laboratory of Continental Dynamics, Department of Geology, Northwest University, Northern Taibai Str. 229, Xi'an 710069, China
[2]Key Laboratory of Orogenic Belt and Crust Evolution, Ministry of Education, School of Earth and Space Sciences, Peking University, Beijing 100871, China
[3]Department of Earth Sciences, University of Hong Kong, Hong Kong, China
[4]School of Earth Science and Resources, Chang'an University, Xi'an 710054, China
[5]Marco Polo Limited liability Company, Ulaanbaatar, Mongolia
[*]E-mail: dhzhang@nwu.edu.cn

Debates of the Permo-Carboniferous paleogeography of the eastern Central Asian Orogenic Belt (CAOB) mainly focus on the existence, extent and thereby evolutionary history of the Paleo-Asian Ocean (PAO) in this period. To the north of the PAO, the spatial-temporal movements of the Mongolia block in the Carboniferous is critical to resolve the above puzzles. South Mongolia locates at a key position that denotes the southernmost margin of the Mongolia block. Here, we present an integrated paleomagnetic and geochronologic study on the Carbo-Permian volcanic-sedimentary strata and intrusive mafic to intermediate dyke swarms developed in Gurvansayhan of the South Mongolia-Xing'an Belt (SMXB). We obtained reliable paleomagnetic data from the 340-330 Ma volcanic-sedimentary strata and the intruding 299 Ma mafic to intermediate dyke swarms in the Gurvansayhan of the SMXB. The 340-330 Ma ChRMs passed fold and PSV tests, and polarity reversal was identified in the dataset. These ChRMs significantly differ from the 299 Ma dyke swarms in geographic coordinates, suggesting for a positive baked-contact test sensus lato; The ChRMs of dyke swarms passed PSV test and the universal negative inclinations likely primary records of the geomagnetic field during the Kiaman Superchron. The inclination values are also consistent with data from the Uliastai Continental Margin and Songliao block, which occupied different parts of the same tectonic unit, the SMXB. The corresponding paleopoles were caculated at Plat = 7.0°S, Plong = 146.8°E (A95 = 5.4°, N = 11 sites; 299 Ma) and Plat = 6.3°S, Plong = 147.0°E (A95 = 5.0°, N = 16 sites; 340-330 Ma). Lastly, integrating our new data and published data, we conclude that Mongolia was situated at paleopositions near 30°N, throughout the Carboniferous. The apparent standstill of the Mongolia block was a counteraction of the southward true polar wander (TPW) in this area and northward migration of the Mongolia lithospheric plate driven by the rollback of the Mongol-Okhotsk Ocean (MOO).

Acknowledgement: This research was funded by the Natural Science Foundation of China (NSFC) (41902229, 41730213, 42072264, 41972237), China Postdoctoral Science Foundation funded project and Hong Kong RGC GRF (17307918).

Finite Element Approach to compute long-wavelength gravity and isostatic anomalies

A. Vasanthi

CSIR-National Geophysical Research Institute, Hyderabad-500007, India
E-mail: vasanthi@ngri.res.in

Gravity measurements on the surface of the Earth reflect the combined effect of deeper and longer wavelength (regional) as well as shallower and short wavelength (residual) geological features. Large-scale Bouguer gravity anomalies have often been used to probe into mass/density variations in the Earth's deep interior. However, for a limited regional survey, there is a need to discriminate the regional and residual mass anomalies separately for the modelling purpose. For this, both graphical as well as analytical methods have been used for over the decades. However, most of these techniques failed to be completely objective, since there was a need to choose the appropriate frequency range in frequency filtering, the degree of polynomial in polynomial fitting and the choice of height in upward continuation etc. Therefore, we developed a new analytical method, based on Finite Element Approach (FEM), which effectively computes the regional and residual gravity components, and fills the long-standing gap. In this technique, only the observed gravity values at the nodes of the element are used in the regional computation, and no other data from the survey space will enter the computation, thereby avoiding the anomalous zones present in the study area. This method is not site-specific and thus does not require any a priori assumptions. In addition, this method also computes the isostatic anomaly, without explicitly invoking any isostatic model – Airy-Heiskanen, Pratt-Hayford or Vening-Meinsz; thereby eliminating the numerous assumptions, and with that overcoming to a great degree the inherent inaccuracies and the ambiguities. This method has been find to be very effective in studying the geological evolution of geodynamically complex regions.

Zircon U-Pb and Hf isotope data from Himalayan Metamorphic Belt, Kaghan Valley, Pakistan constraining crustal growth in Archean and Proterozoic, recycling and regeneration in Paleozoic, and metamorphic regrowth during Mesozoic

Hafiz U. Rehman[1,*], Hao-Yang Lee[2], Sun-Lin Chung[2], Chunjing Wei[3], Zhanzhan Duan[3], Hiroshi Yamamoto[1], Tahseenullah Khan[4]

[1] Kagoshima University, Kagoshima, Japan
[2] Academia Sinica, Taipei, Taiwan
[3] Peking University, Beijing, China
[4] Bahria University, Islamabad, Pakistan
[*]E-mail: hafiz@sci.kagoshima-u.ac.jp

This research presents a comprehensive report of U–Pb isotope age data combined with Hf isotope results conducted on numerous zircon grains separated from Lesser Himalayan Sequence (LHS) and Higher Himalayan Crystalline (HHC) sequence of the Himalayan Metamorphic Belt (HMB), exposed along the Kaghan Valley transect in northern Pakistan. The selected samples comprise slightly to weakly metamorphosed sandstone (sample Ph_01), slate (sample Ph_02), and phyllite (sample Ph_06) that were collected from the LHS, and strongly metamorphosed granitic and pelitic gneisses, pelitic and psammitic schists, and metabasites (eclogites and garnetites) from the HHC. Detailed geology, petrography, geochemistry, and metamorphic and tectonic evolution of the study area are reported in previous studied (e.g., Kaneko et al., 2003; Rehman et al. 2007, 2013, 2016, 2017; Rehman, 2019).

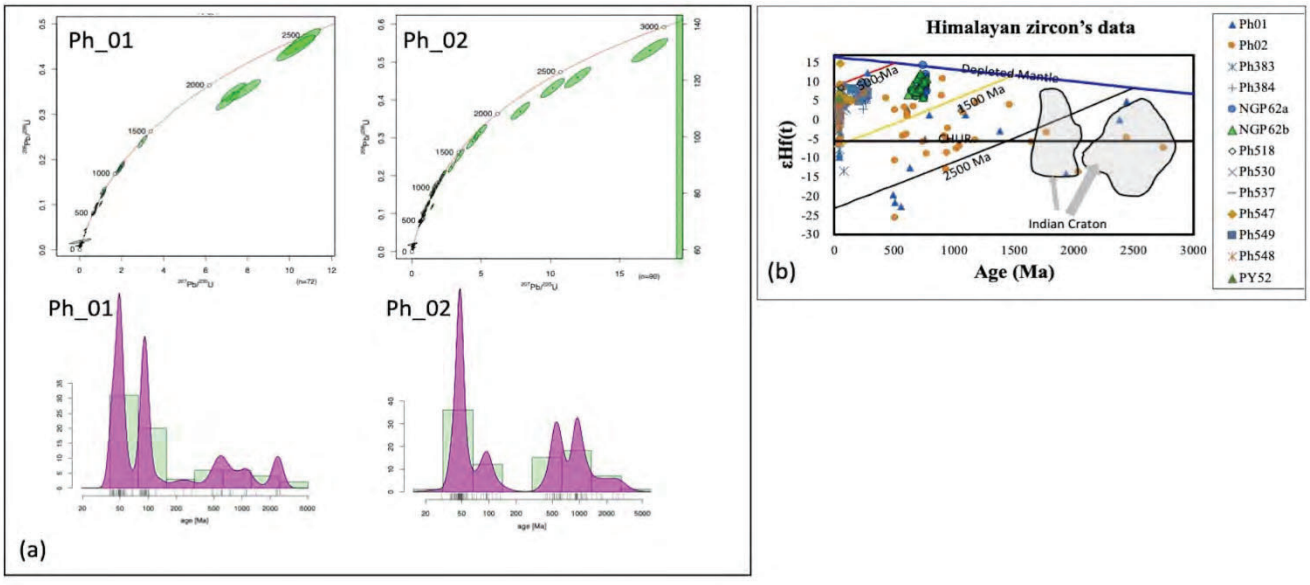

Figure 1(a) U-Pb Concordia diagrams (upper left and right) and age spectrum (lower left and right) of zircon grains from the Himalayan Metamorphic Belt, Kaghan valley, Pakistan. (b) U-Pb age versus εHf(t) diagram of zircon grains analyzed from the Himalayan Metamorphic Belt, Kaghan valley, Pakistan. Zircon data with negative εHf(t) values show crustal contamination or recycled crust. Gray areas are redrawn from the study of Spencer et al. 2019.

Present study focuses on the crustal growth in the initiated during the Archean, evolved through the Proterozoic, Paleozoic, and Mesozoic, and lasted in Early Cenozoic. The U-Pb (207Pb/206Pb, 207Pb/235U, 206Pb/238Pb, and 208Pb/232Th) and Lu-Hf (176Lu/177Hf and 176Hf/177Hf) isotope analyses were conducted in-situ on zircon grains mounted in epoxy, using the split-stream multi-collectorlaser ablation inductively coupled plasma mass spectrometry (LA-ICP-MS) Agilent 7500s quadruple ICP- MS and the Nu Plasma high resolution (HR) multi-collector (MC-) ICP-MS, respectively. All the grains were investigated for internal structures, morphology, and inclusions, and BSE and CL images were recorded using the SEM.

Investigated zircon grains from samples Ph_01 and Ph_02, and sample Ph_06 from the LHS yielded 206Pb/238Pb age spectrum (Fig. 1a) with a maximum value of 2746 ± 54 Ma (representing the initiation of crustal growth), several other zircon grains yielded 206Pb/238Pb age values around 2443 ± 52 Ma, 2380 ± 52, 2438 ± 49 Ma, and 2034 ± 44 Ma,. A number of zircon grain from the above-mentioned samples from the LHS yielded age spectra between 1952 Ma ~ 1642 Ma, followed by next generation of crustal growth around 1300 Ma ~ 900 Ma, additional major peak between 750 Ma ~ 600 Ma, followed by a spectrum of 550 Ma ~ 450 Ma, and the most abundant age data was scattered between 300 Ma ~ 250 Ma in samples from LHS and those from the HHC as well as those selected from the HHC gneissose and schistose rocks. Some scattered age data giving values between 180 Ma and 100 Ma were also obtained from a number of zircon grains from both lithological sequences, suggesting their common detritus source. A peak stage depicting a narrow spectrum between 50 Ma and 45 Ma, was obtained from the majority of zircon grains that were picked from the strongly metamorphosed gneisses, schists, and eclogites. Garnetites yielding similar age values to those obtained from the eclogites, suggest their coeval growth/recrystallization. The same zircon grains were analyzed for Hf isotope ratios where the Hf analyses were performed on the U-Pb dated spots or nearby domain when the U-Pb spot was not possible to be analyzed further. The Hf isotope results, particularly, the εHf(t) values show a broad spectrum between + 15 to -25, in which the plus εHf(t) values indicate juvenile crustal growth whereas the negative εHf(t) values suggest reworked and recycled sedimentary component. The Himalayan zircons show that the Archean and Proterozoic component (age spectrum between 2746 ~ 2034 Ma) was mainly derived from the recycled continental crust as evidenced from the negative εHf(t) values (Fig. 1b), the Late Proterozoic zircons (1000 ~ 700 Ma) producing positive εHf(t) values (Fig. 2), suggest continental crustal growth from a juvenile source, the Paleozoic population of zircons (550 Ma ~ 450 Ma) from both HS and HHC primarily show positive εHf(t) values but with values approaching to zero εHf(t), indicating involvement of sediment or crustal contamination when their magmatic source was generated. The εHf(t) data from Permian magmatism (300 to 250 Ma) is mainly recorded in felsic (granitic gneisses) and mafic components (eclogites) was also showing positive values > 5 εHf(t), advocating their juvenile magmatic source. In addition, the vast majority of zircon population that yielded Eocene age (50 to 40 Ma) is depicting the well-known India-Asia collision-related high- and ultrahigh-pressure metamorphic event.

The U-Pb age and Hf isotope data from the investigated zircons provide insights on the crustal growth and tectono-metamorphic evolution of the HMB. The oldest age of zircon (Archean and Proterozoic) suggests the initial crustal growth before the assembly of supercontinent Nuna. of crust in the Indian plate and by the time India was part of the supercontinent Nuna. The 1900 ~ 1700 Ma spectrum possibly indicates tectonic activities and associated magmatism with the assembly of supercontinent Nuna. Similar age spectrum was also reported from Cathaysia (e.g. Cawood et al., 2018, and references therein). The age spectrum represented by 1300 Ma ~ 900 Ma could have been resulted by the recycling and re-amalgamation within Nuna. The 800 to 600 Ma spectrum represents the Pre-Gondwanan wide-spread magmatism that is well known in the Indian Craton as the LIP (Malani Igneous Suite in India, Nagar Parkar Igneous Complex in southeast Pakistan, South China Block in China, Madagascar, and Seychelles) that were resulted by the subduction of the Mozambique Ocean and mantle plume-related magmatism. The 500 to 450 event can be associated with the Crustal growth in the Gondwana when Indian plate was intact with Antarctica, Australia, and South China. A major magmatic and tectonic activity in the Himalayan region occurred during Permian at the time of Gondwana break-up, having mantle plume along the northern margin spreading to the inner Tethys to produce the bimodal felsic and mafic magmatic rocks (ca. the Permian Panjal Traps comprising basalts, andesites, and rhyolites). These Magmatic lithologies and contemporaneous sedimentary successions subducted beneath the Asian plate and Kohistan Island arc, some parts reaching to the mantle depths and transformed to eclogites during the India-Asia collision in The Eocene (50 to 45 Ma) but the zircons still maintained the positive Hf εHf(t) isotope records from their precursor protolith. Finally, after the possible slab-break off of the Indian slab, the deeply subducted rocks initiated exhumation and that event of retrograde metamorphism is also recorded in some metamorph9ic zircons giving age values of < 40 Ma.

References

Cawood P.A., Zhao G., Yao J., Wang W., Xu Y., Wang Y. 2018. Reconstructing South China in Phanerozoic and Precambrian supercontinents. Earth Scidence Reviews

186, 173-194.

Kaneko, Y., Katayama, I., Yamamoto, H., Misawa, K., Ishikawa, M., Rehman, H.U., Kausar, A.B., Shiraishi, K. 2003. Timing of Himalayan ultrahigh-pressure metamorphism: sinking rate and subduction angle of the Indian continental crust beneath Asia. Journal of Metamorphic Geology 21, 589-599.

Rehman, H.U., Yamamoto, H., Kaneko, Y., Kausar, A.B., Murata, M., Ozawa, H. 2007. Thermobaric structure of the Himalayan metamorphic belt in Kaghan Valley, Pakistan. Journal of Asian Earth Sciences 29, 390-406.

Rehman, H.U., Kobayashi, K., Tsujimori, T., Ota, T., Yamamoto, H., Nakamura, E., Kaneko, Y., Khan, T., Terabayashi, M., Yoshida, K., Hirajima, T. 2013. Ion microprobe U–Th–Pb geochronology and study of micro-inclusions in zircon from the Himalayan high and ultrahigh-pressure eclogites, Kaghan Valley of Pakistan. Journal of Asian Earth Sciences 63, 179-196.

Rehman, H.U., Lee, H.Y., Chung, S.L., Khan, T., O'Brien, P.J., Yamamoto, H. 2016. Source and mode of the Permian Panjal Trap magmatism: Evidence from zircon U-Pb and Hf isotopes and trace element data from the Himalayan ultrahigh-pressure rocks. Lithos 260, 286-299.

Rehman, H.U., Jan, M.Q., Khan, T., Yamamoto, H., Kaneko, Y. 2017. Varieties of the Himalayan eclogites: A pictorial review of textural and petrological features. Island Arc 26: e12209; 1-14.

Spencer C.J., Dyck B., Mottram C.M., Roberts N.M.W., Yao W.H., Martin E.L. 2019. Deconvolving the pre-Himalayan Indian margin -Tales of crustal growth and destruction. Geoscience Frontiers 10, 863-872.

International Association for Gondwana Research 2023 Convention and
20th International Conference on Gondwana to Asia
Niigata, Japan, October 2023
Abstract Volume

Fault delineation, deformation microstructures and temperature estimations from shallow to mid-crustal parts of Main Himalayan Thrust, NW India

Sarkar Dyuti Prakash[1,2,*], Ando Jun-ichi[1,2], Das Kaushik[1,2], Ghosh Gautam[2,3]

[1]Department of Earth and Planetary Systems Science, Hiroshima University, Higashi-Hiroshima, Japan
[2]Hiroshima Institute of Plate Convergence Region Research
[3]Centre for Advanced Study, Department of Geology, Presidency University, Kolkata, India
[*]Email: sarkardp16@hiroshima-u.ac.jp

Fault rock mineralogy and deformation microstructures of crustal-scale faults provide insights on the stress accommodation mechanisms in terms of fault weakening and possibilities of earthquake nucleation. The Main Himalayan Thrust is considered to be the large-scale sub-surface boundary along which Indian plate subducts beneath the Asian plate. The near-surface exposure of the present active boundary of the subduction is considered the Main Frontal Thrust, which separates the Gangetic foreland basin in the south and Sub-Himalayas in the north. Further north we have the Main Boundary Thrust followed by the Main Central Thrust at the northernmost boundary representing the major post-collisional paleo-thrust boundaries between Indian and Asian plates. Here we present a comparative study of our findings on the fault rocks from the Nahan Thrust within the Main Frontal thrust sheet and the Main Boundary thrust in the north, with focus on fault delineation, mesoscopic and microstructures, and temperature estimation using calcite clumped isotope thermometry. This research elucidates the methodologies in delineation of fault boundaries and the heterogenous nature of the deformation mechanisms in fault rocks within a fault zone.

The fault zone from the Nahan Thrust shows dominance of brittle deformation structures consisting of highly brecciated sandstone and a wide gouge zone. The outcrops within the gouge zone, present variably colored red, grey and black gouges. Microstructural observation of the fault rocks using scanning electron microscopy and transmission electron indicates a complex interplay of distributed deformation and progressive stress localization leading to fracture development, cataclasis and frictional sliding with possible seismic slips within the fault zone. Especially the ultra-fine bands of black gouge layer show evidence of amorphous materials, vapor escape structures, and clay clast aggregates, exhibiting a possible fingerprint of seismic faulting and frictional heating during seismic slips. The development of such heterogenous fault architecture in the Nahan thrust has been attributed to composition of the protolith and diachronous fault growth in response to the stress accumulation with ongoing subduction in the Himalayas.

In comparison to Nahan thrust, the studied exposure of the Main boundary Thrust have no clear fault zone. Here we devised the usage of detrital zircon geochronology and litho-structural mapping to delineate the fault boundary. Our U-Pb detrital zircon data indicates a sharp change in age from Neoproterozoic hanging-wall rocks to Cenozoic footwall rocks within an interval of ~1 m. The mesoscopic structures from hanging wall and footwall were studied to elucidate the deformation geometry of the Mian Boundary Thrust.

The calcite clumped isotope thermometry from the calcites within and in proximity of the studied fault zones indicate temperature of 262±30 °C for the Main Boundary Thrust and 170±10 °C for the Nahan thrust suggesting a depth of 10–11 km and 6–7 km respectively.

International Association for Gondwana Research 2023 Convention and
20th International Conference on Gondwana to Asia
Niigata, Japan, October 2023
Abstract Volume

2-D thermal modeling for thrust-related cratonization of hot deep crust: An example from the Eastern Ghats Belt, India

Das, K.[1, 2,*], Sato, F.[1], Nakakuki T.[1,2]

[1]Department of Earth and Planetary Systems Science, Hiroshima University, Japan 739-8526
[2]Hiroshima Institute of Plate Convergence Region Research, Hiroshima, 739-85261
[*]E-mail: kaushik@hiroshima-u.ac.jp

Continents stitching through orogenic belts by accretionary and collisional tectonics was one of the major mechanisms of Precambrian continental growth. The final docking of such hot deep orogenic crust thrusting up on the cold shallow preexisting cratonic crust had one of the major and obvious consequences, i.e. heat dissipation across the boundary. Such large-scale structural boundaries provide also the pathways of crustal fluid flows. Moreover, the resultant shallow crustal processes including sedimentary basin formation are among other consequences at the interface between lithosphere, hydrosphere, biosphere, and atmosphere. However, studies from the exposed rocks across such thrust boundaries often indicate that the effects of heat for such thrusting are speculative due to the "limited" mineralogical growths and lack of data on fluid activities along such structural boundaries.

For the present study, we select the boundary between the Proterozoic Eastern Ghats Belt (EGB) and the Archean Bastar Craton (BC), India. Comprehensive tectonic model until the final cratonization was proposed based on the detailed structural geology, petrological, and geochronological studies (Bhadra et al., 2004; Biswal et al., 2007; Chatterjee et al., 2017a, b; Ganguly et al., 2018: Ganguly and Chatterjee, 2020). On a regional scale, the deep crustal granulites of the EGB preserve the history of ultrahigh-temperature metamorphism that peaked at 1000-900 Ma. However, the youngest thermal event at 650–550 Ma was recorded in monazite grains in felsic gneiss close to the thrust boundary. This youngest metamorphic age has only been found in zircon and monazite grains along tens of kilometers on either side of the boundary and is most pronounced at the boundary. We propose that the regional distribution of this age was caused by the thrust-related thermal activity (~700 °C for zircon and ~600 °C for monazite) during the final cratonization of the EGB and BC. This thermal overprinting reached the amphibolite-granulite transition facies in the presence of crustal fluid.

We have simulated this "hot-on-cold" thrusting (Gupta et al., 2012) in absence and presence of hot fluid at fault to estimate precise spatial temperature distribution patterns during the final cratonization of the EGB crust. The above-mentioned tectonic model provides the initial conditions for this simulation. The numerical simulation is based on the finite volume method with the thermal advection-convection equation. The 2D numerical model is based on geologically appropriate boundary conditions, and a fault angle of about 26.5°, with movement only on the EGB side at a velocity of 2.0 cm/yr. Time sequential thermal profiling is done at 15 km depth (i.e. the present-day surface level after exumation-erosion) across the thrust, both for dry faulting and for faulting associated with hot fluid/melt. The experimental run data show a large temperature increase for the latter case, i.e. up to 700 °C at 5 km, 600 °C between 15 to 30 km from the fault to the Eastern Ghats Belt side, and close to 500 °C at 5 km from the boundary on the BC side. Finally, we have compared the experiment-derived data and those from lithological studies in the study area. The simulation data corroborate closely with the available mineralogical data.

References

Bhadra et al., 2004. Structural evolution across the Eastern Ghats Mobile Belt–Bastar craton boundary, India: hot over cold thrusting in an ancient collision zone. Journal of Structural Geology, 26, 233–245.

Biswal et al., 2007. Timing and dynamics of the juxtaposition of the Eastern Ghats mobile belt against the Bhandara Craton, India: a structural and zircon U–Pb SHRIMP study of the fold–thrust belt and associated nepheline syenite plutons. Tectonics, 26, TC4006.

Chatterjee et al., 2017a. Zircon U–Pb SHRIMP and monazite EPMA U–Th–total Pb geochronology of granulites of the western boundary, Eastern Ghats Belt, India: new possibility for Neoproterozoic exhumation history. Geological Society, London, Spl. Pub. 457, 105–140.

Chatterjee et al., 2017b. Age–integrated tectonic evolution across the orogen–craton boundary: age zonation and shallow–to deep crustal participation during Late Cambrian cratonisation of Eastern Ghats Belts, India. Lithos, 290–291, 269–293.

Ganguly et al., 2018. U–Pb zircon and U–Th–total Pb monazite ages from the Phulbani domain of the Eastern Ghats Belt, India: Time constraints on high–grade metamorphism and magmatism in the lower crust. Precambrian Research, 316, 1–23.

Ganguly and Chatterjee, 2020. Geological evolution of the northern and northwestern Eastern Ghats Belt, India from metamorphic, structural and geochronological records: An appraisal. Journal of Mineralogical and Petrological Sciences, 115, 88–101.

Gupta, S. 2012. Strain localization, granulite formation and geodynamic setting of 'hot orogens': a case study from the Eastern Ghats Province, India. Geological Journal, 47, 334–351.

A late Paleoproterozoic collisional orogenic event in the northern Tarim Craton

Wenbin Zhu[1,*], Rongfeng Ge[1], Hailin Wu[1]

[1]State Key Laboratory for Mineral Deposits Research, School of Earth Sciences and Engineering, Nanjing University, Nanjing 210093, PR China4
[*]E-mail: zwb@nju.edu.cn

Widespread Paleoproterozoic supracrustal rocks in the northern Tarim Craton contain important information about its geological evolution and correlation with adjacent blocks. Field and petrological studies indicate a pelitic to semi-pelitic protolith and a high pressure upper amphibolite-facies peak metamorphic condition for these samples. CL-images reveal that zircons are dominantly metamorphic origin and only a few detrital zircons occur as relics in one sample, the ages of which suggest a maximum deposition age of ca. 2.0 Ga and a sedimentary provenance from the Tarim Craton itself. All metamorphic zircons consistently recorded a metamorphic age of ca. 1.85 Ga, despite of various degrees of discordance probably due to later Pb-loss. Both recrystallization and new zircon growth are recognized for the genesis of these metamorphic zircons. The metamorphic zircon domains in one sample show a relatively large range of initial 176Hf/177Hf ratios similar to the detrital cores, whereas those in the other samples show similar initial 176Hf/177Hf ratios regardless of their internal structures and degrees of discordance. The former is interpreted as a result of complete U-Pb resetting through fluid-mediated recrystallization, whereas the later probably implies a large-scale Hf isotopic homogenization during new zircon growth. Petrological and zircon isotopic evidence supports that the new zircon growth and Hf isotopic homogenization resulted from the mixing of Hf-Zr derived from dissolution of tiny detrital zircons and decomposition of garnet to chlorite in hydrothermal fluids during retrograde metamorphism. Accordingly, the ages of these new zircon growths may postdate the peak metamorphism, which was probably related to a late Paleoproterozoic collisional orogenic event in the northern Tarim Craton.

Formation age and tectonic significance of Yellow River terrace sequences in Xinghai area, northeast Tibetan Plateau

Fubao Chong[1], Yunpeng Dong[1,*], Dengfeng He[1], Shengsi Sun[1], Bo Hui[1], Rutao Zang[1]

[1] State Key Laboratory of Continental Dynamics, Department of Geology, Northwest University, Xi'an 710069, China
[*]E-mail: dongyp@nwu.edu.cn

The uplift of the Qinghai-Tibet Plateau has an important impact on the global landforms change and environmental climate evolution, but geologists have different disputes on the process, magnitude and nature of the uplift. The river terrace formed in the inland of the plateau is mainly controlled by structure, which indicates that the study of river terrace has an important role in revealing the uplift process. In this paper, we establish the terrace sequence of the Yellow River in the Xinghai section of the northeastern Tibetan Plateau, making use of field investigations, gravel analysis, and optically stimulated luminescence (OSL) dating. A total of eight terraces were found here, among which the ages of T1-T8 terraces are 2.0 ka, 3.6 ka, 34 ka, 109 ka, 116 ka, 121 ka, 140 ka and 200 ka. This suggests that the Yellow River existed in Xinghai basins for at least the last 200 ka. The incision rates of the Yellow River in the Xinghai section indicate that there were two distinct phases of uplift of the northeastern Tibetan Plateau, occurring at different rates, with an average uplift rate of ~1.75 mm/yr during the Quaternary. The above research results that the formation of terraces in Xinghai area is mainly controlled by structure and has little influence on climate. The formation time of the highest terrace corresponds to the era of the Gonghe Movement, which caused the rapid rise of the Qinghai-Tibet Plateau to the present height. Therefore, we believe that the emergence of the Yellow River in the Xinghai Basin was caused by the Gonghe movement.

Diapir Melting of Subducted Mélange Generating Alkaline Arc Magmatism and Its Implications for Material Recycling at Subduction Zone Settings

Kai Wang[1], Keda Cai[1,*], Min Sun[2], Xiangsong Wang[2], Xiao-Ping Xia[3], Bo Zhang[4], Bo Wan[5]

[1]School of Earth Sciences and Resources, and State Key Laboratory of Geological Processes and Mineral Resources, China University of Geosciences, Beijing, China
[2]Department of Earth Sciences, The University of Hong Kong, Hong Kong, China
[3]State Key Laboratory of Isotope Geochemistry, Guangzhou Institute of Geochemistry, Chinese Academy of Sciences, Guangzhou, China
[4]The Key Laboratory of Orogenic Belts and Crustal Evolution, School of Earth and Space Sciences, Peking University, Beijing, China
[5]State Key Laboratory of Lithospheric Evolution, Institute of Geology and Geophysics, Innovation Academy for Earth Science, Chinese Academy of Sciences, Beijing, China
[*]E-mail: caikd@cugb.edu.cn

Alkaline rocks crop out in subduction-related volcanic arcs globally, whose genesis is explained by partial melting of hybrid diapiric mélanges in the mantle wedge. Such a new model has not yet been evidenced by field-based investigations, where mélanges and alkaline arc rocks have spatial-temporal and genetic connections. In this study, we identified these two types of rock units exposed in Western Tianshan, and established their petrogenetic relationship through field, geochronologic, geochemical, and thermodynamic investigations. Our results suggest that partial melts produced by melting of the mélange matrix at pressures of 2.8–2.4 GPa and 1.8–1.4 GPa with temperatures of 1000–1200°C can replicate the major-element contents and trace-element abundances of the regional alkaline arc rocks. This finding not only supports the hypothesis that diapir melting of subducted mélanges has a capacity to generate alkaline arc magma, but also provides insight into material recycling at subduction zone settings.

International Association for Gondwana Research 2023 Convention and
20th International Conference on Gondwana to Asia
Niigata, Japan, October 2023
Abstract Volume

SHRIMP U-Th-Pb dating of Rwandan tin mineralisation and associated tectonic processes

Claude Nambaje[1,3,4,*], Ian S. Williams[2], K. Sajeev[1]

[1]Centre for Earth Sciences, Indian Institute of Science, Bangalore-560012, India
[2]Research School of Earth Sciences, Australian National University, Canberra ACT 2601, Australia
[3]Department of Geology, Faculty of Science, Niigata University, 2-8050 Ikarashi, Nishi-ku, Niigata 950-2181, Japan
[4]School of Mining and Geology, University of Rwanda.
[*]E-mail: clauden@iisc.ac.in

Secondary Ion Mass Spectrometry (SIMS) U-Th-Pb dating of cassiterite, zircon and monazite by Sensitive High Resolution Ion MicroProbe (SHRIMP) has provided direct measurements of the ages of Mesoproterozoic–Neoproterozoic pegmatite and quartz vein Sn mineralisation in the Karagwe–Ankole Belt (KAB), Rwanda, and through dates on local igneous rocks, helped to place the mineralisation in a tectonic context. The texture of the studied cassiterite is compositionally controlled, with dark brown zones enriched in Nb, Ta, Ti and Fe relative to the lighter zones, which approach pure (> 99%) SnO2. Internal textures of the cassiterite are also defined by trace element distribution with an enrichment of Ta, Nb, Fe, V, Al and U in darker cathodoluminescence (CL) bands relative to lighter bands (Nambaje et al., 2020), with the majority of the dated cassiterite containing ≤ 1 ppm U. Three stages of Sn mineralisation have been identified, each being associated with magmatic and metamorphic processes during different periods of Rodinian and Gondwanan assembly (Nambaje et al., 2021a,b). The first stage of mineralisation occurred at ca. 1145 Ma. The second stage, which corresponds to the main episode of Sn mineralisation occurred from ca. 1090 to 960 Ma. It started during the period ca. 1090–1040 Ma with fault-controlled Sn mineralisation in quartz veins hosted in quartzite and intra-pegmatitic greisen. This was mainly coeval with the ca. 1078 Ma D2 orogenic event in the KAB during the final amalgamation of Rodinia. Peak Sn mineralisation occurred during the period ca. 1040–960 Ma in quartz veins hosted in mica schists related to shear zones. It was associated with G4 S-type granitic magmatism, with zircon U-Pb and monazite Th-Pb ages between 1011 ± 18 and 976 ± 11 Ma, possibly related to a late/-post-collisional setting linked to the amalgamation of Rodinia (Nambaje et al., 2021a,b). The third and distinct stage of Sn mineralisation occurred at ca. 530 Ma in quartz veins hosted in mica schists within a shear zone located close to reworked basement rocks with meridional foliation. This Sn mineralising event is attributed to hydrothermal fluids, possibly induced by a post-tectonic event associated with the emplacement of G5 S-type granite at 614 ± 9 Ma, during the Pan-African orogeny (Nambaje et al., 2021a). The links established between the mode of Sn mineralisation, its local geological setting, igneous activity and regional tectonism, will help in targeting exploration for ore-grade Sn deposits in Rwanda and nearby countries.

References

Nambaje, C., Eggins, S.M., Yaxley, G.M., Sajeev, K., 2020. Micro-characterisation of cassiterite by geology, texture and zonation: A case study of the Karagwe–Ankole Belt, Rwanda. Ore Geology Reviews 124, 103609. DOI: https://doi.org/10.1016/j.oregeorev.2020.103609.

Nambaje, C., Williams, I.S., Sajeev, K., 2021. SHRIMP U-Pb dating of cassiterite: Insights into the timing of Rwandan tin mineralisation and associated tectonic processes. Ore Geology Reviews 135, 104185. DOI: https://doi.org/10.1016/j.oregeorev.2021.104185.

Nambaje, C., Satish-Kumar, M., Williams, I.S., Takahashi, T., Sajeev, K., 2021. Granitic rocks from Rwanda: Vital clues to the tectonic evolution of the Karagwe–Ankole Belt. Lithos 404-405, 106490. DOI: https://doi.org/10.1016/j.lithos.2021.106490.

International Association for Gondwana Research 2023 Convention and
20th International Conference on Gondwana to Asia
Niigata, Japan, October 2023
Abstract Volume

Eastern South China as an Appalachian-style accretionary orogen

Shoufa Lin[1,*], Lijun Wang[1,2], and Wenjiao Xiao[2]

[1] Department of Earth and Environmental Sciences, University of Waterloo, Waterloo, Ontario N2L 3G1, Canada
[2] National Key Laboratory of Arid Area Ecological Security and Sustainable Development, Xinjiang Institute of Ecology and Geography, Chinese Academy of Sciences, Urumqi 830011, P.R. China
[*]E-mail: shoufa@uwaterloo.ca

South China has traditionally been interpreted to have formed by the collision of two blocks, the Yangtze and the Cathaysia. The proposed timing of collision varies from Proterozoic to Mesozoic, corresponding to that of the various tectono-thermal events documented in South China. We propose, as an alternative interpretation, that eastern South China is an accretionary orogen formed by accretion/collision of multiple terranes (i.e. more than two blocks), and each of the major tectono-thermal events corresponds to an accretional/collisional event. The proposed model includes the following components: (1) The Jiangnan Orogen along the southeastern margin of the Yangtze Block formed as a result of collision between the Yangtze Block and the Greater Huaiyu terrane at ca. 820 Ma. Most of the Greater Huaiyu terrane and part of the Jiangnan orogen rifted away from the Yangtze Block soon after the collision. (2) The West Cathaysia terrane is a composite terrane formed by amalgamation of multiple terranes/arcs at ~1.0–0.7 Ga and is interpreted to be a microcontinent originated from a Grenvillian-aged orogen in the Rodinia supercontinent. (3) West Cathaysia and Yangtze were accreted to two different parts of the northern margin of Gondwana in the Ediacaran to Early Cambrian and were then juxtaposed through margin-parallel large-scale strike-slip motion along the Jiangshan-Shaoxing fault in the late Ordovician. (4) The composite Yangtze-West Cathaysia terrane rifted away from Gondwana in the late Paleozoic. (5) The East Cathaysia terrane, characterized by a ~1.9–1.8 Ga basement and ~250–230 Ma high-grade metamorphism, possibly originated from an Early Mesozoic orogen in the Paleo-Tethyan regime to the south. It was accreted to the east of West Cathaysia in the Mesozoic, through large-scale strike-slip movement along the Northwest Fujian fault. A comparison with the evolution of the Appalachian orogen indicates that the key features of the above model, including multi-terrane accretion/collision, large-scale strike-slip motion and, in particular, separation of two terranes/continents by rifting following their collision, may be common to many orogens.

International Association for Gondwana Research 2023 Convention and
20th International Conference on Gondwana to Asia
Niigata, Japan, October 2023
Abstract Volume

Early Neoproterozoic subduction-related tectonics along the northwestern margin of the Yangtze Block, South China

Bo Hui[1], Yunpeng Dong[1,*], Feifei Zhang[1], Shengsi Sun[1]

[1]State Key Laboratory of Continental Dynamics, Department of Geology, Northwest University, Northern Taibai Str. 229, Xi'an 710069, China
[*]E-mail: dongyp@nwu.edu.cn

The early Neoproterozoic granitoids exposed in the Bikou Terrane preserve vital information for understanding the Tonian tectonic evolution along the northwestern margin of the Yangtze Block, South China. However, their accurate forming age, petrogenesis, and tectonic attributes remain ambiguous. This study reports new results on zircon U–Pb geochronology, zircon Hf isotopes, whole-rock geochemistry, and Sr–Nd isotopes of the Baiquesi and Bahaihe quartz monzonite, Shilingou monzogranite, and Maliupu granodiorite from the Bikou Terrane. Detailed zircon U–Pb dating results reveal that the quartz monzonite and monzogranite were formed at ca. 860 Ma, whereas the granodiorite was emplaced at ca. 825 Ma. The quartz monzonite and monzogranite samples exhibit certain linear correlations in the Harker diagram, congruent distribution patterns of rare earth elements, and consistent isotopic compositions, indicating that they shared the same magma source, whereas the monzogranite was formed by differentiation crystallization of primitive quartz monzonite melt. The quartz monzonite samples are calc-alkaline in composition and have high ratios of Sr/Y and (La/Yb)N, coinciding well with the adakitic rocks. The relatively high contents of MgO, Ni, Cr, and Sr, low contents of Yb and Y, low ratios of La/Ce, Rb/Sr, and Th/La, and positive values of εHf(t) (+4.8–+6.7) and εNd(t) (+1.7–+2.1) indicate that they were formed by the interaction between slab-derived melt and mantle wedge. This mechanism may be triggered by a slab roll- back process in an arc-related setting. The Maliupu granodiorite samples are classified as calc-alkaline I-type granitoids, and have low concentrations of MgO, Cr, Ni, and Y, and low ratios of Sr/Y and (La/Yb)N. They are featured by highly evolved εHf(t) values from −15.0 to −10.9 and εNd(t) values from −11.8 to −11.9, with Hf and Nd model ages ranging between 2.63 and 2.20 Ga, implying they were derived from partial melting of the ancient lower mafic crust and were formed in a subduction-related setting. Therefore, the new data, combined with those from previous studies in the Bikou Terrane, provide an essential link in the evidence chain for the hypothesis that the northwestern periphery of the Yangtze Block was in a persistent subduction-related tectonic regime in the early Neoproterozoic.

International Association for Gondwana Research 2023 Convention and
20th International Conference on Gondwana to Asia
Niigata, Japan, October 2023
Abstract Volume

Yangtze and Cathaysia blocks of South China: Their separate positions in Gondwana until early Paleozoic juxtaposition

Lijun Wang[1,2,*], Shoufa Lin[1], and Wenjiao Xiao[2]

[1]Department of Earth and Environmental Sciences, University of Waterloo, Waterloo, Ontario N2L 3G1, Canada
[2]National Key Laboratory of Arid Area Ecological Security and Sustainable Development, Xinjiang Institute of Ecology and Geography, Chinese Academy of Sciences, Urumqi 830011, P.R. China1
[*]E-mail: lijun.wang@uwaterloo.ca

The Gondwana supercontinent was assembled through a series of subduction and collision processes from the Cryogenian to Cambrian. Although the configuration of the major constituents of Gondwana has been firmly established, the relative positions of the smaller blocks lying outboard of the core with respect to Gondwana and to each other remain controversial. This is particularly true for the various Asian blocks, such as South China, North China, Tarim, and Lhasa. It is generally accepted that South China was located along the northern periphery of East Gondwana. However, its precise position relative to India and Australia is debated, and competing models have been proposed. In all previous models, the Yangtze and Cathaysia blocks, the two major components of South China, were amalgamated by the Tonian, and South China was considered to be a single coherent block in Gondwana.

Based on a summary and critical reevaluation of available paleomagnetic, paleontological, stratigraphic, and detrital zircon data, we propose that the Yangtze and Cathaysia blocks were not juxtaposed until the early Paleozoic and were located at two separate parts of the northern margin of Gondwana before that time. The Yangtze block was located to the northwest of India in the Ediacaran and early Cambrian. Cathaysia was close to or a part of northern Australia in the Ediacaran, when Australia and India were separated by the Kuunga Ocean, and amalgamated with the eastern margin of India in the late Ediacaran to early Cambrian when the ocean closed. Our model implies that the early Paleozoic orogenesis in South China could have been related to two distinct events, the late Ediacaran to early Cambrian collision of Cathaysia/Australia with India (the Kuunga orogeny) and the Late Ordovician amalgamation of Cathaysia with Yangtze. It also implies that the Yangtze and Cathaysia blocks likely occupied two separate positions in Rodinia.

International Association for Gondwana Research 2023 Convention and
20th International Conference on Gondwana to Asia
Niigata, Japan, October 2023
Abstract Volume

Origin and Tectonothermal Evolution of Lodestones in the Layered Ultramafic Intrusions of Coorg Block: Insights from Textural, Chemical, and Geothermometric Constraints

V. Deepchand[1], V. J. Rajesh[2,*], J. Amal Dev[3], Nilanjana Sorcar[3], J. K. Tomson[3], R. B. Binoj Kumar[1]

[1]Department of Geology, University of Kerala, Thiruvananthapuram-695581, India.
[2]Department of Earth and Space Sciences, Indian Institute of Space Science and Technology, Thiruvananthapuram-695547, India.
[3]Solid Earth Research Group, National Centre for Earth Science Studies, Thiruvananthapuram 695011, India
[*]E-mail: rajeshvj@iist.ac.in

Lodestones are naturally magnetised ore bodies commonly found as lenses or bands within mafic-ultramafic rocks (Wasilewski and Kletetschka, 1999; Mills, 2004). Lodestones retain natural remanent magnetism due to their varied mineralogy, microtextural characteristics, and unusual chemical composition (Yamamoto, 2003; Wasilewski and Kletetschka, 1999). Lodestone microtextural and chemical properties shed light on ore genesis and the magmatic cooling history associated with layered igneous processes (Buddington and Lindsley, 1964). There are only two naturally magnetized Fe-Ti magnetite deposits in peninsular India: The Kurihundi lodestone deposit in Nanjangud, Karnataka (Vidyashankar and Govindaiah, 2009) and the Kanthampara lodestone deposit near Periye, Kerala (Sukumaran and Nambiar, 2001). The Periye occurrence is a recognized lodestone deposit in the southern granulite terrain (SGT) located in the Coorg Block, the northernmost crustal block. The microtextural, geochemical, mineralogical, and spectral properties of lodestones from the Periye region of northern Kerala are investigated to understand the magmatic processes associated with their genesis and geothermometric constraints.

In the study area, lodestones form part of the layered igneous complex as a rhythmic layer. The terrain on which the lodestone-bearing mafic-ultramafic layered intrusions were emplaced is comprised of arc magmatic rocks of the Coorg block. The layered mafic-ultramafic units in the Coorg block formed as the oceanic lithosphere subducted southward beneath the block (Santosh et al., 2014; Anoop et al., 2022). The possibility that the present intrusions are part of the Archean Sargur/Wayanad Group, which consists of the supracrustals of the western Dharwar Craton, has also been discussed (Sukumaran & Nambiar, 2001). The lodestone layers are enclosed within laterites as resistant bands, where metamorphosed ultramafic intrusions (meta-peridotite and meta-pyroxenite) are in the basement. These ultramafic intrusions were emplaced into granulitic rocks, such as two pyroxene granulites. The ore bodies are found in three localities (Figure 1), namely Kanthampara, Peraklayi, and Thaynoor, with a notable outcrop apparent at Kanthampara, with an average strike length of 200 metres and a width of 2 metres in the east-west direction.

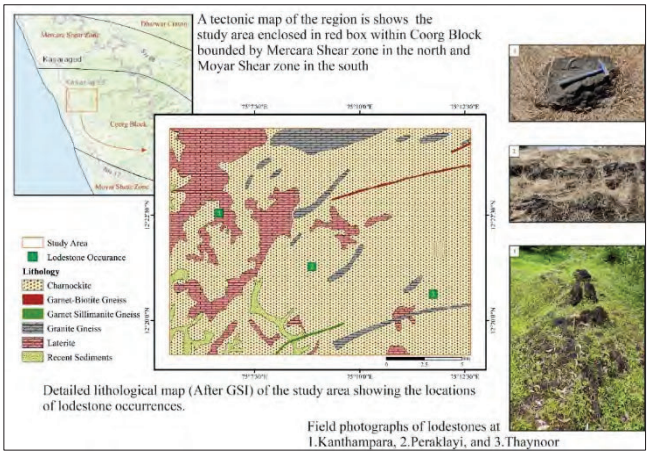

Figure 1: Maps showing lodestone occurrences in the study area, general lithology (after GSI), tectonic framework (Santosh et al., 2014), and field photographs.

The lodestone samples consist primarily of titanomagnetite and ilmenite, with traces of hematite, pleonaste, and ulvöspinel. Ti-magnetite is characterized by the development of a wide range of micro-intergrowth textures that reflect exsolution features resulting from exsolution and oxidation under different temperatures and oxygen fugacity conditions during sub-solidus magma cooling (Lindsley, 1991). The following reaction produces ilmenite and magnetite from ulvospinel:

$$6Fe_2TiO_2 + O_2 \leftrightarrow 6FeTiO_3 + 2Fe_3O_4$$

Ulvospinel intergrowths are interpreted as the result of the exsolution of a magnetite-ulvospinel solid solution under

relatively low oxygen fugacity (Buddington and Lindsley, 1964). Pleonaste usually exsolves at a higher temperature and at an earlier stage than ulvospinel. The granular ilmenite grains surrounded by spots of spinel are formed by the continued solid-state growth of ilmenite crystals during subsolidus cooling because of external granule exsolution (Reynolds, 1978). The XRD pattern exhibits distinct two-theta positions and d-spacing measurements for magnetite (18.2, 30.1, and 63°), ilmenite (20.9, 50.5, 53.2, and 61.6°), hematite (35.5, 33.3, and 57.2°), and spinel (36.9 and 49.19°). This conformation of mineral phases using XRD analysis validates the ability of the present samples to facilitate geothermometric analysis using the magnetite-spinel and hematite-ilmenite buffers. Raman spectral features indicate the presence of magnetite, ilmenite, hematite, chromite, ulvöspinel, and their solid solutions. A major peak in the range 600–800 cm–1 and a few minor peaks at lower wavenumbers correspond to vibration modes A1g, T2g (1), Eg, T2g (2), and T2g (3). The region 600–800 cm–1 is most helpful in discriminating Fe-Ti-Cr-Al substitutions in the magnetite-ulvöspinel, ulvöspinel-chromite, ilmenite-hematite, and chromite-spinel series, but minor peaks in the range 300–600 cm–1 also aid in discrimination.

The bulk rock data reveals varying weight percentages of several oxides, including Fe2O3 (48.5-62.5 wt%), TiO2 (3.5-8.37 wt%), Al2O3 (13-29.5 wt%), V2O5 (0.67-1.38 wt%), and Cr2O3 (3.36-11 wt%). According to several geochemical classification diagrams, the lodestones represent the Fe-V-Ti magnetite type of iron ore, interpreted to have been formed through a magmatic process. Most samples are classified as titanomagnetite-II in the titanomagnetite classification diagram, suggesting that they have undergone late-stage magmatic modifications. The W index value (Fe2O3/Fe2O3+FeO) indicates that the ores have formed from an oxidising magma during the late-stage cooling.

According to mineral chemistry, lodestone magnetite grains include 74.8 to 76.9% FeO(t), 12.9 to 15.8% Cr2O3, and 2.6 to 3.9% Al2O3, whereas ilmenite grains have 37.8 to 41.3% FeO(t) and 53.1 to 53.6% TiO2. Chromium spinels with Cr2O3 contents ranging from 18.4 to 29.6% have also been discovered. The discriminant diagram of Ni+Cr vs. Si+Mg and the triangular diagram based on TiO2-Al2O3-(MgO+MnO) compositions in magnetite indicate that these magnetites are formed in a layered intrusion setting. Mole fractions of ulvospinel in magnetite and hematite in ilmenite were determined by the method of Carmichael (1967), and the temperature and fO2 conditions of coexisting pairs of magnetite and ilmenite were estimated using the methods of Stormer (1968) and Andersen and Lindsley (1985). The results show a temperature range from 479.7 to 673 °C and a fugacity value from -26 to -15.9 for the lodestone samples. The range of fugacity values indicates that the lodestone layers were formed or cooled in an environment with variable oxygen fugacity conditions. The negative fugacity values suggest that the lodestones were formed under higher oxidizing conditions.

Mineral chemistry, textures, and the magnetite-ilmenite geothermometer indicate that the present lodestones are a part of layered igneous intrusion in a subduction zone setting that experienced extensive subsolidus re-equilibration and exsolution at varying conditions of temperature and oxygen fugacity during the magma cooling processes. The lodestone layers were considered to have formed during the early stages of crystallization from an ultramafic magma through gravity settling and introduced into pre-existing fragmented and stratified magmatic intrusions. The presence of lodestone layers can indicate paragenetic and magmatic cooling histories associated with layered igneous complexes observed in similar subduction-related settings worldwide.

References

Andersen, D. J. (1985). New (and final!) models for the Ti-magnetite/ilmenite geothermometer and oxygen barometer. In Abstracts of American Geophysical Union 1985 Spring Meeting. American Geophysical Union.

Anoop, K. S., Anilkumar, Y., Santosh, M., Yu, B., Joy, K. D., Kavyanjali, K. V., Sathyan, A., Mathew, A., & Sajin Kumar, K. S. (2022). Magmatic and metamorphic evolution of a layered gabbro-anorthosite complex from the Coorg Block, southern India: Implications for Mesoarchean supra subduction zone process. Gondwana Research, 103, 105-134.

Buddington, A. F., & Lindsley, D. H. (1964). Iron-titanium oxide minerals and synthetic equivalents. Journal of petrology, 5(2), 310-357.

Carmichael, I. S. (1966). The iron-titanium oxides of salic volcanic rocks and their associated ferromagnesian silicates. Contributions to mineralogy and petrology, 14, 36-64.

Lindsley, D. H. (1991). Oxide minerals: petrologic and magnetic significance. Reviews in Mineralogy, Mineralogical Society of America, pp 509.

Mills, A. A. (2004). The lodestone: History, physics, and formation. Annals of Science, 61(3), 273-319.

Reynolds, R. L., & Goldhaber, M. B. (1978). Iron-titanium oxide minerals and associated alteration phases in some uranium-bearing sandstones. US Geological Survey Journal of Research, 6, 707-714.

Santosh, M., Yang, Q. Y., Shaji, E., Tsunogae, T., Mohan, M. R., & Satyanarayanan, M. (2015). An exotic Mesoarchean microcontinent: the Coorg block, southern India. Gondwana Research, 27(1), 165-195.

Stormer, J. C. (1983). The effects of recalculation on estimates of temperature and oxygen fugacity from analyses of multicomponent iron-titanium oxides. American Mineralogist, 68(5-6), 586-594.

Sukumaran, P. V., & Nambiar, A. R. (2001). Occurrence of

Chromiferous Lodestone near Chalingal, Kasaragod District, Kerala. Geological Society of India, 58(2), 171-173.

Vidyashankar, H. V., & Govindaiah, S. (2009). Ore petrology of the V-Ti magnetite (lodestone) layers of theKurihundi area of Sargur schist belt, Dharwar craton. Journal of the Geological Society of India, 74, 58-68.

Wasilewski, P., & Kletetschka, G. (1999). Lodestone: Nature's only permanent magnet-What it is and how it gets charged. Geophysical research letters, 26(15), 2275-2278.

Yamamoto, Y. (2017). Pull Of History, The: Human Understanding of Magnetism and Gravity Through the Ages. World Scientific.S

Silurian gabbros and granitoids along the Erlangping tectonic belt in Tongbai orogen: Implications for the Late Paleozoic tectonic evolution of the Qinling-Tongbai orogen, China

Zhang Feifei[1,*], Xin Chenghui[1], Gao Hongsen[1], Wang Mingxia[1], Yue Yuangang[1]

[1]State Key Laboratory of Continental Dynamics, Department of Geology, Northwest University, Xi'an 710069, China
[*]E-mail: zhangff@nwu.edu.cn

The Qinling-Tongbai orogen was formed by the multi-stage amalgamation of the North and South China blocks. Tongbai orogen is as the eastern extensional part of Qinling Orogen, but its detail orogenic process and tectonic setting of the late Early Paleozoic are still in dispute. There are some gabbros and granitoids intruded into Erlangping unit. These magmatic rocks provide important constraints on the tectonic evolutionary of the Tongbai orogen. The gabbros selected from Shanshuwan and Zhangjiachong areas yield four weighted mean ages of 432.2 ± 4.3 Ma, 441.3 ± 9.5 Ma, 430.9 ± 3.3 Ma and 432.1 ± 1.6 Ma. Geochemical data shows that these gabbros belongs to tholeiitic basalts series. Their SiO2 content ranges from 46.99 to 50.58 wt.%. They exhibit relative LREE depletion with positive Eu anomalies in the chondrite-normalized REE patterns diagram, and are enrichment in LILEs (Ba, Rb, and Sr) and depleted of HFSE (Nb, Ta, Zr and Hf) in the primitive mantle-normalized diagrams. These rocks have low initial 87Sr/86Sr ratios of 0.7041 – 0.7042 and positive εNd(t) values ranging from +2.3 to +5.3. Our data suggest that the gabbros intruding into the Erlangping tectonic belt have the both the features of N-MORB and IAB. These mafic rocks might be derived from the spinel peridotite mantle source.

The granitoids from Huangjiawan and Bingmasichong areas have identical U–Pb zircon emplacement ages of 436.7 ± 2.8 Ma and 432.9 ± 3.5 Ma, related to northward subduction of the Paleotethyan Ocean. In terms of geochemical compositions, these samples are characterized by high Na2O, and low K2O and TiO2 contents, with enrichment of Rb, Th and Ba and depleted in high field strength elements such as Nb, Ta and Ti in the primitive mantle-normalized diagrams. They also display strong high εNd(t) (+3.7 – +4.7) and zircon εHf (t) (+11.3 – +16.1) values, as well as the young two–stage model ages of Hf isotope (TDM2 = 402 – 643 Ma), suggestive of the involvement of mantle components in the magmatic sources. Therefore, we propose that these granitoids derived from the partial melting of juvenile crust.

Therefore, we consider that the Erlangping back-arc basin has been closed before ca.440 Ma, and the gabbros and granitoids developed in the Erlangping tectonic belt may be related to slab rollback during the northward subduction of the Shangdan ocean or the mafic-magma underplating event caused by the subduction of the mid-ocean ridge.

Mesozoic tectonics of NE China in eastern Central Asian Orogenic Belt

Yongjiang Liu[1,2,*], Boran Liu[1,2], Qingbin Guan[1,2], Sanzhong Li[1,2], Zhaoxu Chen[1,2], Tong Zhou[1,2]

[1]Frontiers Science Center for Deep Ocean Multispheres and Earth System, Key Lab of Submarine Geoscience and Prospecting Techniques, College of Marine Geosciences, Ocean University of China, Qingdao 266100, China
[2]Laboratory for Marine Mineral Resources, Laoshan Laboratory, Qingdao 266237, China
[*]E-mail: liuyongjiang@ouc.edu.cn

The Central Asian Orogenic Belt (CAOB) is the largest accretionary orogen in the world with considerable Phanerozoic juvenile crustal growth. The eastern segment of the CAOB is occupied by NE China and its adjacent areas, which locate in a triangle area surrounded by Siberian Craton to the northwest, North China Craton (NCC) to the south and Pacific oceanic plate to the east. The geophysical data shows that the subducted slab of Paleo-Pacific Plate has reached the Great Xing'an Range, therefore, the entire NE China has been strongly influenced by the subduction process of Paleo-Pacific Plate during Mesozoic time.

In the Middle Jurassic the westward subduction of Izanagi Plat beneath E Asia (Maruyama et al., 1997) and resulted in the back-arc extension, forming extensional faulted basins in the west, while the east area was eroded as highland due to the accretion of Raohe complex to the eastern margin of Jiamusi block triggered by the subduction.

During the Middle-Late Jurassic the subduction direction of Izanagi Plat changed to N/NNW, which resulted in the NE China was controlled by a transtension stress field. A series of sinistral strike-slip faults with NE trending were produced. The offset of the faults decrease from ca. 160 km along Dunhua-Mishan fault in the east to 40-50 km along Nenjiang-Balihan fault in the west, indicating that the deformation stress came from the oblique subduction of Izanagi Plat in the east.

To the time of late Early Cretecouse-early Late Cretecouse, the eastern area started to extension and formed a wide spread fan-basin covered the whole area, probably connecting with the Paleo-Pacific Ocean to the east. With the subduction rollback the extension setting magrited towards east, the western area gradually uplited and the depocenter moved to east. During this period there developed many extensional metamorphic core complexes through E Asia.

During the late Late Cretecouse the subduction direction changed again from NNW to NW and the accretion of the Sihot-Allin terrane to the margin of E Asia, the fan-basin in the NE China was reversed and broken in several small satalite basins (Sanjiang Basin, Hulin Basin, Boli Basin, Jixi Basin, Shuangyashan Basin and Shuanghua Basin). Meanwhile due to the NW-SE compression a set of NW strike-slip faults was produced with a little sinistral offset which cut the previouse NE faults.

Funding: this work was funded by National Natural Science Foundation of China (42130305) and Taishan Scholars (ts20190918).

References

Maruyama S, Isozaki Y, Kimura G. Paleogeographic maps of the Japanese Islands: plate tectonic synthesis from 750 Ma to the present. The Island Arc, 1997, 6(1) : 121-142.

International Association for Gondwana Research 2023 Convention and
20th International Conference on Gondwana to Asia
Niigata, Japan, October 2023
Abstract Volume

Mantle dynamics of the North China Craton originating from slab dehydration

Lin Liu [1,2,3,4,*], Stephen S. Gao [2], Kelly H. Liu[2], William L. Griffin[5], Sanzhong Li[1,4], Siyou Tong[1,4] and Jieyuan Ning[6]

[1]Frontiers Science Center for Deep Ocean Multispheres and Earth System, Key Lab of Submarine Geosciences and Prospecting Techniques, MOE, and College of Marine Geosciences, Ocean University of China, Qingdao 266100, China
[2]Geology and Geophysics Program, Missouri University of Science and Technology, Rolla, MO 65409, USA
[3]Department of Geophysics, Stanford University, Stanford, CA 94305, USA
[4]Laboratory for Marine Mineral Resources, Qingdao National Laboratory for Marine Science and Technology, Qingdao 266237, China
[5]Australian Research Council Centre of Excellence for Core to Crust Fluid Systems (CCFS)/GEMOC, Earth and Planetary Sciences, Macquarie University, Sydney, NSW 2109, Australia
[6]Institute of Theoretical and Applied Geophysics, School of Earth and Space Science, Peking University, Beijing 100871, China
[*]E-mail: Liulin1991@ouc.edu.cn

Cratons are generally defined as stable continental blocks with a strong cratonic root that typically is at least ~200 km thick. Many cratons have undergone little internal tectonism and destruction since their formation, but some of them, such as the eastern part of the North China Craton (NCC), the Dharwar Craton and the Wyoming Craton, have lost their thick cratonic root and become reactivated in recent geological history, leading to widespread Meso-Cenozoic volcanisms. The mechanisms responsible for such decratonization remain debated. To provide new constraints on models leading to decratonization, in this study we stack 612 854 source-normalized P-to-S conversions (receiver functions or RFs) from the 410 and 660 km discontinuities (d410 and d660, respectively) bordering the mantle transition zone (MTZ) recorded at 1986 stations in the NCC. Both the number of RFs and the number of stations are unprecedented in the study area. The average apparent depths of the d410 and d660 and the thickness of the MTZ are 413 ± 6, 669 ± 8 and 255 ± 6 km, respectively. A depression of up to 37 km and mean 11 km of the d660 are clearly observed beneath the eastern NCC, mainly caused by the possible existence of a relatively large amount of water in the MTZ. Our study provides strong observational evidence for geodynamic modelling that suggests water in the MTZ can be driven out into the upper mantle by poloidal mantle flow induced by the subduction and retreat of subducted oceanic slabs. The results are consistent with the weakening of the lithosphere beneath the eastern NCC by the release of water (in the form of structurally bound H/OH) brought down to the MTZ by subduction of the Pacific slab. Continuous slab dehydration and the ascent of fluids would have triggered intraplate volcanism and mantle upwelling in the eastern NCC, as evidenced by the spatial correspondence among the lower-than-normal upper-mantle seismic velocities, unusually large depressions of the d660, Cenozoic basaltic volcanism and thinning of the cratonic lithosphere.

Graphical abstract

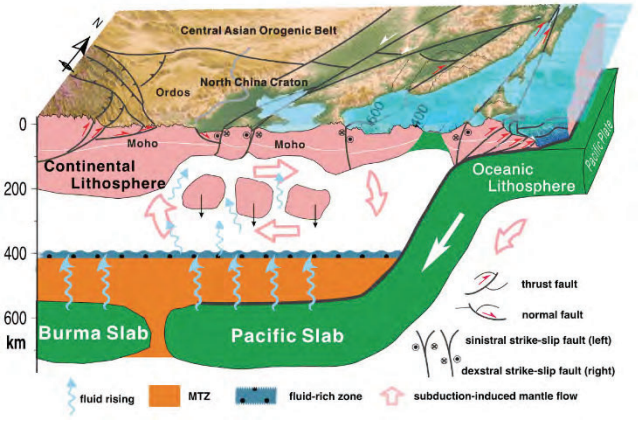

The chemical index of alteration in Permo-Carboniferous strata in North China as an indicator of environmental and climate change throughout the late Paleozoic Ice Age

Longyi Shao

College of Geoscience and Surveying Engineering, China University of Mining and Technology (Beijing), D11 Xueyuan Road, Beijing 100083, China
E-mail: ShaoL@cumtb.edu.cn

The Carboniferous-Permian includes one of the most extreme climate perturbations of the Phanerozoic, entailing the development of profound icehouse conditions in the late Carboniferous-early Permian, followed by the onset of protracted greenhouse conditions towards the end of the Permian. During this interval, glacial deposits were distributed widely in the southern hemisphere, while coal-bearing successions were deposited throughout the paleotropics. The preservation of cyclothems, cyclical repetitions of marine and nonmarine facies including widespread coal beds, in the paleotropical realm including the North China plate, has been attributed to large-scale glacioeustatic sea-level changes, and this interpretation implies that the cyclothemic successions in the low paleolatitudes were also driven by expansions and contractions in southern hemisphere glacial ice on Gondwana.

The chemical index of alteration (CIA), a ratio of mobile elements to immobile elements, can be used as a proxy for calculating chemical weathering intensity. The CIA and estimated land surface temperatures (LSTs) in North China are applied to examine the variations of chemical weathering intensity and temperatures during the late Pennsylvanian-Cisuralian. Then the CIA and LSTs results in North China are compared with equivalent data in synchronous sections in Gondwana Basins. Finally, the timing relationships of glaciation, climate, volcanism, tectonism, and ecosystem changes are considered in the hope of improving understanding of the driving factors of the late Paleozoic Ice Age.

Comparison of CIA and LSTs of the Carboniferous and Permian coal-bearing series in North China with the middle- to high-paleolatitude successions of Gondwana facilitates reconstruction of global climate changes during the late Paleozoic Ice Age. Four synchronous excursions between the North China and Gondwana Basins toward lower CIA and LSTs are recognized and interpreted as four cooling events, respectively. Two severe cooling event occurred around 300 Ma and 287Ma, respectively, with large decreases in global temperatures (mostly >5°C), while another two less-pronounced cooling events at 297.5 Ma and 295 Ma with global temperature drops of <5°C are defined as discrete pulses superimposed on the earlier, more severe cooling interval. Overlap in the timing of decreased chemical weathering intensity in different parts of North China and glaciations in some Gondwanan Basins that coincide with stepwise decreases in pCO2 suggest that CO2-forced climate change was likely one of the most important driving factors for the continental weathering changes and the onset and demise of glaciations. Local tectonism, atmospheric and ocean circulation, and orbital parameters also played the roles in driving the glaciations and deglaciations. The continued effects from weathering of worldwide mafic rocks along with expansion of paleotropical forests are considered to be contributors to the cooling intervals along with glacial events and evolution of ecosystems during the late Pennsylvanian-Cisuralian.

International Association for Gondwana Research 2023 Convention and
20th International Conference on Gondwana to Asia
Niigata, Japan, October 2023
Abstract Volume

Rheology of basement complex from the middle and lower crust of the North Qinling Orogenic Belt

Li Yixi[1,*], Sun Shengsi[1], Dong Yunpeng[1,2], Yu Kecheng[1], Li Yongcheng[1]

[1] State Key Laboratory of Continental Dynamics, Department of Geology, Northwest University, Xi'an 710069, China
[2] Collaborative and Innovation Research Centre of Continent Tectonics, Northwest University, Xi'an 710069, China
[*]E-mail: yixi_li0629@163.com

The basement complex in the middle part of the North Qinling Orogenic Belt is characterized by strong migmatization, with deformation features of deep plastic rheology and ductile shear zones, implying the rheological weakening processes in the middle and lower crust under different conditions. High-grade metamorphic rocks such as migmatized gneiss and lenticular amphibolite are exposed in the middle part of the North Qinling Orogenic Belt, which provide an ideal object for research on rheological weakening and strain localization of the middle and lower continental crust. Banded migmatites are widely exposed in the study area, usually accompanied by the formation of strongly deformed domains, while the weakly deformed domains usually develop granitic rocks, weakly deformed amphibolite and a small amount of marble. The migmatites are generally amphibolite-facies metamorphosed with structures such as boudinage structures, flowage folds, and S-C fabric, indicating north-south compression and NWW-SEE sinistral shearing. Zircon morphology and U-Pb ages show that the anatexis of Precambrian basement complex was constrained at 400–386 Ma, and ductile deformation of 132 Ma was superimposed in the Shagou area on the south side. Migmatites were formed at 595–691℃ and 2.32–6.31 kbar, and the occurrence of peritectic amphibole, melt pockets, and variation of mineral major compositions indicated a relatively water-rich environment. The mesosomes of migmatites are composed of gneiss and plagioclase amphibolite, which inherit the parental strong deformation characteristics. Quartz in the gneiss has a high temperature fabric caused by prism <a> slip, while the deformation of feldspar is dominated by intragranular dislocation slip, forming the B-type fabric caused by (010) [100] slip. Amphibole in the amphibolite is dominated by (100) [001] dislocation slip, while plagioclase doesn't display clear fabric. The deformation of melanosome is jointly controlled by intragranular plastic deformation and grain boundary sliding. Due to the effect of aqueous fluid, the deformation mechanism of plagioclase amphibolite is dominated by dissolution-precipitation creep with the formation of type I fabric of amphibole, while amphibolite is dominated by semi-brittle deformation, together with rigid body rotation and grain boundary sliding, and forms type II fabric due to the infiltration of melt (fluid). The leucosome is characterized by magma flow, but quartz shows the characteristics of coaxial flattening and forms the fabric caused by the prism <a> slip, while feldspar forms B-type fabric caused by (010) [100] slip in the continuous progressive deformation processes. The formation of migmatites is accompanied by strain localization, while the increase in melt content leads to a decrease in the strength of the middle and lower crust and the formation of the North Qinling island arc terrane. Combined with regional geological data, it can be seen that the anatexis of the basement complex in the middle part of the North Qinling occurred under the background of the collision between the North China block and the South China block after the closure of the Shangdan Ocean, which led to the formation of amphibolite-facies migmatites and strain localization in the orogenic belt.

International Association for Gondwana Research 2023 Convention and
20th International Conference on Gondwana to Asia
Niigata, Japan, October 2023
Abstract Volume

Micro-textures, in-situ trace elements and C-H-O isotopes from the Baguamiao gold deposit, Western Qinling, Central China: Implication for mineralization processes

Hui-Dong Yu[1], Yu-Zhen Fu[1], Nuru Said[2], Hua-Wen Cao[1], Wei-Xuan Fang[3], Jia-Jun Liu[4], Hai-Feng Chen[1], Chang-Cheng Huang[1], Hao Zou[1*]

[1] State Key Laboratory of Oil and Gas Reservoir Geology and Exploitation, Chengdu University of Technology, Chengdu, Sichuan 610059, China
[2] Department of Mineral and Rocks, King Abdul-Aziz University, Jeddah 20206, Saudi Arabia
[3] China Non-ferrous Metals Resource Geological Survey, Beijing 100012, China
[4] State Key Laboratory of Geological Process and Mineral Resources, China University of Geosciences, Beijing 100083, China
[*]E-mail: zouhao21@gmail.com

The Baguamiao gold deposit, located in the Fengxian-Taibai ore district, is one of the largest gold deposits in the West Qinling orogen, central China (Wang et al., 2020; Ding et al., 2021). However, the occurrence state and mechanism of gold precipitation are still unclear. In addition, there is no consensus on the source of metals and ore-forming fluids. The relationship between gold mineralization and magmatic activity, and the classification of ore deposits are also poorly understood. Therefore, more systematic geochemical studies are urgently needed to obtain the detailed process of the deposit formation and mechanism of metal precipitation (Mao et al., 2002; Chen et al., 2004; Chen and Santosh, 2014).

In this contribution, ore characteristics, the mineralogical texture, in-situ trace elements and chemical mapping of sulfide, as well as the C-H-O isotopes of quartz, ankerite and calcite were used to define occurrence state of gold, the evolution of ore-forming fluid and the mechanism of gold precipitation. This combined with previous studies, assists to better constrain the genesis of the Baguamiao gold deposit and explore the tectonic evolution and genetic model of gold deposits in the West Qinling, we draw the following conclusions:

(1) Invisible gold occurs dominantly as solid solutions (Au^{+}) in the lattice of pyrite and pyrrhotite, and the occurrence of Cu and Te promotes the enrichment of lattice gold. Pb-Bi-Ag-Sb occur as galena and sphalerite micro-inclusions in the pyrite and pyrrhotite.

(2) The ore-forming fluid is a mixed source of metamorphic water, magmatic water and meteoric water, and the carbon is dominantly derived from deep magma. During its evolution, phase separation, fluid-rock interaction and fluid mixing are the main mechanisms of gold precipitation in the Baguamiao gold deposit.

(3) The Baguamiao gold deposit is an orogenic gold deposit under the crustal continuum model which related to the closure of the East Paleo-Tethys Ocean.

References

Wang, Y.T., Mao, J.W., Zhang, J., Wang, R.T., Chen, G.M., Hu, Q.Q., Chen, S.C., Liu, X.L., 2020. Geochronological constraints on the Baguamiao gold deposit, West Qinling orogen, central China: Implications for ore genesis and geodynamic setting. Ore Geol. Rev. 122, 103508.

Ding, L.L., Zhu, L.M., Xiong, X., Zhang, G.W., Li, S.H., 2021. Genesis of the Maanqiao gold deposit in the western Qinling orogen, central China: Constraints from fluid inclusions and in-situ sulfur isotopes. Geochemistry 81, 125691.

Mao, J.W., Qiu, Y.M., Goldfarb, R.J., Zhang, Z.C., Garwin, S., Fengshou, R., 2002. Geology, distribution, and classification of gold deposits in the western Qinling belt, central China. Mineral. Deposita. 37, 352–377.

Chen, Y.J., Zhang, J., Zhang, F.X., Pirajno, F., Li, C., 2004. Carlin and Carlin-like gold deposit in Western Qinling mountains and their metallogenic time, tectonic setting and model. Geological Rev. 50, 134–152 (in Chinese with English abstract).

Chen, Y.J., Santosh, M., 2014. Triassic tectonics and mineral systems in the Qinling Orogen, central China. Geol. J. 49, 338–358.

International Association for Gondwana Research 2023 Convention and
20th International Conference on Gondwana to Asia
Niigata, Japan, October 2023
Abstract Volume

Petrography and Rb-Sr mineral age of mafic dyke rocks on Niban-Rock, Lützow-Holm Complex (LHC), East Antarctica

Tomoharu Miyamoto[1,*], Katsuyuki Yamashita[2], Daniel J. Dunkley[3], Toshiaki Tsunogae[4], and Mutsumi Kato[5]

[1]Department of Earth and Planetary Sciences, Faculty of Science, Kyushu University, 744 Motooka, Nishi-ku, Fukuoka, 819-0395, Japan
[2]Department of Earth Sciences, Okayama University, 1-1-1 Tsushima-naka, Kita-ku, Okayama 700-8530, Japan
[3]Department of Polar and Marine Research, Institute of Geophysics, Polish Academy of Sciences, PL-01452, Warsaw, Poland
[4]Faculty of Life and Environmental Sciences, University of Tsukuba, 1-1-1 Tennodai, Tsukuba, Ibaraki, 305-8577, Japan
[5]Nittetsu Mining Consultants Co., Ltd. Minato–ku, Tokyo 108–0014, Japan
[*]E-mail: miyamoto@geo.kyushu-u.ac.jp

The LHC of the Dronning Maud Land, situated west of the Rayner Complex and east of the Yamato–Belgica Complex of East Antarctica, is a high-grade metamorphic terrane within the East Antarctic Shield. Niban Rock is a 2.5 km × 3.5 km exposure located at northeast LHC and is corresponded into the amphibolite–facies zone defined by Hiroi et al. (1991). Niban Rock is composed of Niban–higashi Rock and Niban–nishi Rock, and is underlain mainly by sillimanite–garnet–biotite gneiss, biotite gneiss, and biotite–hornblende gneiss along with minor metabasite, calc–silicate gneiss, granite, and aplite (Kizaki et al., 1983). Recently, metamorphic facies analysis and geochronological results for the metamorphic rocks have been reported (Dunkley et al., 2020; Kitano et al., 2021; Mori et al., 2023).

Although the intrusive rocks were less voluminous than the widespread metamorphic rocks, the emplacement of the mafic dyke which cut metamorphic textures and structures was recognized in the Niban-higashi Rock. At the Niban-higashi Rock, the mafic dyke was a few tens cm width intrusive to 10 m length at least, oriented mostly to the WNW-ESE direction, and cut sharply through the foliage of the surrounding host gneisses. The dyke does not exhibit textures resembling the major metamorphic structures found in the surrounding basement rocks. The boundary between the dyke and surrounding host gneisses had no reactive textures. Therefore, the dykes intruded after peak metamorphism at the Niban-Rock.

The mafic dyke rocks are commonly holocrystalline and aphyric. They consisted mainly of alkali feldspar, plagioclase, biotite, hornblende, quartz, apatite, and titanite. The crystals often grow in parallel arrays in the intrusive direction of the dyke. The mafic dyke rocks from Niban-Rock have alkalic compositions and enriched to incompatible elements. On the spidergram, the normalized incompatible element patterns generally display a slow downward trend to the right, with enrichment in Ba and Rb more than 110 and 150 times that of the primitive mantle, respectively, and high values of large ion lithophile element-to-high field strength element ratios (LILE/HFSE). In the spidergram, troughs are evident for Nb, Ti, and Sr, whereas peaks of variable size are present for Pb. For chronological research, the mafic fractions (biotite and hornblende) and felsic fractions (plagioclase and orthoclase) were separated from crushed mafic rock samples. The Sr isotope compositions as well as the total Rb and Sr concentrations were determined by TIMS using a Finnigan MAT-262 system at Okayama University. Their 87Rb/86Sr and 87Sr/86Sr values are aligned on the isochron diagram, and the age showed 500.9 ± 0.2 Ma and IR = 0.704665 ± 0.000016). Mafic dykes at Niban-Rock suggest the presence and timing of mantle-involved igneous activity after major metamorphism at the NE LHC. Besides, the higher Sr initial isotopic compositions of mafic rocks than the CHUR or depleted mantle values at that time is also suggested that the possibility of assimilation of crustal material during mafic magma formation.

Regarding mafic dyke intruded after LHC metamorphism, the intrusive direction of the mafic rocks in Niban-Rocks was NW-SE, but at Akebono Rock in the eastern part of the LHC, the intrusion direction of mafic dykes was N-S or NW-SE (Hiroi et al., 1986). At the Cape Hinode in the eastern part of the LHC, mafic dykes intruded in the NE-SW or N-S direction (Yanai and Ishikawa, 1978). On the other hand, the direction of intrusion of ultrapotassic mafic rocks, which were intruded just after peak metamorphism in the western part of the LHC (Innhovde, Rundvågshetta, etc.) is generally N-S, which is different from that in the eastern part of the LHC (Arima and Shiraishi, 1993; Miyamoto et al., 2023). Although there are some unknown factors in their detailed intrusion timing, considering that the direction of intrusion is closely related to the stress field at that time, the stress field just after

metamorphism was different between the eastern and western parts of the LHC, otherwise, there is a possibility that the zonal structure changed after the intrusion.

References

Arima, M. and Shiraishi, K. (1993): Proc. NIPR Symp. Antarct. Geosci., 6, 103-115.

Dunkley, D. J., Hokada, T., Shiraishi, K., Hiroi, Y., Nogi, Y. and Motoyoshi, Y. (2020): Polar Science, 26, 100605.

Hiroi, Y., Shiraishi, K. and Motoyoshi, Y. (1991): In Thomson, Crame, and Thomson (eds.) Geological Evolution of Antarctica. Cambridge University Press, 83-87.

Kitano, I., Hokada, T., Baba, S., Kamei, A., et al. (2021): the 12th Symposium on Polar Science. National Institute of Polar Research.

Kizaki, K., Hiroi, Y. and Kanisawa, S. (1983): Geological map of Niban Rock, Antarctica. Geol. Map. Ser., Sheet 17, Natl. Inst. Polar Res.

Miyamoto, T., Yamashita, K., Dunkley, Daniel J., Shimada, K., Tsunogae, T., Kato, M. (2023): Journal of Mineralogical and Petrological Sciences, 118, Issue ANTARCTICA, (in print).

Mori, Y., Hokada, T., Miyamoto, T., and Ikeda, T. (2023): Journal of Mineralogical and Petrological Sciences, 118, Issue ANTARCTICA, S005.

International Association for Gondwana Research 2023 Convention and
20th International Conference on Gondwana to Asia
Niigata, Japan, October 2023
Abstract Volume

Preliminary works on the structural interpretation of the Seosan-Taean area, western Gyeonggi Massif, Korea

Seongjae Park[1,*], Donghyeok Lee[2], Minho Kang[1], Yirang Jang[1], Sanghoon Kwon[2]

[1]Department of Geological and Environmental Sciences, Chonnam National University, Gwangju 61186, Republic of Korea.
[2]Department of Earth System Sciences, Yonsei University, Seoul 03722, Republic of Korea.
[*]E-mail: star980518@jnu.ac.kr

Over the past two decades, various geological studies have been conducted in the western Gyeonggi Massif, yielding crucial evidence regarding the plate marginal processes from the Proterozoic to the Mesozoic (e.g., Oh et al., 2005; Kwon et al., 2009; Kim et al., 2013; Park et al., 2018). This led to the western Gyeonggi Massif as a prominent contractional orogenic belt in the East Asian continental margin (e.g., Kwon et al., 2009; Kim et al., 2015; Kee et al., 2019). The Seosan-Taean area is located at the west margin of this region, preserving evidence of the multiple tectono-thermal events related to subduction and collision of the tectonic Wilson cycle with typical fold-thrust belt features.

In the Seosan-Taean area, the Proterozoic Seosan Group served as basement for the overlying Paleozoic Taean and Mesozoic Seokmun formations, showing distinct map patterns defined by systematically repeated NE-SW striking quartzites, schists, and calc-silicate layer of the Seosan Group. To understand the structural geometry of this area, we have conducted detailed field mapping and realistic geometric interpretations using down-plunge projections (Marshak and Mitra, 1988). Preliminary results indicate that the repetition of NE-SW striking layers in the study area can be attributed to synformal depressional folding, which plunges to the southwest in the northern part and northeast in the southern part. The spatial and temporal evolution of these structures as well as their structural relationship with the overlying Taean Formation will provide a better understanding of a prominent mountain belt in the Seosan-Taean area of the western Gyeonggi Massif. This eventually will help to understand the role of the western Gyeonggi Massif during tectonic evolution of the East Asian continents over its evolution history.

References

Kee, W.-S., Kim, S.W., Kim, H., Hong., P., Kwon, C.W., Lee, H.-J., Cho, D.-L., Koh, H.J., Song, K.-Y., Byun, U.H., Jang, Y., Lee, B.C., 2019b. Geologic map of Korea. KIGAM, scale 1:1,000,000.

Kim, S.W., Kee, W.-S., Lee, S.R., Santosh, M., Kwon, S., 2013. Neoproterozoic plutonic rocks from the western Gyeonggi massif, South Korea: Implications for the amalgamation and break-up of the Rodinia supercontinent. Precambrian Res 227, 349-367.

Kim, S.W., Kwon, S., Park, S.-I., Yi, K., Santosh, M., Ryu, I.-C., 2015. Early to Middle Paleozoic arc magmatism in the Korean Peninsula: Constraints from zircon geochronology and geochemistry. J. Asian Earth Sci. 113, 866-882.

Kwon, S., Sajeev, K., Mitra, G., Park, Y., Kim, S.W., Ryu, I.-C., 2009. Evidence for Permo-Triassic collision in Far East Asia: The Korean collisional orogen. Earth Planet. Sci. Lett. 279, 340-349.

Oh, C.W., Kim, S.W., Choi, S.G., Zhai, M., Guo, J., Krishana, S., 2005. First finding of eclogite facies metamorphic event in South Korea and its correlation with the Dabie-Sulu Collision Belt in China. J. Geol. 113, 226-232.

Park, S.-I., Kwon, S., Kim, S.W., Hong, P.S., Santosh, M., 2018. A Mesozoic orogenic cycle from post-collision to subduction in the southwestern Korean Peninsula: New structural, geochemical, and chronological evidence. J. Asian Earth Sci. 157, 166-186.

Marshak, S., Mitra G., 1988. Basic Method of Structural Geology: Prentice Hall, 446p.

International Association for Gondwana Research 2023 Convention and
20th International Conference on Gondwana to Asia
Niigata, Japan, October 2023
Abstract Volume

The garnet effect on hafnium isotope compositions of granitoids during crustal anatexis

Long Chen[1,2,3,*], Chris Yakymchuk[4], Kai Zhao[2], Zifu Zhao[2,3,5], Dongyong Li[1], Peng Gao[6], Yixiang Chen[2,3,5], Guochao Sun[2], Zhibin Liu[2]

[1]Frontiers Science Center for Deep Ocean Multispheres and Earth System, Key Lab of Submarine Geosciences and Prospecting Techniques, MOE and College of Marine Geosciences, Ocean University of China, Qingdao 266100, China
[2]CAS Key Laboratory of Crust-Mantle Materials and Environments, School of Earth and Space Science, University of Science and Technology of China, Hefei 230026, China
[3]Center of Excellence for Comparative Planetology, Chinese Academy of Sciences, Hefei 230026, China
[4]Department of Earth and Environmental Sciences, University of Waterloo, Waterloo, Ontario N2L 3G1, Canada
[5]Frontiers Science Center for Planetary Exploration and Emerging Technologies, University of Science and Technology of China, Hefei 230026, China
[6]School of Earth Science and Geological Engineering, Sun Yat-sen University, Guangzhou 510275, China
[*]E-mail: chenlong@ouc.edu.cn

Radiogenic Hf isotope disequilibrium during crustal anatexis complicates petrogenetic studies that link sources to sinks in granitoids systems and hinders the applications of Hf isotope to evaluate long-term crustal growth and evolution. Garnet can be a dominant host of radiogenic Hf in crustal rocks and its behavior in granitoid sources may play a crucial role in isotopic decoupling between residue and melt. We document covariation between (Gd/Lu)N ratios and εHf(t) in post-collisional granitoids from the Dabie orogen. This covariation reflects different garnet modal contents in the residue during anatexis. Quantitative modeling further confirms the dominant role of mixing between melts derived from garnet-rich and garnet-poor residua in producing the observed covariation patterns, but results are inconsistent with the entrainment of garnet rich in radiogenic Hf in the melt. Our results demonstrate that the garnet effect on Hf isotope ratios during crustal anatexis is a crucial factor in elucidating the granitoids source and complicates interpretations of crustal growth from the global zircon archive.

Trondhjemites from the Western Dharwar Craton, Southern India: Implications for Mesoarchean crustal growth

Ming-Xian Wang[1], M. Santosh[1,2,*], M. Jayananda[3], Cheng-Xue Yang[1], Tarun T. Thomas[3], Sung Won Kim[4]

[1]School of Earth Sciences and Resources, China University of Geoscience Beijing, Beijing 100083, P.R. China
[2]Department of Earth Science, University of Adelaide, Adelaide SA 5005, Australia
[3] Centre for Earth, Ocean and Atmospheric Sciences, University of Hyderabad, Hyderabad - 500 046, India
[4]Geology Division, Korea Institute of Geoscience and Mineral Resources, Daejeon 34132, Republic of Korea
[*]E-mail: santosh@kochi-u.ac.jp

Trondhjemite, together with tonalite and granodiorite (TTG) are important building blocks of the Archean continental crust and their studies provide insights into the formation of the early continents. The Western Dharwar Craton (WDC) in southern India contains voluminous TTG rocks that record prolonged Archean crustal evolution history with evidence for multiple episodes of magmatic accretion and metamorphic events from the Paleoarchean (~3600 Ma) to Archean-Proterozoic transition (~2500 Ma ago). In this study, we investigate trondhjemites from different typical locations in the WDC. Petrological, geochemical and zircon U-Pb, REE and Lu-Hf data are presented and evaluated to understand the timing of magmaemplacement and petrogenetic history. The trondhjemites in our study were generated from partial melting of juvenile hydrous basalt with arc features. The melting depth is variable, mainly shallow, while some melts originated at greater depths with variable plagioclase, amphibole with or without garnet, ilmenite or rutile in source residue. The age data presented here suggest that the crust accretion of the Mesoarchean Western Dharwar Craton occurred dominantly at 3.13-3.27 Ma followed by reworking of lower crustal basement 3.0-2.9 Ga.

International Association for Gondwana Research 2023 Convention and
20th International Conference on Gondwana to Asia
Niigata, Japan, October 2023
Abstract Volume

New zircon U–Pb geochronology of high-pressure schists from the Itoigawa-Omi area in the Hida Gaien Belt, Japan

Ippei Kitano[1,2,*], Yasuhito Osanai[1], Tatsuki Tsujimori[3], Ko Takenouchi[4], Nobuhiko Nakano[1]

[1]Kyushu University, Fukuoka, Japan
[2]Hokkaido University, Sapporo, Hokkaido, Japan
[3]Tohoku University, Miyagi, Japan
[4]Fossa Magna Museum, Itoigawa, Niigata, Japan
[*]E-mail: kitano@museum.hok

Late Paleozoic high-pressure (HP) schists occur as large tectonic blocks (up to ~6 km in length) in an antigorite-bearing serpentinite mélange in the Itoigawa-Omi area (western part of Niigata Prefecture), which is located in the northmost Hida Gaien Belt (e.g., Matsumoto et al., 2011). The HP schists record mainly greenschist/blueschist transitional-facies to amphibolite-facies and locally preserve blueschist- to eclogite-facies metamorphism. The serpentinite mélange also includes blocks of Early Paleozoic metagabbro, amphibolite, and rare jadeitite (e.g., Tsujimori, 2002; Kunugiza et al., 2004, 2017; Matsumoto et al., 2011). Based on the preservation of blueschist- to eclogite-facies mineral assemblages and the distribution of Banno (1958)'s "garnetiferous bed", Tsujimori (2002) divided the HP schists' exposure into the Eclogitic Unit (EC unit) and non-Eclogitic Unit (non-EC unit). Note that the non-EC unit represents the Banno (1958) and Matsumoto et al. (2011)'s Biotite Zone. Although previous studies have shown no significant difference among phengite K–Ar (or Ar/Ar) ages in two different units, no systematic zircon U–Pb geochronology has been applied yet. This contribution presents our new zircon geochronology from four samples (garnet blueschist: 805T01A, 805T01G; quartz-rich mica schist: 80504, 80501) from the EC unit of the Agero area and two samples (biotite-bearing metasedimentary schist: 80401C and 80402A) from the non-EC unit of the Hashidate area. All analyzed zircon grains exhibit a core-rim texture in the CL image, with normally rounded detrital cores rimmed by thin rims. In the EC unit samples, detrital cores of samples 805T01A, 805T01G and 80504 have concordant U–Pb ages ranging from 1462 ± 66 to 365 ± 21 Ma (n = 44), from 3008 ± 122 to 375 ± 12 Ma (n = 75), from 2361 ± 61 to 450 ± 16 Ma (n = 11), respectively. Similar range from 2785 ± 79 to 338 ± 16 Ma (n = 69) was also obtained from sample 80501. In the non-EC unit samples, detrital cores ages in samples 80401C and 80402A range from 506 ± 35 to 332 ± 19 Ma (n = 19) and from 2065 ± 60 to 315 ± 17 Ma (n = 22), respectively.

These new data confirmed that protoliths of both two units contain Early to Middle Paleozoic detrital zircons (~470 Ma, ~450 Ma, and ~400 Ma), which are significantly younger than hydrothermal zircons from jadeitite (~530–520 Ma) and igneous relict zircon (~590 Ma) of some jadeitites in the same mélange (Kunugiza et al., 2017). Moreover, we did confirm the presence of Mesoproterozoic to Archean detrital zircons in both units, which are common feature of the Japanese Late Paleozoic geotectonic units. Naturally, the provenance of such old zircon can be linked to the eastern portion of the North China Craton. Although we have not yet constrained the age of the metamorphic thin rims, discordance arrays suggest a Late Paleozoic HP metamorphic event in both two units. To further our understanding of the precise timing of HP metamorphism, more detailed geochronology is required than that documented in previous studies.

References

Basupi, T.O., Tsunogae, T., Tsutsumi, Y., 2022. Petrology and geochronology of sapphirine-bearing granulites from the Limpopo Complex in eastern Botswana: Implications for Paleoproterozoic long-lived high-pressure/ultrahigh-temperature metamorphism and rapid exhumation. Geol. J., 57, 4194-4215.

Kunugiza, K., Goto, A., Itaya, T., & Yokoyama, K., 2004. Geological development of the Hida Gaien belt: Constraints from K-Ar ages of high P/T metamorphic rocks and U–Th–Pb EMP ages of granitic rocks affecting contact metamorphism of serpentinite. Geol. Soc. Japan, 110, 580–590 (in Japanese with English abstract).

Kunugiza, K., Nakamura, E., Goto, A., Kobayashi, K., Ota, T., Miyajima,H., & Yokoyama, K., 2017. In–situ U-Pb zircon age dating deciphering the formation event of the omphacite growth over relict edenitic pargasite in omphacite–bearing jadeitite of the Itoigawa-Omi area of the Hida-Gaien belt, central Japan. J. Mineral. Petrol. Sci., 112, 256–270.

Matsumoto, K., Sugimura, K., Tokita, I., Kunugiza, K., & Maruyama, S., 2011. Geology and metamorphism of the Itoigawa-Omi area of the Hida Gaien Belt, central Japan: Reconstruction of the oldest Pacific type high P/T type metamorphism and hydration metamorphism during exhumation. J. Geog., 120, 4–29 (in Japanese with English abstract).

Tsujimori, T., 2002. Prograde and retrograde P-T paths of the Late Paleozoic glaucophane eclogite from the Renge Metamorphic Belt, Hida Mountains, Southwestern Japan. Int. Geol. Rev., 44, 797–818.

Geochemical evolution of fertile upper mantle peridotite implies unbroken mantle keel beneath East Asia

Vinod O. Samuel[1], Sanghoon Kwon[1], Yirang Jang[2,*], Youngwoo Kil[3], M. Santosh[4,5,6]

[1]Department of Earth System Sciences, Yonsei University, Seoul 03722, Republic of Korea
[2]Department of Earth and Environmental Sciences, Chonnam National University, Gwangju 61186, Republic of Korea
[3]Department of Energy and Resources Engineering, Chonnam National University, Gwangju 61186, Korea
[4]School of Earth Sciences and Resources, China University of Geosciences Beijing, Beijing 100083, China
[5]Department of Earth Science, University of Adelaide, Adelaide SA 5005, Australia
[6]Faculty of Science, Kochi University, Kochi 780-8520, Japan
[*]E-mail: yirang@jnu.ac.kr

Whether upper mantle roots of continents are evolved geochemically or have been delaminated and replaced by new mantle is a major unresolved question. One of the prominent geochemical change observed globally in mantle peridotites is the transformation of depleted harzburgite to fertile lherzolite. In this study, we present direct evidence of geochemical evolution of peridotite xenoliths preserved in the Cenozoic alkali basalts from the Jeju Island, Korea. The xenoliths mainly consist of olivine, clinopyroxene, orthopyroxene, and minor spinel, showing visible partial alteration of orthopyroxene to clinopyroxene, olivine, and minor spinel. Salient geochemical features include high-Na, Cl concentration in melt pockets and in minerals, spoon shaped earth element pattern, and low oxygen isotope ratios of minerals. These characteristics imply that chloride - carbonatite (kimberlite) melt could have infiltrated from the deeper mantle during Paleozoic. Further interaction of these xenoliths with Cenozoic alkali basalt melt have generated enrichment in Fe, light REE's, and oxygen isotope ratios of minerals. Our results suggest that harzburgitic upper mantle partially evolved to a lherzolitic in composition during interaction with melts/fluids originated from the deep mantle, preserving an unbroken upper mantle root of the East Asian continents.

International Association for Gondwana Research 2023 Convention and
20th International Conference on Gondwana to Asia
Niigata, Japan, October 2023
Abstract Volume

Mineral chemistry and thermobarometry of xenoliths from the Kyrgyz-Tianshan basalts

Nancy Hui-Chun Chen[1,*], Peter A.Cawood[2], Yoshiyuki Iizuka[3]

[1]Department of Resources Engineering, National Cheng Kung University, Tainan 70101, Taiwan
[2]School of Earth, Atmosphere and Environment, Monash University, Clayton, VIC 3800, Australia
[3]Institute of Earth Sciences, Academia Sinica, Taipei 11529, Taiwan
[*]E-mail: huichun@gs.ncku.edu.tw

We present a detailed chemical study of mantle xenoliths from the Ortosuu and Uchkuduk basalt sites, located at the central portion of the Kyrgyz-Tianshan orogenic belt. Establishing the xenolith geotherm in the regions is essential for reconstructions associated with upper mantle and lower crustal processes. Two groups of clinopyroxene can be identified from the studied xenoliths based on their Mg number (Mg #) and trace element patterns. Group 1, primitive clinopyroxenes, has lower Mg #, 86–90, and LREE-depleted patterns than group 2, depleted clinopyroxenes, which are characterized by a relatively high Mg numbers (91–92) and LREE-enriched patterns. The REE distribution in group 1 clinopyroxenes suggests that they were controlled by partial melting, whereas group 2 clinopyroxenes are far more complex involving partial melting degree of 6–11 %, and later modification by carbonatite and/or silicate melts during metasomatism. Coupled P-T estimations from geothermobarometry indicate that the more fertile group 1 xenoliths were probably derived from the uppermost mantle and the more depleted group 2 xenoliths were likely transported from a depth close to the crust mantle boundary beneath the Tianshan.

International Association for Gondwana Research 2023 Convention and
20th International Conference on Gondwana to Asia
Niigata, Japan, October 2023
Abstract Volume

Preliminary studies on structural evolution at an oblique Transverse Zone, Okcheon fold-thrust belt, Korea

Changyeob Kim[1,*], Jungrae Noh[1], Dawon Kim[1], Sanghoon Kwon[1], Yirang Jang[2]

[1]Department of Earth System Sciences, Yonsei University, Seoul 03722, Republic of Korea
[2]Department of Geological and Environmental Sciences, Chonnam National University, Gwangju 61186, Republic of Korea
[*]E-mail: kcy0202@yonsei.ac.kr

The NE-SW trending Okcheon Belt is a prominent fold-thrust belt(FTB) that preserved multiple phases of orogeny that provides significant evidence related to the evolution of the southern part of the Korean peninsula. Within this belt, two distinct zones named Taebaeksan and Okcheon zones have been conventionally divided based on differences in lithology, deformation structures, and metamorphic conditions. The geological relationship between them is still debated because of the lack of insufficient information for explaining their differences along a transverse zone, namely the Kwanbong Transverse Zone.

To figure out the nature of the Kwanbong Transverse Zone, we have delineated the structural geometry of each zone with detailed kinematic analyses, where overall structural trend changes at the Kwanbong area to unveil the geologic contact relationship between the two zones. The structural geometry of the area is reinterpreted by constructing cross-section profiles using down plunge projection with additional information from the detailed field mapping, SHRIMP U-Pb age dating, and biomarker analysis as a chemical fossil. Kinematic analyses including the maximum stretching directions of the finite strain and the maximum shortening directions from the acute bisectors of the conjugate fracture sets were also conducted to derive the kinematic directions at different stages. The results indicate that (1) the Hwanggangri and Seochangri formations are folded into a first-order anticline-syncline pair, and the Gounri Formation and the age-unknown lime-silicate rock at its eastern limb are in fault contact with the Seochangri Formation, (2) a folded Bonghwajae thrust placed the older Ordovician limestone on top of the younger Yongam formation defining a tectonic window, namely the Yongam tectonic window hereafter, (3) differences in structural styles are preserved along the Kwanbong area of the Okcheon Belt, and are represented by the NE-SW trending anticline-syncline pair in the Okcheon Zone and refolded NS trending anticline-syncline pair and Bonghwajae thrust in the Taebaeksan Zone, respectively.

Further studies are necessary to figure out better structural geometric interpretation and kinematics of the study area for defining the geological relationship between the two zones along a oblique transverse zone. Our findings will help us understand the structural evolution of the Okcheon Belt as a whole and the nature of the transverse zone in fold-thrust belt in general.

Meso- to Neoarchean Geological Evolution of the Wutai Complex, North China Craton: Implications from Geochemistry and Zircon Geochronology on the Metavolcanics

Pin Gao[1, 2], M. Santosh[1, 3, 4, *], Toshiaki Tsunogae[2, 5], Cheng-Xue Yang[1, 6]

[1]School of Earth Sciences and Resources, China University of Geosciences Beijing, 29 Xueyuan Road, Beijing 100083, P.R. China
[2]Graduate School of Life and Environmental Sciences, University of Tsukuba, Ibaraki, Japan
[3]Department of Earth Sciences, University of Adelaide, Adelaide SA 5005, Australia
[4]Faculty of Science, Kochi University, Kochi 780-8520, Japan
[5]Department of Geology, University of Johannesburg, Auckland Park, South Africa.
[6]Institute of Earth Sciences, China University of Geosciences Beijing, 29 Xueyuan Road, Beijing 100083, P.R. China
[*]E-mail: santosh@cugb.edu.cn

Precambrian terranes offer valuable insights into the early crustal evolution history of the Earth. The Wutai Complex located at the central part of the Trans-North China Orogen in the North China Craton (NCC) preserves the Precambrian basement of the craton. This study presents whole-rock geochemistry, zircon U-Pb geochronology, and the zircon Lu-Hf isotope data on the metavolcanic rocks (metabasalt and felsic tuff) from the Wutai Complex. The whole-rock geochemistry indicates that the Mesoarchean and Neoarchean volcanics can be divided into calc-alkaline IAB-type and tholeiitic MORB-type volcanics. The metabasalt shows a 207Pb/206Pb weighted mean age of 2884 ± 16 Ma, which is the oldest zircon U-Pb age reported from the Wutai Complex.The felsic tuff sample shows 207Pb/206Pb weighted mean age of 2557 ± 10 Ma. Zircon Lu-Hf results indicate that the felsic tuff was derived from enriched juvenile sources. The results of the study suggest that plate tectonics may have been active from Meso- to Neoarchean; the initial subduction in the Wutai Complex started from Mesoarchean, and the Neoarchean is the major time of the subduction-related magmatism in the Wutai Complex corresponding to the initial cratonization of the NCC.

International Association for Gondwana Research 2023 Convention and
20th International Conference on Gondwana to Asia
Niigata, Japan, October 2023
Abstract Volume

Proterozoic intracratonic reworking in southern Africa: implications for episodic thermal events related to supercontinent amalgamation

Toshiaki Tsunogae [1,2,*], Prince Mandingaisa [3], Mzee Nkhwachi Nyirongo [3]

[1]Faculty of Life and Environmental Sciences, the University of Tsukuba, Ibaraki 305-8572, Japan
[2]Department of Geology, University of Johannesburg, Auckland Park 2006, South Africa
[3]Degree Program in Geosciences, the University of Tsukuba, Ibaraki 305-8572, Japan
[*]E-mail: tsunogae@geol.tsukuba.ac.jp

The basement rocks in southern Africa are composed of Archean cratons (e.g., Zimbabwe, Kaapvaal, Congo, and Tanzania Cratons) and orogenic belts dissecting them. The orogenic belts are traditionally classified into four units based on their ages; ca. 2.7–2.6 Ga Limpopo Complex, ca. 2.0–1.9 Ga Magondi and Ubendian Belts, ca. 1.1–1.0 Ga Kibaran–Irumide and Namaqua–Natal Belts, and ca. 650–550 Ma Pan-African Belt (e.g., Mozambique, Zambezi, and Damara Belts). Previous studies suggest that most of them were formed by continent-continent collisional events related to the assembly of supercontinents (Columbia, Rodinia, and Gondwana). However, detailed petrological and geochronological studies as well as field investigations on some of the orogenic belts indicate that southern Africa was not formed by simple continent-continent collisional events, but multiple thermal events probably took place even in a single orogenic belt. For example, the 2.7–2.6 Ga Limpopo Complex, which sutures the Kaapvaal Craton to the south and the Zimbabwe Craton to the north was locally overprinted by 2.0 Ga granulite-facies event (e.g., Jacket et al., 1997; Basupi et al., 2022). Similar ca. 2.0 Ga event was also found from the southernmost part of the Zimbabwe Craton adjacent to the Limpopo Complex (Tsunogae and Belyanin, 2020). As another example, the ca. 2.0 Ga Magondi Belt was affected by the ca. 1.2-1.1 Ga low-pressure amphibolite facies metamorphism (Mandingaisa et al., 2022), whereas ca. 2.0 Ga Ubendian Belt was overprinted by Pan-African (ca. 560-540 Ma) high-pressure metamorphism. The ages of the second thermal events that affected the belts are also consistent with the timing of global supercontinent amalgamation, therefore we infer intracratonic reworking affected most of the Neoarchean to Mesoproterozoic orogens in southern Africa.

References

Basupi, T.O., Tsunogae, T., Tsutsumi, Y., 2022. Petrology and geochronology of sapphirine-bearing granulites from the Limpopo Complex in eastern Botswana: Implications for Paleoproterozoic long-lived high-pressure/ultrahigh-temperature metamorphism and rapid exhumation. Geological Journal, 57, 4194-4215.

Jaeckel, P., Kröner, A., Kamo, S.L., Brandl, G., Wendt, J.I., 1997. Late Archaean to early Proterozoic granitoid magmatism and high-grade metamorphism in the central Limpopo belt, South Africa. Journal of the Geological Society 154, 25-44.

Mandingaisa, P., Tsunogae, T., Uthup, S., Basupi, T.O., Meck, M.L., Tsutsumi, Y., 2022. Latest Mesoproterozoic (ca. 1.2–1.1 Ga) amphibolite-facies metamorphism from the Dete-Kamativi Inlier, NW Zimbabwe: Implications for a Rodinia-related intracratonic orogen in Southern Africa. Precambrian Research 376, Article No. 106688, 1-20.

Tsunogae, T., Belyanin, G.A., 2020. P-T and Ar-Ar age constraints on low- to high-grade metabasites from the Buhwa Greenstone Belt, southern Africa: Implications for Neoarchean to Paleoproterozoic thermal evolution along the Limpopo Complex-Zimbabwe Craton boundary. Journal of African Earth Sciences, 162, Article 103722, 1-17.

International Association for Gondwana Research 2023 Convention and
20th International Conference on Gondwana to Asia
Niigata, Japan, October 2023
Abstract Volume

Traversing the Himalayan Orogen 2023-Report of the 11th Student Himalayan Field Exercise Tour

M. Yoshida[1,2,*], M.R. Paudel[2], K. Arita[3], T. Sakai[4], B.N. Upreti[5]

[1]Gondwana Institute for Geology and Environment, Hashimoto, Japan
[2]Department of Geology, Tri-Chandra Campus Tribhuvan University, Kathmandu
[3]Hokkaido University Museum, Sapporo, Japan
[4]Faculty of Science and Technology, Shimane University, Matsue, Japan
[5]Nepal Academy of Science and Technology, Kathmandu
[*]E-mail: gondwana@oregano.ocn.ne.jp

A student who visits the Himalaya feels the movement of the crust and understands the principal importance of studying geology and geomorphology in the field. The Student Himalayan Field Exercise Project (SHET-HP, 2023) has been conducting two weeks (depart from and return to Japan) Student Himalayan Field Exercise Tour (SHET) in March every year since 2012 in the west-central Nepal Himalaya with its full traverse from the north, the Trans Himalaya to the south, the Indo-Gangetic Plain (Fig. 1). The Gondwana Institute for Geology and Environment in collaboration with the Department of Geology, Tri-Chandra Campus, Tribhuvan University have been taking charge of the practical fulfillment of the tour.

The 11th SHET was successfully carried out in March 2023 as follows; the details are given in Yoshida (2023). The tour team was composed of 18 people including 11 Japanese, 2 Nepalese and 1 Chinese (supported by IAGR) students and a Japanese mountain photographer, a Japanese and a Nepalese teacher and a Nepalese guide.

The COVID-19 pandemic was still in Japan and some other countries; however, Nepal was quite safe with only one or less newly infected person per day, appearing far safer than Japan which had around 10,000 newly infected people per day. To enter Nepal, two times of vaccination or PCR

negative certificates were necessary. To enter Japan, however, the Department of Foreign Affairs of Japan identified Nepal as the danger level 1, "strong caution should be paid to visit and stay" and had the regulation that people from Nepal should be negative in PCR examination or have completed three times of vaccination. These regulations, anyway were cleared by all the participants with less problems.

The field exercise tour was mostly the same as before, however, observations were insufficient in the section Kagbeni - Kalopani due to cold rain and snow fall. Especially it was a pity that at Chaktan Khola, which is the important STDS valley (STD of Fig. 1) where we did detailed observations every year, we could only collect some pebbles but could not do detailed observations due to very cold and wet conditions which prevented drawing and writing. Further in the Gangetic Plain, we could not get a full view of the Himalayan ranges and view all geologic zones of the Himalayan Orogen, which was one of the highest expectations of the tour.

After returning Kathmandu, on the first day in the morning, some members received the PCR examination, and in the afternoon, all members joined the summary seminar at the Tri-Chandra Campus and delivered their reports in English, and in the evening, a farewell dinner assembly was conducted at a Japanese restaurant in Thamel inviting 4 TU staff. Next day, all students were escorted by TU students for the one day city tour. Next day in the noon time, the Japanese members departed Kathmandu for Japan. Bringing of rock samples to Japan was no problem due to the special permission letter of DMG that we prepared during the field tour.

The participation fee for the SHET-11 was 215,601 JPY, the highest among the 11 tours so far, even though the team collected some donations which could support 22,730 JPY for each participant. Some highlight views in the field, details of new regulations by the Nepal DMG for the geological survey in Nepal and sample transportation to Japan, and details of the account of the SHET-11 will be disclosed at the presentation.

References

SHET-HP, 2023, Student Himalayan Field Exercise site, in the GIGE homepage, http://www.gondwanainst.org/geotours/Studentfieldex_index.htm

Yoshida, M., 2023 (ed.), Traversing the Himalayan Orogen 2023--A Record of the 11th Student Himalayan Field Exercise Tour in March 2023 (in Japanese and English). Field Science Publishers, Hashimoto, 231 pages.

International Association for Gondwana Research 2023 Convention and
20th International Conference on Gondwana to Asia
Niigata, Japan, October 2023
Abstract Volume

Paleozoic sedimentary history of the Hida Gaien belt (Inner zone of Southwest Japan) in relation to the breakup of Gondwana and the assembly of Northeast Asia

Keisuke Suzuki[1, *], Toshiyuki Kurihara[2]

[1] Geological Survey of Japan, AIST, 1–1–1 Higashi, Tsukuba, Ibaraki 305–8567, Japan
[2] Department of Geology, Faculty of Science, Niigata University, Niigata 950–2181, Japan
[*]E-mail: suzuki.k@aist.go.jp

The Hida Gaien belt in the Inner zone of Southwest Japan consists mainly of a basement of Ordovician mafic pyroclastic rocks and lavas and the overlying Silurian–Permian shallow marine shelf deposits. This belt corresponds to the southeastern termination of the Central Asian Orogenic Belt (CAOB) (Suzuki et al., 2021). Therefore, to understand the Paleozoic sedimentary history of the Hida Gaien belt, we must focus on the tectonic relationships with microcontinents in the area west of the eastern end of the CAOB such as the Jiamusi–Khanka and Songliao–Xilinhot blocks and their collisional sutures. Several studies suggested that such microcontinents were dispersed from the northeastern margin of Gondwana or the southeastern margin of the Siberia Craton (Zhou et al., 2018). From this perspective, the paleogeography of the Hida Gaien belt is expected to have changed with the microcontinents of the eastern CAOB during the Paleozoic.

Previous studies in the Hida Gaien belt accumulated important data of paleobiogeography and biostratigraphy from carbonate rocks (Williams et al., 2014). However, geochronologic and -chemical data from clastic and volcanic rocks were not sufficient, disturbing our understanding of the sedimentary history of this belt. This presentation provides an opportunity to introduce the Paleozoic sedimentary history of the Hida Gaien belt based on recent studies of us (Suzuki et al., 2021; 2023). A detailed stratigraphy from the Devonian to Permian and a combination of detrital zircon U–Pb age spectra and geochemistry from their clastic and volcanic rocks will help us to understand the paleogeographic change from the breakup of Gondwana to the assembly of Northeast Asia, including the eastern CAOB and Japan. The main findings are as follows.

Devonian (~398–383 Ma) strata consist mainly of clastic rocks and limestones. Devonian sandstones contain intermittent and small amounts of Precambrian zircons (~3268–556 Ma) with the Cambrian–Silurian zircon grains (~540–480 Ma and ~460–420 Ma). Detrital zircon U–Pb age spectra similar to those of the Devonian strata of the Hida Gaien belt are also observed in the Tasmanides of eastern Australia (e.g., the Thomson, Lachlan, and Delamerian orogens), the Jiamusi–Khanka–Bureya (NE China and the Russian Far East) and Songliao–Xilinhot (Inner Mongolia) blocks in the eastern CAOB, and the Jiangyu continental arc of the Jilin area. These suggest that the Hida Gaien belt and microcontinents and magmatic arcs of the eastern CAOB were located along the northeastern extension of NE Gondwana during the Devonian.

Carboniferous (~346–301 Ma) strata are characterized by a change in the dominant lithology from volcanic rocks to limestone. Early Carboniferous (~346 Ma) volcanic rocks consist of basalt and rhyolite. Such bimodal volcanic rocks in the Hida Gaien belt are also present in South Kitakami belt, the southeastern margin of the South China block (Hainan), and the Jilin area. The volcanism observed along these regions is close in time to the rifting and the opening of the Paleo-Tethys Ocean that resulted in the breakup of Gondwana and may have been some related to those events.

Permian (~283–256 Ma) volcano-sedimentary sequence is characterized by Lower Permian felsic tuffs and tuffaceous clastic rocks, Middle Permian andesites and sandstones rich in volcanic detritus, and upper Middle to Upper Permian feldspathic sandstones and mudstones. This sequence can be correlated with those of the Jilin, Suolun and Xi Ujimqin areas in the eastern CAOB. In addition to their stratigraphic similarities, the Permian sandstones contain few Precambrian zircons from the South and North China block but are dominated by zircons in the 500–400 Ma age range derived from the Jiamusi–Khanka and Songliao–Xilinhot blocks. Permian strata in the Hida Gaien belt and the eastern CAOB would have been deposited proximal to each other in the same tectonic setting along a single subduction zone in the western Paleo-Pacific Ocean.

In summary, the Hida Gaien belt records a sedimentary history in response to tectonics from orogeny along NE Gondwana to the development of the eastern CAOB during the Paleozoic. Although the paleogeographic change characterized by the drifting of microcontinents by the opening of the Paleo-Tethys Ocean has been reconstructed

primarily from the continental sutures of South Asia, these phenomena may also have influenced the assembly of Northeast Asia with Japan.

References

Suzuki, K., Kurihara, T., 2021. U–Pb ages and sandstone provenance of the Permian volcano-sedimentary sequence of the Hida Gaien belt, Southwest Japan: Implications for Permian sedimentation and tectonics in Northeast Asia. Journal of Asian Earth Sciences 219, 104888. https://doi.org/10.1016/j.jseaes.2021.104888

Zhou, J. B., Wilde, S. A., Zhao, G. C., Han, J., 2018. Nature and assembly of microcontinental blocks within the Paleo-Asian Ocean. Earth-Science Reviews 186, 76–93. https://doi.org/10.1016/j.earscirev.2017.01.012

Williams, M., Wallis, S., Oji, T., Lane, P., 2014. Ambiguous biogeographical patterns mask a more complete understanding of the Ordovician to Devonian evolution of Japan. Island Arc 23, 76–101. https://doi.org/10.1111/iar.12067

Suzuki, K., Kurihara, T., Sato, T., Ueda, H., Takahashi, T., Wilde, S. A., Satish-Kumar, M., 2023. Detrital zircon U–Pb ages and geochemistry of Devonian–Carboniferous sandstones and volcanic rocks of the Hida Gaien belt, Southwest Japan: Provenance reveals a Gondwanan lineage for the early Paleozoic tectonic evolution of proto-Japan. Gondwana Research 115, 224–255. https://doi.org/10.1016/j.gr.2022.12.005

International Association for Gondwana Research 2023 Convention and
20th International Conference on Gondwana to Asia
Niigata, Japan, October 2023
Abstract Volume

Tracing crustal evolution using detrital zircon and monazite from beach placers of Gondwana

P.G. Athira[1,2,*], K. Sajeev[1], Daniel J. Dunkley[3], M. G. Zhai[4], S. P.K. Malaviarachchi[5], T. Razakamanana[6], B.F. Windley[7], V.A. Ayisha[8]

[1]Centre for Earth Sciences, Indian Institute of Science, Bengaluru, India
[2]Department of Geology, Faculty of Science, Niigata University, Ikarashi 950-2181, Japan
[3]Department of Polar and Marine Research, Institute of Geophysics, Polish Academy of Sciences, Warsaw, Poland
[4]Institute of Geology and Geophysics, Chinese Academy of Sciences, Beijing, China
[5]Department of Geology, Faculty of Science, University of Peradeniya, Sri Lanka
[6]Department of Earth Sciences, Université de Toliara, Toliara 601, Madagascar
[7]School of Geography, Geology and the Environment, University of Leicester, Leicester LE1 7RH, UK
[8]Department of PG Studies and Research in Geology, MES Ponnani College, Kerala, India
[*]E-mail: athirapg1990@gmail.com

Southern India occupied a central position in East Gondwana in the Late-Neoproterozoic-Cambrian (650 – 500 Ma). During this period several shear/suture zones were formed within and bordering crustal blocks that can be correlated with neighboring continental blocks and continents such as Madagascar, Sri Lanka, Australia and Antarctica (Braun et al., 2003; Meert et al., 2003; Ishwar-Kumar et al., 2013; Collins et al., 2014). Accordingly, all these continental areas preserve important records of the collision and amalgamation of Gondwana. In addition to the available rock data from different crustal blocks and shear zones in southern India and its neighboring areas, we compare the beach placer zircon and monazite geochronological data from all these regions. In the present study, we utilize LA-ICP MS U-Pb ages of zircon and monazite, and Hf isotopes of zircon from the coastal sands of India, Sri Lanka and Madagascar in order to understand their provenance and crustal evolution.

Detrital zircon grains from SW India display a wide range of ages of 650–450 Ma, 1100–650 Ma, 2300–1600 Ma, 2800–2300 Ma and 3500–2800 Ma. For zircons from SW Sri Lanka the ages are in the ranges of 650 – 450 Ma, 1000 – 650 Ma to 2300 -1600 Ma, and a few grains are >2500 Ma. From SE Madagascar the ages are in the ranges 650 to 450 Ma and from 1900 to 1700 Ma. Ages >2500 Ma are not common for samples from Sri Lanka and Madagascar, but they are present in Indian samples, hence they may be derived from gneisses that formed at this time in the Dharwar Craton, as magmatic protoliths of similar age in the Madurai Block and/or the western part of Coorg Block. Similarly, ages ranging from 650 Ma to 850 Ma common in Indian samples can be linked to the magmatic events at Achankovil Shear Zone and southern Madurai Block during early to mid-Neoproterozoic. Paleoproterozoic ages from India and Sri Lanka exhibit a prominent peak at 1800 Ma, similar to samples from Madagascar. These zircons mostly occur as elongate grains with igneous growth zones, which indicates derivation from igneous sources.

The similarity between the Paleoproterozoic age peaks of zircons with comparable Hf isotopic signatures of beach sands from India and Sri Lanka suggest derivation from a similar rock provenance. Moreover, the ages of metasediments and magmatic rocks from India and Sri Lanka are comparable to those from granulite terranes in Madagascar and East Africa. The similarities in age distributions and Hf isotope signatures suggest that during the Paleoproterozoic to early Mesoproterozoic, East Africa and central Madagascar were juxtaposed, while southern India and Sri Lanka were contiguous with Madagascar. Thus, the comparable Paleoproterozoic age peaks of beach sands from four contiguous terranes provide a major constraint on the distribution and configuration of the Columbia Supercontinent. The higher percentage of younger ages range from 600 Ma to 450 Ma for zircon and monazite, which is common for India, Madagascar and Sri Lanka corresponding to recorded major tectonothermal events related to the evolution of the Gondwana Supercontinent. Furthermore, we conclude that these beach sands were mostly derived from metasedimentary rocks that were metamorphosed under granulite facies conditions during the assembly of East Gondwana.

References

Braun, I., Kriegsman, L.M., 2003. Proterozoic crustal evolution of southernmost India and Sri Lanka. Geol. Soc. Spec. Publ. 206, 169–202.

Meert, J.G., Torsvik, T.H., 2003. The making and unmaking of a supercontinent: Rodinia revisited. Tectonophysics

375, 261–288.
Ishwar-Kumar, C., Windley, B.F., Horie, K., Kato, T., Hokada, T., Itaya, T., Yagi, K., Gouzu, C., Sajeev, K., 2013. A Rodinian suture in western India: New insights on India-Madagascar correlations. Precambrian Res. 236, 227–251.
Collins, A.S., Clark, C., Plavsa, D., 2014. Peninsular India in Gondwana: The tectonothermal evolution of the Southern Granulite Terrain and its Gondwanan counterparts. Gondwana Res. 25, 190–203.

International Association for Gondwana Research 2023 Convention and
20th International Conference on Gondwana to Asia
Niigata, Japan, October 2023
Abstract Volume

Monazite dating of pelitic gneisses in the Dai Loc Complex, Truong Son Belt, Vietnam

Vuong Bui Thi Sinh[1,2,*], Ippei Kitano[1,2], Yasuhito Osanai[2], Nobuhiko Nakano[2]

[1] Hokkaido University Sapporo, Hokkaido, Japan
[2] Kyushu University, Fukuoka, Japan
[*]E-mail: buisinhvuongdc@gmail.com

Locating on the south Truong Son Belt, the Dai Loc granitic complex is considered as one of the most key tectonic complexes in Vietnam, which separated from the northern Kontum Massif, via the early Paleozoic Tam Ky–Phuoc Son suture zone (e.g., Hieu et al., 2016). Although the high temperature pelitic gneisses, which have been discovered from the Dai Loc Complex (Osanai et al., 2018; Bui et al., 2022), play an important role to reveal tectonic evolution of the Complex, its metamorphic evolution is controversial whether polymetamorphism occurred during Silurian and Triassic (Nam et al., 2023) or only single metamorphism around Silurian (Bui et al., 2022; Kitano et al., 2022). This study conducted preliminary EMP monazite geochronology for four pelitic gneisses (73102B, 73102D, 73102E and 73102I) from the Dai Loc Complex to unreveal the possible timeline of the metamorphic evolution.

The petrography of all these samples is characterized by primary higher temperature assemblages of garnet (core-mantle) + biotite ± cordierite ± orthopyroxene ± spinel ± sillimanite and secondary lower temperature one of garnet (dusty rim) + biotite + kyanite ± staurolite ± gedrite. All analyzed monazites occur in the matrix, contacting with biotite, quartz, kyanite and garnet. Firstly, monazites in orthopyroxene-bearing garnet–cordierite–biotite gneiss (73102B) exhibit core–mantle–rim texture based on the different BSE emission and geochemistry. Its core domain is characterized by the darkest BSE with relatively high Y2O3 contents of 1.19–1.33 wt% and weighted mean age of 435 ± 54 Ma (n = 5, MSWD = 0.69). The grey mantle part shows the highest Y2O3 contents (1.86–2.39 wt%) and the calculated age at 426 ± 15 Ma (n = 9, MSWD = 0.80). Finally, the brightest BSE rim displays the lowest Y2O3 values (0.41–0.89 wt%) and the youngest weighted mean age at 398 ± 34 Ma (n = 5, MSWD = 1.30). Similarly, monazites in garnet–cordierite–biotite gneiss of 73102I are featured by the heterogenous texture of dark core, grey mantle and bright BSE rim. The Y2O3 concentration increases from the core to mantle (highest values of 1.82–2.89 wt%) then decreases again toward the rim (lowest one at 0.08–1.52 wt%). Correspondingly, the calculated age for the monazite core domain stays at 420 ± 18 Ma (n = 7, MSWD = 1.12) which is consistent with the reported zircon age of 429.1 ± 5.4 Ma from this sample (Bui et al., 2022) and older than those obtained at the mantle and rim domains of 398 ± 11 Ma (n = 22, MSWD = 0.57) and 399 ± 34 Ma (n = 6, MSWD = 1.3), respectively. Whereas garnet–biotite gneiss (73102D) contains patchy or structureless monazite grains with high Y2O3 concentrations in the wide range of 1.46–2.66 wt%. A weighted mean age of 422.5 ± 6.1 Ma (n = 72, MSWD = 1.00) is calculated from all analyzed grains. Finally, monazite from another garnet–biotite gneiss (73102E) indicates the homogenous internal texture, but the distinct geochemistry and relative ages can be separated into two groups. The first group features the high Y2O3 concentration of 1.45–2.31 wt% and the calculated age by using unmixed age peaks at 394.4 ± 7.1 Ma and 440 ± 27 Ma (n = 20) which is similar to reported zircon age of 442.4 ± 5.1 Ma from this sample (Bui et al., 2022). The second group characterized by lower Y2O3 concentrations of 0.54–1.11 wt%, and weighted mean age of 407.5 ± 5.5 Ma (n = 37, MSWD = 1.12).

Due to high errors, the calculated ages from core, mantle and rim monazite domains from analyzed samples are occasionally overlapped, however the distinguished internal textures, geochemical features and consistence with previous zircon ages can constrain on the timing of metamorphic evolution. The medium- to high-Y core to mantle domains of monazite show the similar reported zircon ages of 440–430 Ma, which is considered to be in equilibrium with garnet core to mantle part. Although monazite mantle co-exists with garnet, the high Y2O3 concentration can be explained by the presence of melt which could be a Y supplier for the growth of monazite mantle. The low Y2O3 monazite rim or group showing the youngest clustered age of 410–400 Ma might suggest the equilibrium with the dusty garnet rim. The recrystallization of monazites during the overgrowth of dusty garnet rim produces the low Y2O3 monazite rim domains. Therefore, the monazite dating in this study might imply the high temperature metamorphic stage at 440–430 Ma, and subsequent cooling stage which produces secondary garnet dusty rim at 410–400 Ma happened within a single metamorphic event. However, further monazite dating for pelitic gneisses and granitoids in the Dai Loc Complex is required to clarify the possibility of above thermal history.

International Association for Gondwana Research 2023 Convention and
20th International Conference on Gondwana to Asia
Niigata, Japan, October 2023
Abstract Volume

Structural evolution and stratigraphic relations in the Western Dharwar Craton (WDC) and its implications in regional scale tectonics

Lakshmanan Sreehari[1,*], Keisuke Suzuki[3], A.S. Silpa[1], Tsuyoshi Toyoshima[2], Hayato Ueda[2], Madhusoodhan Satish-Kumar[2], Atsushi Kamei[1]

[1]Department of Earth Science, Shimane University, Matsue, Shimane 690-8504, Japan
[2]Department of Geology, Faculty of Science, Niigata University, Niigata 950-2181, Japan
[3]Geological Survey of Japan, AIST, 1–1–1 Higashi, Tsukuba, Ibaraki 305–8567, Japan
[*]Email: sreehari@riko.shimane-u.ac.jp

The Western Dharwar Craton (WDC) plays a crucial role in understanding the regional-scale tectonics due to its preservation of mutual relations between major geological units in the Dharwar Craton (DC). This study focuses on the field and structural relationships among different geological units in the Chitradurga Schist Belt (CSB) of the WDC, along with the selection of key samples for zircon U-Pb geochronological and whole-rock geochemical analysis. Geological investigations reveal the presence of five main units in the study area: the Basement Gneiss, Sargur, Bababudan, Chitradurga and Hiriyur Groups. Each Group is separated by unconformities or fault contacts with older units, including the Basement Gneiss. Our findings indicate that the Sargur and Bababudan Groups were formed by distinct rifting events associated with mantle plumes. Based on zircon U-Pb dating of matrix and granitic pebble samples from the Sargur Group conglomerate, the initiation of rifting is estimated to have occurred around 3300 Ma. Gneisses in the western margin of the CSB and the Kibbanahalli Schist Belt (KSB) yield upper intercept ages of approximately 3200 Ma, indicating concurrent granitic magmatism associated with Sargur Group rifting. Rifting in the Bababudan Group began < 3000 Ma, and its cessation is linked to convergence and subduction in the far east. Rifting in the Chitradurga and Hiriyur Groups initiated during this convergence and subduction event, around 2700 Ma. Thus, these Groups are interpreted as two distinct stages of back-arc rifting. The Chitradurga Group's rifting commenced approximately 2600 Ma, inferred from the age of felsic volcanic rocks, while the Hiriyur Group's rifting began around 2560 Ma, based on the youngest cluster age in the conglomerate. Geochemical analysis of felsic and mafic samples from different Groups supports our interpretation of plume-related rifting in the Bababudan and Sargur Groups, and subduction-related back-arc rifting in the Chitradurga and Hiriyur Groups. However, our observations indicate that none of the rifting events in the study area led to the formation of an oceanic plate; instead, they appear to be failed rifts.Structural analysis in the study area reveals two major regional-scale deformation events: D2 and D3. D2 deformation is characterized by upright F2 folds with NNW-SSE trending axial planes, and east-dipping NNW-SSE trending reverse faults that enclose these folds. Similarly, D3 deformation represents the reactivation of D2 structures into strike-slip and likely transpressional movements. These structural elements are connected to the formation of a back-arc fold-thrust belt, associated with a shallowing subduction angle. In the final stage of deformation, a probable collision occurred, converting the back-arc fold-thrust belt into a hinterland thrust belt. Consequently, the present structural architecture represents a hinterland fold-thrust belt.

International Association for Gondwana Research 2023 Convention and
20th International Conference on Gondwana to Asia
Niigata, Japan, October 2023
Abstract Volume

Mineralogical and Chemical characterization of Allanite from Moyar Shear Zone, India

V. T. Muhammed Shamil[1,*], Ishwar-Kumar C[1], and K. Sajeev[2]

[1]Department of Earth Sciences, Indian Institute of Technology Kanpur, India
[2]Centre for Earth Sciences, Indian Institute of Science, Bangalore, India
[*]E-mail: shamil20@iitk.ac.in

Southern India was part of the eastern Gondwana supercontinent, composed of crustal nuclei separated by deep crustal shear/suture zone. The high-grade terranes of Coorg, Nilgiri, Salem, Madras, and Trivandrum are the significant crustal blocks of the Southern Granulite terrane (SGT), which is separated by the Dharwar craton on the north by the major collisional boundary such as Palghat Cauvery and Moyar Bhavani shear/suture zone. The Moyar shear zone forms the southern boundary of the Coorg block, which separate the Nilgiri Block of SGT. The Moyar shear zone has a strike-slip component with dextral displacement. The highly sheared rocks of the Moyar shear zone witnessed large-scale tectonothermal activities in the Precambrian (Naha and Srinivasan.,1996).

The chemical characterization and genesis of the Allanite found in the Hornblende-Biotite gneiss from the study area are the primary focus of this study. Allanite is an epidote group mineral and an LREE repository in the continental crust. The petrography of Allanite in the study area shows a euhedral shape and is surrounded by the anhedral epidote grain.

Mineral inclusions identified in Allanite consist of apatite and Fe-oxides, with the apatite crystals exhibiting a well-defined euhedral morphology. Anastomosing fractures present in the outer boundary of Allanite towards the epidote formed due to the increase in the grain volume during the metamictization. These fractures show enrichment of La, Ce, and Nd. The geochemical signature of the Allanite in the present study shows that Allanite-Ce has been formed from the late-stage crystallization of meta-aluminous granitoid. The considerable difference in the Fe3+/Fetotal of the surrounding epidote (0.297) to that of early-formed Allanite (0.705) implies that the epidote is formed in more oxidized condition. The elemental mapping of the Allanite from the study area shows a compositional, especially LREE zonation. The boundary region of the grain is depleted in REE, while the core is enriched. The REE-enriched zones show Ca and Al depletion. This variation in the compositional range suggests that the Allanites are primary, and redistribution LREE might happen during the post-crystallization tectonothermal activity. Anastomosing fractures, and LREE-depleted rim of the Allanite, and the overgrowth of epidote indicate that these are produced by metasomatism. Geochemically similar Allanite occurrences have been reported from the Singhbhum shear zone (Pal et al., 2021), with their formation attributed to LREE metasomatism. The geochronological data suggest that the Allanite of Singhbhum shear zone has been formed through multiple stages of the formation, and with subsequent REE re-mobilization. Therefore, mineral chemistry and geochronology of the Allanites associated with the shear zones can be used as a tectonothermal indicator, as well as a potential target for REE mineral exploration.

References

Pal, D. C., Basak, S., McFarlane, C., & Sarangi, A. K. (2021). EPMA geochemistry and LA-ICPMS dating of allanite, epidote, monazite, florencite and titanite from the Jaduguda uranium deposit, Singhbhum Shear Zone, eastern India: Implications for REE mineralization vis-à-vis tectonothermal events in the Proterozoic Mobile Belt. Precambrian Res. 359, 106208.

Naha, K., & Srinivasan, R. (1996). Nature of the Moyar and Bhavani shear zones, with a note on its implication on the tectonics of the southern Indian Precambrian shield. Proceedings of the Indian Academy of Sciences-Earth and Planetary Sciences, 105, 173-189.

International Association for Gondwana Research 2023 Convention and
20th International Conference on Gondwana to Asia
Niigata, Japan, October 2023
Abstract Volume

Zircon geochemistry of felsic gneisses from Harvey Nunatak, Napier Complex in East Antarctica

Mami Takehara[1,*], Kenji Horie[1,2], Tomokazu Hokada[1,2], 58th Japanese Antarctic Research Expedition Geological Field Survey Team

[1]National Institute of Polar Research, 10-3, Midori-cho, Tachikawa-shi, Tokyo 190-8518, Japan
[2]The Graduate University for Advanced Studies, SOKENDAI
[*]E-mail: takehara.mami@nipr.ac.jp

Zircon ($ZrSiO_4$) is the most widely used mineral for geochronological and geochemical investigations owing to its favorable properties, such as high physicochemical stability, adequate content of trace elements such as U, rare-earth elements (REE) (e.g., Armstrong-Altrin et al., 2018 and references therein), Li (e.g., Ushikubo et al., 2008) and exhibits good retention of radiogenic Pb (>900°C; e.g., Cherniak, 2010 and references therein). Trace elements in zircon serve as indicators for estimating the source melt and the environment where it crystallized. Zircon U-Pb geochronology combined with trace-element geochemistry is a powerful tool for investigating the geochemistry of rocks that have experienced high-temperature environments. Zircon has become a powerful geochemical tool for Antarctic geological and petrological research. We found extremely lithium (Li)-enriched zircons (Li content, [Li]: ~300-600 ppm) in an orthopyroxene-felsic-gneiss collected from Harvey Nunatak in the Napier Complex, East Antarctica by JARE-58 Geological Field Survey Team. The Napier Complex, including Harvey Nunatak experienced extremely high temperatures (>1100°C) based on the mineral assemblage of sapphirine + quartz (Harley, 2016 and reference therein). The thermal history is essential for unraveling the earth's crustal evolution, including deep crust; however, geochronological constraints, such as the timing and duration of the metamorphic events, are still debated. We characterized the zircons of Harvey Nunatak based on the concentration of trace elements analyzed by a sensitive high-resolution ion microprobe (SHRIMP-IIe) in the National Institute of Polar Research (NIPR). The Li and oxygen isotope ratios of zircons are also analyzed by SHRIMP-IIe/AMC in NIPR.

The zircon grains in the Grt-bg. Opx-Qtz-Pl gneiss (sample No. 170223-2A-09) had no core-rim structure and were characterized by sector zoning and nebulous to fir-tree zoning, which is a common feature of zircon in granulite facies rocks. The U-Pb data of the unaltered domains of the zircons are scattered from 2524–2342 Ma, and the weighted average is 2493.1±9.7 Ma (MSWD =15). This weighted average age is statistically meaningless owing to the large MSWD, which indicates a mixture of multiple elements. The largest peak was centered at ca. 2470 Ma and was consistent with the weighted average ages of the zircon rims of the Opx-Pl gneisses (Sample Nos. 170223-2A-08 and 170223-2A-10). Therefore, it is considered that the zircons crystallized by regional metamorphism continued from 2524–2342 Ma, similar to the 170223-2A-08 and 170223-2A-10 samples.

The REE patterns of the 170223-2A-09 zircons were similar to those of the 170223-2A-08 and 170223-2A-10 zircons. The LREE-enriched patterns are probably affected by the altered domains and are probably derived from the altered domains surrounding the fractures (Takehara et al., 2018). The HREE-depleted patterns are similar to the REE patterns of zircon co-existing with garnet, shown in the sample of Mt. Riiser-Larsen reported by Hokada and Harley (2004). Lower Ti-in-zircon temperature (about 865°C) is obtained from HVN 09 zircons, which show the average Ti-in-zircon temperature of 934°C. The garnets localized in the 170223-2A-09 sample indicate that zircon grains were not entirely related to the garnets during regional metamorphism. The REE pattern of a spot, which indicates the U-Pb age of 2520 Ma, is similar to the lower middle-REE pattern in the 170223-2A-10 sample. There is a possibility that the REE pattern is derived from different crystallization conditions or inheritance affected by the U-Pb system disturbance; however, further studies are necessary.

The oxygen isotope ratios were consistent regardless of age, suggesting that the oxygen atoms were taken up into the zircons from the environment that was buffered from the minerals or melts, except for the zircon domains in the altered grains. The average $\delta^{18}O$ value is 4.93±0.12 ‰ and slightly lower than that of zircon in equilibrium with the mantle materials (5.3 ± 0.3 %; Valley, 2003), but it does not indicate that the protoliths of the sample rocks are of the mantle derivation because these zircons crystallized during UHT metamorphism. The $\delta^{18}O$ values in the unaltered domains of the altered grains are widely scattered compared to those of the unaltered grains. Some of them are probably attributed to the altered domains surrounding the fractures.

References

Armstrong-Altrin, J.S., Ramos-Vázquez, M.A., Zavala-León, A.C., Montiel-García, P.C., 2018. Provenance discrimination between Atasta and Alvarado beach sands, western Gulf of Mexico, Mexico: Constraints from detrital zircon chemistry and U–Pb geochronology. Geological Journal, 5, 2824-2848.

Cherniak, D.J., 2010. Diffusion in accessory minerals: Zircon, titanite, apatite, monazite and xenotime. In: Rosso, J.J. (Ed.), Diffusion in Minerals and Melts, Reviews in Mineralogy and Geochemistry. 72. Mineralogical Society of America, Washington, DC, pp. 827–869.

Harley, S.L., 2016. A matter of time: the importance of the duration of UHT metamorphism. Journal of Mineralogical and Petrological Sciences, 111, 50-72.

Hokada, T., Harley, S.L., 2004. Zircon growth in UHT leucosome: constraints from zircon-garnet rare earth elements (REE) relations in Napier Complex, East Antarctica. Journal of Mineralogical and Petrological Sciences 99, 180-190.

Takehara, M., Horie, K., Hokada, T., and Kiyokawa, S., 2018. New insight into disturbance of U-Pb and trace-element systems in hydrothermally altered zircon via SHRIMP analyses of zircon from the Duluth Gabbro. Chemical Geology, 484, 168-178.

Ushikubo, T., Kita, N.T., Cavosie, A.J., Wilde, S.A., et al., 2008. Lithium in Jack Hills zircons: Evidence for extensive weathering of Earth's earliest crust. Earth and Planetary Science Letters, 272, 666-676.

Valley, J.W., 2003. Oxygen isotopes in zircon. Reviews in mineralogy and geochemistry, 53, 343–385.

International Association for Gondwana Research 2023 Convention and
20th International Conference on Gondwana to Asia
Niigata, Japan, October 2023
Abstract Volume

Form line map, geological structures, and crustal unit divisions of the Lützow-Holm Complex, East Antarctica

Tsuyoshi Toyoshima

Department of Geology, Faculty of Science, Niigata University, Niigata 950-2181, Japan
E-mail: ttoyo@geo.sc.niigata-u.ac.jp

In this paper, a form line map, cross sections, and division of crustal units (Toyoshima, 2017) of the Lützow-Holm Complex (LHC), East Antarctica, are revised with reference to Nogi et al. (2013) and Takahashi et al. (2017). In the revised division, the LHC are divided into seven units: Srtrandnibba, Rundvågshetta, Skallen, Onglu-Scarvsnes, Cape Hinode, Okuiwa-Kasumi, and Akarui Point units. Vergence of folds and dip directions of foliations are taken into account when drawing cross sections. The revised form line map and cross sections suggest that the crustal rocks of the LHC were originally subhorizontal in geological structure, but were folded so strongly that they became a fold and thrust belt. It appears that the LHC has NE- and SW-dipping thrust sheets.

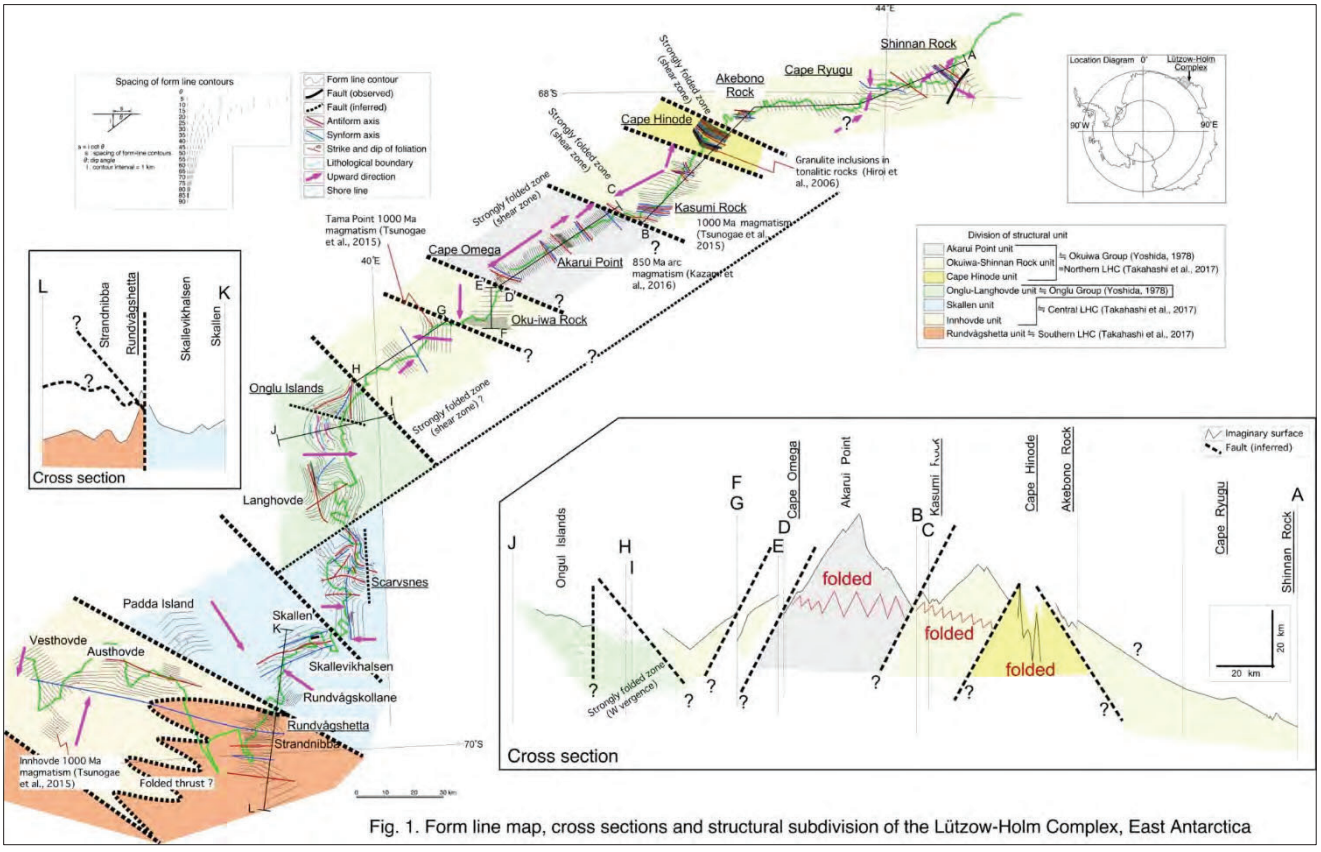

Fig. 1. Form line map, cross sections and structural subdivision of the Lützow-Holm Complex, East Antarctica

The revised form line map and crustal unit divisions show that the LHC is not uniform and includes several types of crustal units or fragments of crust. The LHC is the result of poly-phase continental collisions during the Late Achaean to Early Palaeozoic.

Based on lithostratigraphy, Yoshida (1978) has divided the Lützow-Holm Complex (LHC), East Antarctica, into three groups: Okuiwa, Onglu, and Skallen Groups. Based on geophysical data, Nogi et al. (2013) have divided the complex into four discrete blocks that may be bounded by NE–SW-trending right-lateral strike-slip faults. Based on petrological, geochemical, and zircon U-Pb geochronological data, Takahashi et al. (2017) have divided the complex into three crustal units: a 2.5 Ga unit in the

southern LHC, a 1.0 Ga unit in the northern LHC, and a supracrustal unit in the central LHC with fragments of 1.8 Ga and minor 2.5 Ga and 1.0 Ga magmatic arcs. These divisions are based on different viewpoints, so there are many similarities, but also many differences. In this paper, these divisions are compared, and the megascopic geological structures and crustal unit division of the LHC are discussed.

References

Nogi, Y., Jokat, W., Kitada, K., Steinhage, D., 2013, Geological structures inferred from airborne geophysical surveys around Lützow-Holm Bay, East Antarctica. Precambrian Research, 234, 279–287.

Takahashia, K., Tsunogae, T., Santosh M., Takamura, Y., Tsutsumi, Y., 2017, Paleoproterozoic (ca. 1.8 Ga) arc magmatism in the Lützow-Holm Complex, East Antarctica: Implications for crustal growth and terrane assembly in erstwhile Gondwana fragments. Journal of Asian East Science, 157, 245-268. http://dx.doi.org/10.1016/j.jseaes.2017.07.053.

Toyoshima, T., 2017, Geological structures, crustal units, and tectonics of the Lützow-Holm Complex, East Antarctica. In: Abstracts of the Eighth Symposium on Polar Science, NIPR.

Geological control of the eastern Great Wall: Mountain-basin relationships in the eastern North China Craton

Boran Liu[1,2], Sanzhong Li[1,2], Franz Neubauer[3,*], Chengyue Liang[4]

[1]Frontiers Science Center for Deep Ocean Multispheres and Earth System, Key Lab of Submarine Geosciences and Prospecting Techniques, and College of Marine Geosciences, Ocean University of China, Qingdao 266100, China
[2]Laboratory for Marine Mineral Resources, Laoshan Laboratory, Qingdao 266100, China
[3]Department of Environment and Biodiversity, Geology Division, Paris-Lodron-University of Salzburg, 5020 Salzburg, Austria
[4]College of Earth Sciences, Jilin University, Changchun 130061, China

The E–W trending Yanshan belt, an intraplate fold-thrust belt located in the northern North China Craton, has experienced several episodes of Mesozoic deformation, which resulted in the widely distributed magmatism and mountain-basin tectonics that completely re-shaped the topography of the eastern North China Craton. Our study focuses on which tectonic processes created such mountain-basin couple in the Mid-Late Mesozoic times. The detailed field investigations, structural and paleo-stress analysis, U-Pb zircon geochronology of granite intrusions and volcanic tuffs and provenance analysis of sandstones have been done in the Qinglong area, northeastern North China Craton. The U-Pb LA-ICP-MS dating of zircons yield ages of 114 to 201 Ma for various granites and 115 to 116 Ma for volcanic rocks from Zhangjiakou Formation. The detrital zircons from the Lower Cretaceous sandstones yield four age groups of 2587 to 2460 Ma, 2222 to 1828 Ma, 297 to 190 Ma and 187 to 100 Ma, which are all sourced from the Qinglong and surrounding areas and indicating that the Qinglong area started to uplift after Middle Jurassic.

The Qinglong area underwent multiple deformation overprinting by NE–SW compression in Middle-Late Jurassic times, WNW–ESE compression in Late Jurassic to Early Cretaceous, ENE–WSW extension in Early Cretaceous and NNW–SSE compression in Late Cretaceous during the Yanshanian orogeny. Meanwhile, widely distributed granite intrusions and emplacement of Upper Jurassic-Lower Cretaceous volcanic rocks indicate a large amount of magma input to the area.

The Qinglong area with the Great Wall along its southern margin close to plain adjacent to the south was uplifted to form the Qinglong highland and surrounding related basins by combination of the multiple tectonic compression, extension and the regional magma inflation at depth during the Late Jurassic to Late Cretaceous.

Neoproterozoic paleo-ocean fluid inclusions inside Himalayan magnesite crystals

Prakash Chandra Arya[1,*], M. Satish-Kumar[2], K. Sajeev[1]

[1]Centre for Earth Sciences, Indian Institute of Science, Bangalore 560 012, India
[2]Department of Geology, Niigata University, Niigata 950-2181, Japan
[*]E-mail: prakasha@iisc.ac.in

The Neoproterozoic time plays an important role in the Earth's biological evolution because its roots are connected to the Snowball Earth glaciations and a major oxygenation event in the Earth's history. During this time, the oceans have undergone several physical and chemical changes due to extreme climatic and environmental changes. However, we do not know much about these past oceans as they are tectonically destroyed. In the present work, we have identified microscopic remnants of the Neoproterozoic sweater droplets along with freshwater (i.e., glacial melt water) inclusions in the magnesium carbonates of the Himalayas. The paleo-ocean fluid inclusions are dense (1.19–1.15 g/cc) and saline (25.02–20.52 eq. NaCl), while the freshwater inclusions are low in density (1.05–1.0 g/cc) and salinity (7.73–0.18 eq. NaCl) (Arya et al., 2023). The interaction between these two fluids resulted in the formation of intermediately dense (1.13–1.08 g/cc) and saline (17.87–10.86 eq. NaCl) fluid inclusions. These findings have immense significance in the field of Earth Science as they can provide firsthand information on the paleo-oceanographic parameters (pH, EC, chemical, and isotopic composition etc.), which were long anticipated or calculated with large uncertainty.

Figure 1: Photomicrograph showing trapped droplets of paleo-ocean as fluid inclusions in the sparry magnesite of the Kumaun Himalayas

References

Arya, P.C., Nambaje, C., Kiran, S., Satish-Kumar, M. and Sajeev, K., 2023. Himalayan magnesite records abrupt cyanobacterial growth that plausibly triggered the Neoproterozoic Oxygenation Event. Precambrian Research, 395, p.107129.

Paleozoic tectonothermal evolution of the Jinchuan Ni-Cu sulfide deposit, NW China: New constraints from 40Ar/39Ar and (U-Th)/He thermochronology

Ni Tao[1,2,*], Jun Duan[1], Martin Danišík[3], Jiangang Jiao[1], Yunpeng Dong[2*], Noreen J. Evans[3], Yalin Gao[4], Ruohong Jiao[5], Meinert Rahn[6]

[1]School of Earth Science and Resources, Xi'an Key Laboratory for Mineralization and Efficient Utilization of Critical Metals, Chang'an University, Xi'an, China
[2]State Key Laboratory of Continental Dynamics, Department of Geology, Northwest University, Xi'an, China
[3]John de Laeter Centre, Curtin University, Perth, Australia
[4]State Key Laboratory for Comprehensive Utilization of Nickel and Cobalt Resources, Jinchang, China
[5]School of Earth and Ocean Sciences, University of Victoria, Victoria, Canada
[6]Institute of Geo- and Environmental Sciences, University of Freiburg, Freiburg, Germany
[*]E-mail: ni.tao@chd.edu.cn | dongyp@nwu.edu.cn

The world's third largest and China's largest magmatic Ni-Cu sulfide deposit – the Jinchuan ore deposit, is hosted in the Proterozoic basement of the Longshoushan Terrane, a NW-extending elongated orogen on the southwestern margin of the North China Craton. The Paleozoic tectonothermal history of the Jinchuan Ni-Cu sulfide deposit is crucial to understand ore formation and spatial occurrence in the area. Accordingly, this study applies multimineral (hornblende, biotite, and K-feldspar) 40Ar/39Ar and zircon (U-Th)/He thermochronology to the Neoproterozoic Jinchuan ore-hosting intrusion, as well as to the Paleoproterozoic migmatitic country rocks and an early Paleozoic granitic intrusion in the Longshoushan Terrane. Hornblende 40Ar/39Ar ages of 543 Ma and 489 Ma from the migmatitic country rocks constrain the age of amphibolite facies metamorphism in Jinchuan to the Ediacaran to late Cambrian. The presence of nearby Silurian to Devonian sediments suggests that the Jinchuan ore deposit was exhumed to the surface by the Silurian. Exhumation occurred in an extensional setting during the spreading and subduction of the North Qilian Ocean. Syn-orogenic (Qilian Orogeny) magmatic reheating up to ~400 ˚C in the Silurian occurred in the middle of the pre-Silurian surface exposure and Devonian thermal event as illustrated by biotite 40Ar/39Ar plateau ages of 406 Ma and 380 Ma, respectively. The late Carboniferous plagioclase and K-feldspar 40Ar/39Ar mini plateau ages of ca. 318 Ma and ca. 301 Ma, together with Mississippian (ca. 334 Ma) to Guadalupian (ca. 272 Ma) zircon (U-Th)/He mean ages, suggest protracted late Paleozoic cooling to <150 ˚C, associated with the Qilian orogenic collapse.

International Association for Gondwana Research 2023 Convention and
20th International Conference on Gondwana to Asia
Niigata, Japan, October 2023
Abstract Volume

Subcontinental Lithospheric mantle evolution in Archean: insights from the geochemistry of mafic dyke swarms

Silpa A.S[1,*], Satish-Kumar M.[2], Sajeev K.[3], Takazawa Eiichi[2], Takahashi Toshiro[2]

[1]Department of Earth Science, Shimane University, 1060 Nishikawatsu-cho, Matsue, Shimane 690-8504, Japan
[2]Department of Geology, Faculty of Science, Niigata University, 8050 Ikarashi-ninocho, Nishi-ku, Niigata 950-2181, Japan
[3]Centre for Earth Sciences (CEaS), Indian Institute of Science, Bangalore 560 012, India
[*]E-mail: silpa@riko.shimane-u.ac.jp

Archean subcontinental lithospheric mantle (SCLM) is peculiar due to the presence of certain rock types and distinct geochemical characteristics that are not found in the younger mantle. The evolution of SCLM from Archean to Proterozoic Era is closely related to various geological processes such as continental growth, episodic mafic volcanism, rifting and break-up of the protocontinents and subsequent subduction-recycling processes. SCLM underwent significant transformations, and such changes can be understood from the nature and composition of mantle derived rocks. Archean cratons which are principal constituents of several ancient supercontinents are characterized by the presence of regional scale mafic dyke swarms. Such mafic dyke swarms are often correlated with major Large Igneous Provinces (LIPs), the magmatic events during which large volumes of mantle generated materials are emplaced within a short period of time (Ernst and Bleeker., 2010; Ernst et al., 2005). The Archean Dharwar Craton of southern India is one such craton where dyke swarms of varying generations and dimensions are present and is the focus of the current study.

Similar to the Archean cratons of the world, Dharwar craton (DC) is composed of tonalite trondhjemite-granodiorite (TTG) type gneisses (c. 3.4–3.2 Ga), volcano-sedimentary greenstone belts (c. 3.35–3.10 Ga Sargur Group and younger c. 2.9–2.6 Ga Dharwar Supergroup) and calc-alkaline to potassic granitoid rocks (Peucat et al., 2013; Jayananda et al., 2018). DC is divided into three crustal blocks (western, central, and eastern) separated by major shear zones. Mafic dykes intruded into the older Western Dharwar craton (WDC) are considered and are categorized into two as: older metadolerite dykes (?-~3.0 Ga) and younger dolerite dykes (~2.7 Ga- 1.8 Ga), each of which can be further divided into three generations based on the petro-geochemical characteristics.

Metadolerite dykes exhibit weak metamorphism and are chiefly composed of plagioclase, clinopyroxene and amphibole along with opaque phases. Even though the medium to fine-grained plagioclase shows varying degrees of alteration, lath shapes are distinguishable and show remnant ophitic textures (Silpa et al., 2023). The dolerite dykes on the other hand are undeformed, essentially composed of plagioclase and clinopyroxene and are characterized by well-preserved ophitic- poikilitic textures. A few contained olivine (olivine dolerite dykes) and orthopyroxene (Silpa et al., 2021a).

Metadolerite dykes show depleted mantle source characteristics and low isotope initial ratios (87Sr/86Sr = 0.70041) whereas the dolerite dykes show gradual enrichment of the SCLM (87Sr/86Sr = 0.70653). Rare earth element depleted patterns are observed for metadolerite dykes indicating a primitive homogenous mantle source. For the dolerite dykes, a depleted MORB source mantle (DMM) enriched by recycled oceanic crust, followed by continental crustal sediments are suggested, which lead to the heterogeneity of the mantle and formation of different source magmas. The trace and rare earth element geochemistry of clinopyroxene form dolerite dykes also substantiate distinct source mantle characteristics within the younger dolerite group (Silpa et al., 2021b). The multiple sulfur isotope characteristics of the studied dykes show a combination of weak mass-independent fractionation (MIF) signatures and mass-dependent (MDF) signatures (Silpa and Satish-Kumar, 2022). Microbial sulfate reduction during the changing atmospheric chemistry in Archean and the isotopically distinct sulfur aerosols formed in the Archean atmosphere which later incorporated into the sediments lead to such isotope signatures. The systematic modification of the subcontinental lithospheric mantle (SCLM) by recycling of the crustal components are evident from multiple sulfur isotope characteristics. The geochemical characteristics of the mafic dykes from Dharwar craton demonstrate gradual enrichment of the SCLM from a depleted mantle and suggest that subduction-recycling has a crucial role in altering the composition of SCLM over time.

References

Ernst, R. and Bleeker, W., 2010. Large igneous provinces (LIPs), giant dyke swarms, and mantle plumes: significance for breakup events within Canada and adjacent regions from 2.5 Ga to the Present.Canadian Journal of Earth Sciences, 47(5), pp.695-739.

Ernst, R.E., Buchan, K.L. and Campbell, I.H., 2005.

Frontiers in large igneous province research. Lithos, 79(3-4), pp.271-297.

Jayananda, M., Santosh, M. and Aadhiseshan, K.R., 2018. Formation of Archean (3600–2500 Ma) continental crust in the Dharwar Craton, southern India. Earth-Science Reviews, 181, pp.12-42.

Peucat, J.J., Jayananda, M., Chardon, D., Capdevila, R., Fanning, C.M. and Paquette, J.L., 2013. The lower crust of the Dharwar Craton, Southern India: Patchwork of Archean granulitic domains. Precambrian Research, 227, pp.4-28.

Silpa, A.S., Satish-Kumar, M. and Takahashi, T., 2021. Sr-Nd isotopic study of dolerite dykes in the Western Dharwar craton, southern India: Implications for the evolution of the subcontinental lithospheric mantle in late Archean. Lithos, 388, p.106023.

Silpa, A.S., Satish-Kumar, M., 2022. Multiple Sulfur Isotope Geochemistry of the Precambrian Mafic Dykes and Komatiites in the Dharwar Craton, Southern India: Evidence for Crustal Recycling and Enrichment in the Subcontinental Lithospheric Mantle. Lithosphere. (Special 8): 4679300 A. S. Silpa, M. Satish-Kumar; Multiple Sulfur Isotope Geochemistry of the Precambrian Mafic Dykes and Komatiites in the Dharwar Craton, Southern India: Evidence for Crustal Recycling and Enrichment in the Subcontinental Lithospheric Mantle. Lithosphere 2022;; 2022 (Special 8): 4679300

Massive abiotic methane production in eclogite during cold subduction

Lijuan Zhang[1,*], Lifei Zhang[1]

[1]Key Laboratory of Orogenic Belts and Crustal Evolution, MOE, School of Earth and Space Sciences, Peking University, Beijing 100871, China
[*]E-mail: lijuanzhang@pku.edu.cn

Methane (CH_4) is a critical but overlooked component in the study of deep carbon cycle. Abiotic CH_4 produced by serpentinization of ultramafic rocks has received extensive attention, but its formation and flux in mafic rocks during subduction remain poorly understood. Here, we report massive CH_4-rich fluid inclusions in well zoned garnet from ultrahigh-pressure (UHP) eclogites in the Western Tianshan, China. Petrological characteristics and carbon–hydrogen isotopic compositions confirm the abiotic origin of this CH_4. Reconstructed P–T–fO2–fluid trajectories and Deep Earth Water modeling imply that massive abiotic CH_4 was generated during prograde HP–UHP metamorphism at depths of 50–120 km, whereas CO_2 was produced during exhumation. The massive production of abiotic CH_4 in eclogites may result from multiple mechanisms during prograde HP-UHP metamorphism. Our flux calculation proposes that abiotic CH_4 formed in HP-UHP eclogites in cold subduction zones may represent one of the largest, yet overlooked, sources of abiotic CH_4 on Earth.

Tibetan Plateau growth linked to crustal thermal transitions since the Miocene

Xiu-Zheng Zhang[1,2,*], Qiang Wang[2], Wei Dan[2]

[1]State Key Laboratory of Isotope Geochemistry, Guangzhou Institute of Geochemistry, Chinese Academy of Sciences, Guangzhou 510640, China

[2]CAS Center for Excellence in Deep Earth Science, Guangzhou, 510640, China

[*]E-mail: zhangxz@gig.ac.cn

The topographic transition of central–northern Tibetan Plateau since the early Miocene has created a consistently high and flat plateau similar to that of today. However, to date, the associated deep crust and/or /mantle events are poorly understood, mainly due to an early Miocene metamorphic–magmatic lull within the Qiangtang Block, central–northern Tibetan Plateau. To address this issue, we undertook a study of crustal xenoliths and zircon xenocrysts in 6.0–2.3 Ma lavas in the Qiangtang Block. The occurrence of 22.6–12.9 Ma high-temperature–low-pressure granulite xenoliths implies that the middle crust of the block has been very hot since that time. Zircon xenocrysts and granitic xenoliths from 6.0–2.3 Ma lavas were studied and shown to have high zircon δ18O values, which supports Miocene crustal melting and the formation of unexposed, coeval felsic plutons. Combined with paleoelevation data from the Tibetan Plateau, our results suggest that the early Miocene cold–hot thermal transition of the middle–lower crust was near-synchronous with topographic evolution from high-relief mountains to a flat plateau, which supports crustal flow as the main topographic smoothing mechanism for central–northern Tibetan Plateau.

International Association for Gondwana Research 2023 Convention and
20th International Conference on Gondwana to Asia
Niigata, Japan, October 2023
Abstract Volume

Ultramafic-Hosted Magnesite Deposits of Salem Mafic-Ultramafic Complex, Southern India: Insights from Spectral and C-O Isotope Studies

A. Haritha[1,*], V. J. Rajesh[1], and M. Satish-Kumar[2]

[1]Department of Earth and Space Sciences, Indian Institute of Space Science and Technology, Thiruvananthapuram 695 547, India
[2]Department of Geology, Niigata University, Niigata 950-2181, Japan
[*]E-mail: harithaa.18@res.iist.ac.in

Magnesite ($MgCO_3$) is an important carbonate mineral that has many uses in industry and is thought to be an excellent refractory material. It forms mainly through the alteration of magnesium-rich host rocks in diverse geological environments. The common types of magnesite occurrences are sparry or macro-crystalline (Veitsch type), cryptocrystalline (Kraubath type), and fluviatile-limnic (Bela Stena type). Massive cryptocrystalline magnesite deposits are often associated with ophiolitic sequences and/or mafic-ultramafic complexes. Ultramafic-hosted magnesite mineralization is often linked to H2O and CO2 processes like serpentinization and near-surface meteoric weathering of ultramafic bodies (Abu Jaber et al., 1992). In southern India several magnesite deposits are found in ultramafic complexes, where they form complex networks of veins and fracture fillings inside the ultramafic body. Spectroscopic techniques and stable C-O isotope geochemistry were used to study magnesite deposits found in Neoproterozoic ultramafic rocks in Salem, in the southern peninsula of India. We focused on: (i) the spectral characterization of the magnesite, (ii) understanding the prevailing physicochemical conditions that controlled the formation of magnesite deposits, and (iii) understanding the source of the fluids that led to the formation of magnesite.

The Salem Mafic-Ultramafic Complex (SMUC) is one of the Precambrian mafic-ultramafic complexes that have been emplaced into the older supracrustals of the Southern Granulite Terrane (SGT) (Fig 1a) of southern peninsular India. The complex is an ENE-WSW trending semicircular to elongate body of Neoproterozoic age (maximum length of 20 km) is located in the Salem block of the SGT. Dunites, serpentinites, pyroxenites, wehrlite, peridotite, hornblendite, charnockite, hornblende gneiss, mafic intrusions like gabbro, amphibolite, and dolerites, quartzo-feldspathic alkaline

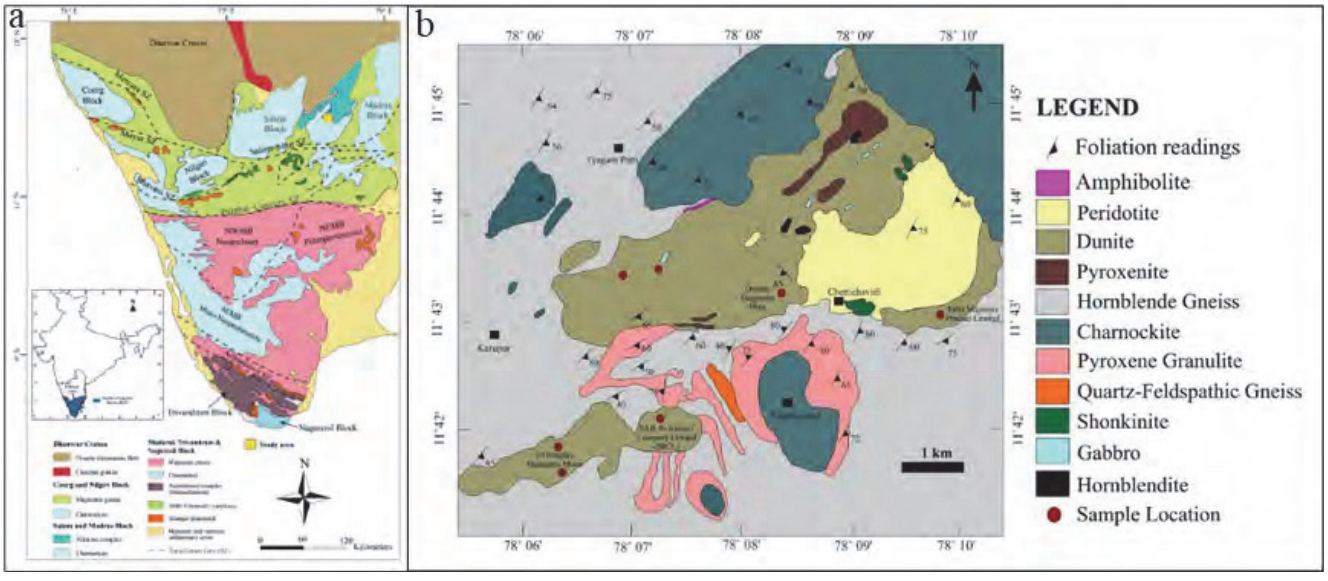

Figure. 1. (a) Generalized geological map and tectonic framework of the Southern Granulite Terrain (SGT) of India showing major crustal blocks and intervening shear/suture zones (modified after Santosh et al., 2015) with an inset image of India showing the location of SGT. (b) A simplified geological map of the study area illustrating the distribution of various lithological units. The map also shows the sample locations (modified after Yellappa et al., 2019).

rocks, and ultra-potassic intrusions like shonkinites and lamprophyres are the major lithounits in the SMUC (Fig 1b). The geochemistry of dunites and peridotites suggest that arc signature (Yellappa et al., 2019) with similarities of Alaskan type complexes. The magnesite mineralization within the Salem mafic-ultramafic complex is mostly confined to major faults/joint planes of the dunite body. It occurs in two belts, i.e., the west hills – Jagir Ammapalayam (4 sq. km) on the south and the Karuppur-Red hills – Kurumbapatti-Chettichavadi Jagir (26 sq. km) on the north. The magnesite deposits occur as veins, stockwork, and extensive fracture fillings. The most prominent magnesite vein occurs along with fractures in a NE-SW direction in the dunite intrusion. The thickness of the magnesite veins ranges from a few centimeters to meters. Lenticular and lumpy masses of magnesite are also observed in the study area. The massive and granular magnesite mineralization of the Salem stretches down to a depth of 360 m, according to the available drill hole data.

The spectral characterization of magnesite was conducted using visible-near infrared (Vis-NIR) reflectance spectroscopy, Laser Raman spectroscopy, and Fourier-Transform Infrared (FTIR) spectroscopy. The Vis-NIR spectra shows a paired absorption at 2.3 and 2.5 µm, attributed to C-O bond vibration overtones and combination tones of C-O stretching and bending. Jayabal et al., 2011 established a relationship between the radius of curvature of 2.3 µm absorption feature and the carbonate abundance in order to qualitatively estimate the grade of magnesites. The smaller the radius of curvature, the higher the carbonate abundance in magnesites. The parameters such as albedo, band position, and band depth were also utilized to estimate the grade of magnesites (Ranganathan and Siddan, 2020). Infrared spectroscopy is widely used to distinguish the minerals in the carbonates and their solid solution series. The FTIR spectral pattern obtained for magnesite samples in the 600 to 2000 cm-1 range. The characteristic vibrational frequencies are observed in and around 1434 cm−1, 880 cm−1, and 747 cm−1. The three major infrared active vibrations present in natural carbonates are out-of-plane bending (ν2), the asymmetric stretching (ν3), and the in-plane bending (ν4) modes of carbonate ions. Laser Raman data showed peaks at or near 212, 332, 735, 1096, and 1460 cm−1. Magnesium content and crystal structure of magnesites significantly control the Laser Raman peak. Mg-carbonates exhibit four symmetric (υ1) and asymmetric stretching (υ3) due to the internal vibration of the (CO3)2 group as well as translation (T) and librational (L) of the (CO3)2 group due to the external vibration of the crystal lattice. The utilization of these spectroscopic methods enabled the characterization of magnesites, providing insights into their spectral characteristics and grade determination. The spectral parameters from these methods offer powerful techniques for identifying high-quality magnesites, and the developed spectral library may prove valuable for future planetary missions.

The δ13CVPDB (3.6±1.2‰) and δ18OSMOW (25.4± 0.7‰) (n = 10), values of magnesite suggest a meteoric source of CO2 and that the magnesite mineralization resulted from the alteration of the ultramafic rocks by low-temperature (49 ± 3.3 °C) fluids. Based on field observations and stable isotopic signatures, we propose a model for the genesis of Salem magnesites. This model propose that meteoric water seeped into the ultramafic rocks through weak planes and cracks, causing the alteration. The stable isotopic values, characterized by lighter carbon and heavier oxygen, imply that the mineralizing fluid cannot be solely sourced from the deep mantle, with the heavier oxygen indicating a meteoric/atmospheric origin. The oxygen isotopes are considered paleo-thermometers, and the analysis depicts the precipitation temperature of Salem magnesite as ~50°C, indicative of a low-temperature alteration process. Studies of stable isotopes in ultramafic-hosted magnesite deposits around the world support two different ideas about where fluids come from: (i) the mantle and (ii) meteoric water. Our results, compared with data from similar magnesite occurrences globally, will provide a better understanding of the source of fluids responsible for the genesis of similar magnesite deposits.

References

Abu-Jaber, N. S., & Kimberley, M. M. 1992. Origin of ultramafic-hosted magnesite on Margarita Island, Venezuela. Mineralium Deposita, 27, 234-241.

Ranganathan, P.C., Siddan, A., 2020. Geospatial assessment of ultramafic rocks and ore minerals of Salem. India. Arabian Journal of Geosciences 13 (20), 1–16.

Jayabal, S.K., Shanmugam, S., Sukkiri, G., 2011. Hyperspectral Radiometry to Characterise Dunite Alteration and Magnesite Deposits of Salem, South India. Journal of the Indian Society of Remote Sensing 39 (4), 497–505.

Santosh, M., Yang, Q.-Y., Shaji, E., Tsunogae, T., Mohan, M.R., Satyanarayanan, M., 2015. An exotic Mesoarchean microcontinent: the Coorg Block, southern India. Gondwana Res. 27, 165–195.

Yellappa, T., Santosh, M., Manju, S., 2019. The mafic–ultramafic complex of Salem, southern India: An analogue for Neoproterozoic Alaskan-type complex. Geological Journal 54 (5), 3017–3040.

International Association for Gondwana Research 2023 Convention and
20th International Conference on Gondwana to Asia
Niigata, Japan, October 2023
Abstract Volume

Correlating multiple-stage exhumation processes in central Tibetan Plateau and its margins: Implications for plateau uplift and growth

Zhiwu Li[1,*], Shugen Liu[1,2], Kui Tong[1], Peter J.J. Kamp[3], Ganqing Xu[3], Zijian Wang[1], Jinxi Li[1], Yuehao Ye[1], Wenhui Wu[1]

[1]State Key Laboratory of Oil and Gas Reservoir Geology and Exploitation, Chengdu University of Technology, Chengdu 610059, China
[2]Xihua University, Chengdu 610039, Sichuan, China
[3]School of Science, University of Waikato, Hamilton 3240, New Zealand
[*]E-mail: lizhiwu06@cdut.edu.cn

How and when the Tibetan Plateau (TP) uplifted and grew is an open question, and an enduring research hotspot in geoscience as well. Wang et al. (2008, 2014) proposed an inside-out growth model which suggested the elevated central TP (namely proto-TP) by ~45 Ma has undergone outward expansion and associated uplift processes since then. Recent paleoaltimetry (e.g. Xiong et al., 2020, 2022) and low-temperature thermochronology studies (e.g. Bi et al., 2022; Tong et al., 2020, 2022; Li et al., 2023) in the central TP and its eastern, northeastern margins have confirmed that the Plateau has experienced more complex uplift and growth histories with significantly temporal and spatial variability. Our new low-temperature thermochronology data (Tong et al., 2022; Li et al., 2023), integrated with previously published data, allows a comprehensive correlation of uplift-and-exhumation history between the central TP and its margins, which shed significant implication for the growth model of the TP.

In the central TP, previously published multiple-system thermochronology dataset (AHe-apatite (U-Th)/He, AFT-apatite fission track, ZHe-zircon (U-Th)/He, ZFT-zircon fission track) recorded cooling ages varying between ~160 Ma and 40 Ma, indicative of a complex uplift and growth history since the Late Jurassic (Tong et al., 2022, and reference therein). Our new AHe, AFT and ZFT data in the Gaize region, central-western TP, in combination with thermal history modeling, depicted a three-episode exhumation scenario (Tong et al., 2022), i.e. a phase of Late Cretaceous rapid exhumation followed by an accelerated Eocene-early Oligocene exhumation event and then a moderate exhumation episode since the early Miocene. These results are consistent with those from the northern Lhasa (Rohrmann et al., 2012) and Qiangtang terranes (e.g. Wang et al., 2008; Rohrmann et al., 2012; Zhao et al., 2020; Bi et al., 2022). Besides, recent low-temperature thermochronology studies in the central-southern Qiangtang terrane revealed an earlier exhumation episode during Late Jurassic-Early Cretaceous (Zhao et al., 2017; Qian et al., 2021; Zhang et al., 2021).

In the eastern TP margin, we recently reported new low-temperature thermochronology data for samples from four deep vertical sections (one in outcrop and three in deep drill-holes) and linking surface samples along a NW-SE transect (Li et al., 2023). Together with comparable data published for surface samples (e.g. Xu and Kamp, 2000; Tian et al., 2013) and another two steep vertical sections in outcrop (Xuelongbao and Pengguan massifs) (Wang et al., 2012; Furlong et al., 2021), our results revealed a three-episode rapid exhumation scenario with significantly spatial variability in the eastern TP margin, namely the Early Cretaceous (~130 Ma), Late Cretaceous (~90 – 70 Ma) and Late Cenozoic (~27 Ma – present day) (Li et al., 2023, and reference therein). The Early Cretaceous (~130 Ma) exhumation episode involved quite a part of the eastern TP and Longmen Shan Thrust Belt. The Late Cretaceous exhumation episode affected the whole eastern TP margin as far east as the Anxian-Guanxian Fault in the Longmen Shan front. The Late Cenozoic exhumation episode is recorded by the region east of the Longriba Fault System to the Longquan structure within the western Sichuan Basin, but not represented on the Eastern TP west of the Longriba Fault System at all.

To the northeastern TP margin, lots of previous low-temperature thermochronology studies have revealed multiple-episode exhumation events during early Late Cretaceous, early Late Eocene, and Late Oligocene – Middle Miocene and since the late Miocene, respectively (e.g. Zhuang et al., 2018; Tong et al., 2020, and reference therein; An et al., 2020). The early Late Cretaceous and early Late Eocene exhumation episodes were mainly localized to the pre-existing tectonic boundaries dividing rigid blocks. The Late Oligocene – Middle Miocene exhumation episode overspread the northeastern TP margin which is generally characterized by spatial propagation northwards from the East Kunlun Shan to the Qilian Shan-Nan Shan tectonic belt (e.g. Li et al., 2021; Tong et al., 2020, and reference therein).

By comparing the aforementioned uplift and exhumation processes between the central TP and its eastern,

northeastern margins, we suggest a three-stage differential exhumation and growth model of the TP since the Cretaceous.

(1) The eastern TP margin experienced two rapid exhumation events at ~130 Ma and ~90 – 70 Ma, followed by an extremely slow Cenozoic cooling process for the eastern TP west of the Longriba fault system (Li et al., 2023), suggesting a peneplain process with significant topography building of the eastern TP since the late Cretaceous, which we referred to as the Zoige paleo-Plateau (Liu et al., 2019). Of important note is that the central-southern Qiangtang terrane in the central TP also experienced an early Cretaceous rapid exhumation event, followed by a uniform rapid uplift and exhumation episode during the late Cretaceous, which likely resulted in surface uplift and topography growth in the Qiangtang and Lhasa terranes. Taken together, we suggest that the high topography in the central TP likely extended eastwards to the Zoige paleo-plateau, forming a united paleo-plateau by the late Cretaceous, here called the Qiangtang-Lhasa-Zoige paleo-plateau. We interpret the continued collision between Qiangtang and Lhasa terranes contributed to the formation of the Qiangtang-Lhasa-Zoige paleo-plateau, and also resulted in the reactivation of pre-existing tectonic belt associated with localized uplift and exhumation at the Qilian Shan-Nan Shan fold-and-thrust belt and Longmen Shan thrust belt in the northeastern and eastern TP margins, respectively.

(2) During ~55 Ma to ~30 Ma, the central TP experienced a rapid exhumation episode, which can be related to the hard collision of Indo-Asia Plates. Meanwhile, the early Cenozoic rapid exhumation event was sparsely localized in the eastern (e.g. Tian et al., 2022) and northeastern TP margins due mainly to the reactivation of former thrust faults.

(3) Since the early Oligocene, the central TP experienced a limited exhumation process with an extremely slow erosion rate, suggesting the establishment of present low-relief, high-elevation topography in the central TP. This high-elevation and flat topography in the central TP might produce a lateral horizontal compressional stress to its peripheral region, which subsequently, coupled with continuous India-Asia convergence, resulted in the thrusting and rapid uplift both in the eastern and northeastern TP margins by the Late Oligocene-Middle Miocene. In the eastern TP margin, a 150-km-wide Late Cenozoic (< 27 Ma) extraordinary exhumation zone bounded by the Longriba Fault system and the Wenchuan-Maoxian Fault was triggered by the development of a doubly-vergent orogenic wedge of the Longmen Shan Thrust Belt. To the northeastern TP margin, this thrust-related rapid uplift episode is generally characterized by a spatial propagation northwards from the East Kunlun Shan at Late Oligocene to the Qilian Shan-Nan Shan tectonic belt at Middle Miocene, which consequently contributed to significant topography building throughout the northeastern TP margin.

References

An, K., Lin, X., Wu, L., Yang, R., Chen, H., Cheng, X., Xia, Q., Zhan,g F., Ding, W., Gao, S., Li, C., Zhang, Y., 2020. An immediate response to the Indian-Eurasian collision along the northeastern Tibetan Plateau: Evidence from apatite fission track analysis in the Kuantan Shan-Hei Shan. Tectonophysics 774, 228278.

Bi, W., Li, Y., Kamp, P.J.J., Xu, G., Zhang, J., Han, Z., Du, L., Wang, C., He, H., Xu, T., Ma, Z., 2022. Cretaceous–Cenozoic cooling history of the Qiangtang terrane and implications for Central Tibet formation. GSA Bulletin 135 (5-6): 1587–1601.

Bi, W.J., Han, Z.P., Li, Y.L., Li, C.M., Wang, C.S., Zhang, J.W., Han, L.Y., He, H.Y., Qian, X.Y., Xu, T.K., Ma, Z.N., 2021. Deformation and cooling history of the Central Qiangtang terrane, Tibetan Plateau and its tectonic implications. Int. Geol. Rev. 63 (15), 1821–1837.

Furlong, K.P., Kirby, E., Creason, C.G., Kamp, P.J.J., Xu, G., Danišík, M., Shi, X., Hodges, K.V., 2021. Exploiting thermochronology to quantify exhumation histories and patterns of uplift along the margins of Tibet. Front. Earth Sci. 9, 688374.

Li, C., Zheng, D., Zhou, R., Yu, J., Wang, Y., Pang, J., Wang, Y., Hao, Y., Li, Y., 2021. Late Oligocene tectonic uplift of the East Kunlun Shan: Expansion of the northeastern Tibetan Plateau. Geophysical Research Letters, 48, e2020GL091281.

Li, Z.W., Kamp, P.J.J., Liu, S.G., Xu, G.Q., Tong, K., Danišík, M., Wang, Z.J., Li, J.X., Deng, B., Ran, B., Ye, Y.H., Wu, W.H., 2023. Late Cretaceous – Cenozoic thermal structure and exhumation of the Eastern Tibetan Plateau margin: A doubly-vergent orogenic wedge. Earth-Science Reviews 238, 104319.

Liu, S.G., Li, Z.W., Ran, B., Li, J.X., Deng, B., Wang G.Z., Yang, D., Wang, Z.J., 2019. Discovery of the Mesozoic Zoige paleo-plateau in eastern Tibetan Plateau and its geological significance. Journal of Chengdu University of Technology (Science & Technology Edition) 46 (1), 1–28. (in Chinese with English abstract)

Qian, X.Y., Li, Y.L., Dai, J., Wang, C.S., Han, Z.P., Zhang, J.W., Li, H., 2021. Apatite and zircon (U–Th)/He thermochronological evidence for Mesozoic exhumation of the Central Tibetan Mountain Range. Geol. J. 56, 599–611.

Rohrmann, A., Kapp, P., Carrapa, B., Reiners, P.W., Guynn, J., Ding, L., Heizler, M., 2012. Thermochronologic evidence for plateau formation in central Tibet by 45 Ma. Geology 40, 187–190.

Tian, Y.T., Kohn, B.P., Gleadow, A.J.W., Hu, S.B., 2013. Constructing the Longmen Shan eastern Tibetan Plateau

margin: Insights from low-temperature thermochronology. Tectonics 32, 576–592.

Tian, Y.T., Liu, Y.M., Li, R., Sun, X.L., Zhang, Z.J., Carter, A., Vermeesch, P., 2022. Thermochronological constraints on Eocene deformation regime in the Long-Men Shan: Implications for the eastward growth of the Tibetan Plateau. Global and Planetary Change 217, 103930.

Tong, K., Li, Z.W., Zhu, L.D., Xu, G.Q., Zhang, Y.X., Kamp, P.J.J., Tao, G., Yang, W.G., Li, J.X., Wang, Z.J., Jiang, X., Zhang, H.S., 2022. Thermochronology constraints on the Cretaceous-Cenozoic thermo-tectonic evolution in the Gaize region, central-western Tibetan Plateau: Implications for the westward extension of the proto-Tibetan Plateau. Journal of Asian Earth Sciences 240, 105419.

Tong, K., Li, Z.W., Zhu, L.D., Tao, G., Zhang, Y.X., Yang, W.G., Zhang, J.L., 2020. Fold-and-thrust deformation of the hinterland of Qilian Shan, northeastern Tibetan Plateau since Mesozoic with implications for the plateau growth. Journal of Asian Earth Sciences 198, 104131.

Wang, C.S., Dai, J.G., Zhao, X.X., Li, Y.L., Graham, S.A., He, D.F., Ran, B., Meng, J., 2014. Outward-growth of the Tibetan Plateau during the Cenozoic: a review. Tectonophysics 621, 1–43.

Wang, C.S., Zhao, X.X., Liu, Z.F., Lippert, P.C., Graham, S.A., Coe, R.S., Yi, H.S., Zhu, L.D., Liu, S., Li, Y.L., 2008. Constraints on the early uplift history of the Tibetan Plateau. P. Natl. Acad. Sci. USA 105 (13), 4987–4992.

Wang, E., Kirby, E., Furlong, K.P., van Soest, M., Xu, G., Shi, X., Kamp, P.J.J., Hodges, K.V., 2012. Two-phase growth of high topography in eastern Tibet during the Cenozoic. Nat. Geosci. 5, 640–645.

Xiong, Z., Ding, L., Wang, X., Spicer, R.A., Farnsworth, Wang, X., Valdes, P.J., Su, T., Zhang, Q., Zhang, L., Cai, F., Wang, H., Li, Z., Song, P., Guo, X., Yue, Y., 2020. The early Eocene rise of the Gonjo Basin, SE Tibet: from low desert to high forest. Earth Planet. Sci. Lett. 543, 116312.

Xiong, Z., Liu, X., Ding, L., Farnsworth, A., Spicer, R.A., Xu, Q., Valdes, P., He, S., Zeng, D., Wang, C., Li, Z., Guo, X., Su, T., Zhao, C., Wang, H., Yue, Y., 2022. The rise and demise of the Paleogene Central Tibetan Valley. Sci. Adv. 8, eabj0944.

Xu, G., Kamp, P.J.J., 2000. Tectonics and denudation adjacent to the Xianshuihe fault, eastern Tibetan Plateau: constraints from fission tract thermochronology. J. Geophys. Res. 105, 19231–19251.

Zhang, J.W., Li, Y.L., Xu, M., Dai, J.G., Qian, X.Y., Han, Z.P., Zhang, H.P., Pang, J.Z., 2021. New apatite fission track evidence from the northern Qiangtang terrane reveal two-phase evolution of central Tibet. Terra Nova 33, 95–108.

Zhao, Z.B., Bons, P.D., Li, C., Wang, G.H., Ma, X.X., Li, G.W., 2020. The Cretaceous crustal shortening and thickening of the South Qiangtang Terrane and implications for proto-Tibetan Plateau formation. Gondwana Res. 78, 141–155.

Zhao, Z.B., Bons, P.D., Stubner, K., Wang, G.H., Ehlers, T.A., 2017. Early Cretaceous Exhumation of the Qiangtang Terrane During Collision with the Lhasa Terrane, Central Tibet. Terra Nova 29, 382–391.

Zhuang, G.S., Johnstone, S.A., Hourigan, J., Ritts, B., Bobinson, A., Sobel, R.E., 2018. Understanding the geologic evolution of Northern Tibetan Plateau with multiple thermochronometers. Gondwana Res. 58, 195–210.

International Association for Gondwana Research 2023 Convention and
20th International Conference on Gondwana to Asia
Niigata, Japan, October 2023
Abstract Volume

A review of the prolonged early Paleozoic retreating subduction and accretionary orogenesis of the Altai Zone, Central Asian Orogenic Belt

Xing Cui[1,*], Min Sun[1], Guochun Zhao[1,2]

[1]Department of Earth Sciences, The University of Hong Kong, Pokfulam Road, Hong Kong, China
[2]Department of Geology, Northwest University, Xi'an, 710069, China
E-mail: tongkui@cdut.edu.cn

The Paleozoic western Mongolia Collage evolved along the southern margin of the Siberian Craton, which provides a detailed documentation of orogenic and continental stabilization processes that occurred in an accretionary plate margin. In this research, data review on sedimentation, magmatism, deformation and metamorphism establishes a comprehensive chronology of events that characterize the early-middle Paleozoic accretionary orogenesis of the Altai Zone from the western Mongolia Collage. At the onset of the Paleozoic, docking of the Lake Zone Island arc towards the Precambrian microcontinents in western Mongolia was succeeded by the establishment of a north-dipping subduction zone along the western margin of the Lake Zone. The subduction-related arc magmatism clustered at ca. 530-490 Ma, during which time accumulations of the flysch-like sequences from the Cambrian to early Silurian constituted the giant accretionary wedge of the Altai Zone. The subduction was in a retreat mode driven by slab rollback, manifested by the gradual migration of the arc from the Lake Zone to the Altai Zone. From the late Cambrian to Devonian, the mantle-derived mafic magma consolidated to the juvenile lower crust of the Altai Zone, while underplating-facilitated crustal anatexis signified the maturation and stratification of the upper crustal lithosphere. Data on deformation and metamorphism reveals switching between compression and extension of the upper plate during the accretionary history. Geological data integration and interpretation emphasize that the slab-roll back induced mantle flow during trench retreat dramatically influenced the wedge growth, creating tectonic switches in the upper plate and determining the magmatism and metamorphism of the accretionary complex. The resultant diachronous upper plate deformation and extensive magmatism are inferred to be a recurrent and global phenomenon, and the magmatism spanning from mantle melting to crustal anatexis is indicative of the stabilization of an immature accretionary wedge. This work was financially supported by Hong Kong RGC GRF (17302317), National Key R&D Program of China (2017YFC0601205), NSFC Projects (41730213, 42072264, 41902229, and 41972237).

International Association for Gondwana Research 2023 Convention and
20th International Conference on Gondwana to Asia
Niigata, Japan, October 2023
Abstract Volume

Mantle impressions of East Asian subduction history

Douwe G. van der Meer[1,2,*], D.J.J. van Hinsbergen[1], W. Spakman[1]

[1]Department of Earth Sciences, Utrecht University, 3584 CB Utrecht, the Netherlands
[2]CNOOC International, 90 Oxford Road, Uxbridge UB8 1LU, United Kingdom
[*]E-mail: douwevdm@gmail.com

Seismic wave tomography of the mantle reveals subducted lithosphere (slabs) as positive wave speed anomalies, which provide geodynamic constraints to understanding basin evolution. In 2018 a global framework was published wherein slabs had been correlated with their geological record, accessible online at www.atlas-of-the-underworld.org. This compilation summarized slabs from the upper mantle down to the core-mantle boundary, documenting subduction from ~300 Myr to Present. In our research we have correlated shallow slabs to active subduction and have interpreted progressively deeper slabs with older geological records. On their downward journey, slabs decelerate due to increased mantle viscosity, and stack/thicken as imaged in tomography. We do not observe slabs stagnating in the upper mantle indefinitely, all slabs have travelled through the upper mantle in <60 Myr. Along the East Asian margin, plate convergence has occurred since at least the Jurassic. Several detached slabs in the lowermost mantle, underneath the Asian continent, document the continental formation by closure of the Paleo-Asian and Mongol-Okhotsk Oceans. Further east, slabs under the continental margin, document semi-continuous subduction of oceanic plates. Under the continental margin, actively subducting slabs are imaged, but are detached from a prominent deeper slab. This separation is inferred to be largely the result of late Cretaceous-early Cenozoic approach and subduction of the Pacific-Izanagi ridge. This led to several slabs, lying flat within and just below the upper-lower mantle transition zone. Meanwhile throughout the Mesozoic, intra-oceanic subduction in the Panthalassa Ocean led to slabs below the present Pacific Ocean. Once intra-oceanic subduction ceased, with continued growth of the Pacific Plate, extinct arcs were transported to the Asian and American margins and accreted as exotic terranes. In this poster, we show some of the imaged slabs that have led to a more thorough understanding of the East Asian subduction history.

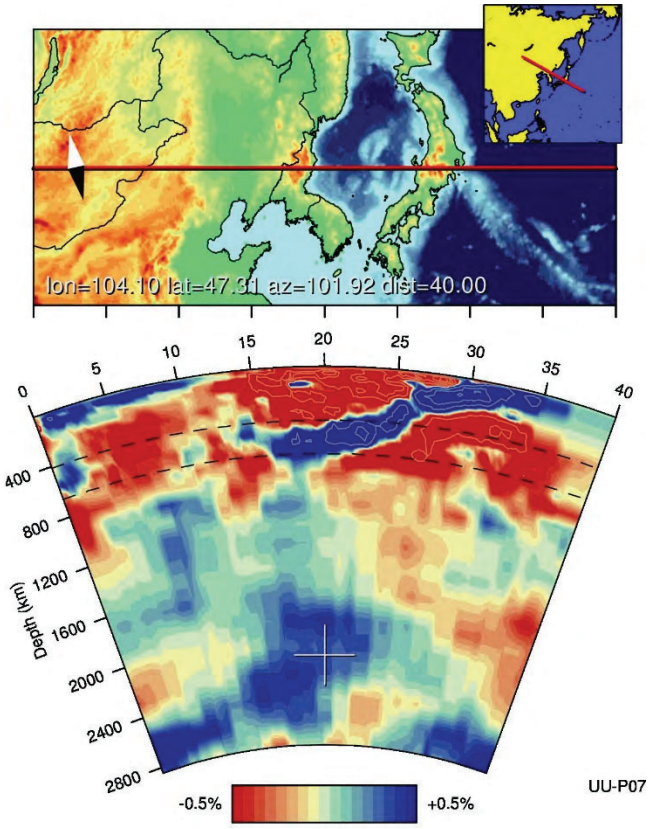

Figure 1: Tomographic image of the mantle under east Asia, displaying several actively subducting and detached slabs.

International Association for Gondwana Research 2023 Convention and
20th International Conference on Gondwana to Asia
Niigata, Japan, October 2023
Abstract Volume

Radiolaria- and zircon U–Pb-dated Permian strata on Sado Island, central Japan, and their geotectonic significance

Toshiyuki Kurihara[1,*], Keisuke Suzuki[2], Hirotaka Ishida[3]

[1]Department of Geology, Faculty of Science, Niigata University, Niigata 950–2181, Japan
[2]Geological Survey of Japan, AIST, 1–1–1 Higashi, Tsukuba, Ibaraki 305–8567, Japan
[3]Niigata City Office, 1-602-1 Gakkouchodori, Chuo-ku, Niigata 951-8550, Japan
[*]E-mail: kurihara@geo.sc.niigata-u.ac.jp

The pre-Cretaceous basement rocks of Sado Island (Niigata Prefecture), located in the Sea of Japan, are essential for understanding the relationship of basement rocks on Honshu Island and in northeast China and Far East Russia. However, the detail of their geology and age have remained uncertain due to the thick volcanic and sedimentary covers of the Cenozoic age. We investigated Permian strata in the Ota area of the Kosado Hills, Sado Island, central Japan, to determine their depositional age based on radiolarian biostratigraphy and zircon U–Pb dating. We also focused on the geology of the region and its geotectonic significance.

The Paleozoic rocks in the Kosado Hills are exposed from the coastline of Ota and its surrounding mountains to Mikawa in the west. The Paleozoic strata consist mainly of alternating sandstone and mudstone, along with limestone and basaltic rocks. The strata generally strike WNW–ESE to E–W and dip 20°–80° to the north and northeast. Late middle Permian radiolarians from mudstone exposed on a forest road in Ota have been reported Suzuki et al., 2003. Limestone boulders containing late middle Permian fusulinids have been found around Mikawa Ichida et al., 2010.

The radiolarian analysis revealed the presence of Follicucullus porrectus and Follicucullus dilatatus in mudstone exposed on the coastline of Ota, indicating a middle–late Capitanian to early Changhsingian age. Mudstone exposed along the forest road of Ota yielded Cariver charveti, suggesting a late Capitanian–early Changhsingian age. Zircon U–Pb dating of a tuff layer intercalated within the Follicucullus-bearing mudstone resulted in a weighted mean age of 260 ± 2 Ma, corresponding to a Capitanian–Wuchiapingian age. The tuffaceous sandstone with mudstone, including C. charveti, yielded a weighted mean age of 264 ± 6 Ma, spanning the Rodian to Wuchiapingian. Its youngest model peak age (256.6 ± 2.6 Ma) obtained through peak separation provides the most reliable estimation for the maximum depositional age, corresponding to a Wuchiapingian age.

The Permian strata in the Kosado Hills have been investigated with the objective of their correlation with geologic units in neighboring regions. The strata have previously been considered to have a strong relationship to the Ultra-Tamba or Maizuru belts based on lithological similarities and fossil affinities Suzuki et al., 2003, Ichida et al., 2010. However, the absence of chert and undeformed rocks in the Kosado Hills suggest that these are not part of the Ultra-Tamba belt. The Permian strata of the Kosado Hills have closer affinities to the Maizuru Group in the Maizuru belt.

References

Suzuki, H., Kuwahara, K., 2003. J. Geol. Soc. Japan 109, 489–492.
Ichida, M., Suzuki H., Kondo, M., Nogami, Y., 2010. Fossils 87, 29–34.

International Association for Gondwana Research 2023 Convention and
20th International Conference on Gondwana to Asia
Niigata, Japan, October 2023
Abstract Volume

Magmatic and crustal evolution of volcanic arcs through back-arc spreading: A case study of the opening of the Japan Sea

Raiki Yamada[1,*], Toshiro Takahashi[1]

[1]Faculty of Science, Niigata University, Niigata 950-2181, Japan
[*]E-mail: yamada.raiki.geo@gmail.com

Introduction

As continents have grown in subduction zones through the earth's history (Sawada et al., 2018), back-arc spreading is considered to have provided complementary information on tectono-thermal evolution of active continental margins (Wolfram et al., 2019). Therefore, arc volcanism during back-arc spreading is considered to be a significant key to reveal process of evolution of volcanic arcs. However, many unsolved issues are still remaining in such magmatism.

Opening of the Japan Sea (Japan Sea opening), which occurred from 44 to 15 Ma, is one of typical Cenozoic back-arc basin formations in the western Pacific region (Jolivet et al., 1994). Extensive arc volcanism occurred especially in the Japan Sea side of the Japan arc during back-arc spreading in the Japan Sea. Although many researchers have revealed temporal change of chemical variations in related volcanic rocks (e.g., Shuto et al., 2015), only basalts and andesites have been selected as the main objects. Therefore, petrogenesis and significance of rhyolites, which is also distributed widely in the Japan arc, is waiting to be solved. Considering these situations, we studied whole-rock chemical compositions (major and trace elements and Sr–Nd isotope) of Oligocene to Miocene andesitic to rhyolitic volcanic rocks from the Toyama basin in the SW Japan arc in order to understand magmatic and crustal evolution of volcanic arcs through back-arc spreading.

Geological settings and sample description

The Toyama basin, one of the large sedimentary basins in the SW Japan arc, is characterized by voluminous andesites and rhyolites (Yamada and Takahashi, 2021). Volcanic rocks which formed during the Japan Sea opening in the Toyama basin consists mainly of alkalic rhyolite (Tori F.; F. indicates formation), sub-alkalic to alkalic andesites (Iwaine F.) and sub-alkalic rhyolites (Iozen F.). These formations considered to have been formed in 23–22 Ma, 18–17 Ma and 17–16 Ma, based on radiometric ages and chronostratigraphy (Nakajima et al., 2019; Yamada and Takahashi, 2021).

Collected volcanic rock samples can be classified into five rock types, on the basis of petrographic features: biotite-bearing rhyolitic pyroclastic rocks (Type-1 rhyolite; Tori F.), olivine two-pyroxene andesite (Type-2 andesite; Iwaine F.), two-pyroxene amphibole andesite (Type-3 andesite; Iwaine F.), two-pyroxene andesite (Type-4 andesite; Iwaine F.) and aphyric rhyolite (Type-5 rhyolite; Iozen F.). Type-1 rhyolite shows alkalic chemical composition, whereas Type-5 rhyolite is composed of sub-alkalic dacite to rhyolite. Type-2 is high-magnesian andesite (HMA) characterized by high MgO content (7.81 wt.% in the maximum). Type-3 andesite is high-Sr andesite characterized by unusually high Sr concentration (>2000 ppm). Type-4 andesite is tholeiitic andesite showing differentiated chemical compositions (Mg# = 41–49).

Results and discussion

Results of whole-rock geochemical compositions and model calculations provide following petrogenesis and magmatic evolution processes. Arc magmatism related to the Japan Sea opening in the Toyama basin initiated with eruption of rhyolitic pyroclastic flows (Type-1 rhyolite) at 23 Ma. It is considered that Type-1 rhyolite magma was generated by high-rate crustal assimilation of contemporaneously active basaltic magma, which are distributed in the Noto peninsula as Kamiwazumi and Matsunagi Fs., with the Hida belt in the continental crust. After magmatic hiatus between 22–18 Ma, andesitic lava flows were effused as Type-2 to -4 andesites in stratigraphic ascending order in 18–17 Ma. Type-2 andesite magma was produced by partial melting of the mantle peridotite saturated by H_2O derived from slab fluid, meanwhile Type-3 andesite magma is considered as low-SiO2 adakite (LSA; Martin et al., 2005), generated by partial melting of the mantle wedge metasomatized by slab melt. In addition, partial melting of the mantle wedge produced parental sub-alkalic basaltic magma, and this basaltic magma assimilated the continental crust to generate Type-4 andesite magma. Type-5 rhyolite, effused just after andesitic magmatism, is thought to have been generated by mixing between andesitic magma and crustal melt. Although Type-5 rhyolite is affected by crustal material as well as Type-1 rhyolite, the degree of effect for Type-5 rhyolite seems to be lower than that for Type-1 rhyolite. Arc magmatism related to the Japan Sea opening in the Toyama basin terminated with the rhyolitic magmatism at 16 Ma. This magmatic evolution suggests that upwelling of the asthenospheric mantle into the

mantle wedge caused melting of the subducting Pacific plate, and that basaltic to andesitic magmatism caused crustal melting and assimilation to generate rhyolitic magma. Moreover, back-arc spreading in the Japan Sea was driven by upwelling of the asthenospheric mantle into the mantle wedge. In particular, Type-1 and -5 rhyolites with large volumes have significantly similar chemical composition to the upper continental crust, suggesting that rhyolitic magmatism during back-arc spreading contributes recycling and growth of the arc crust.

References

Jolivet, L., Tamaki, K., Fournier, M., 1994. Japan Sea, opening history and mechanism: A synthesis. Journal of Geophysical Research 99, 22237–22259.

Martin, H., Smithies, R.H., Rapp, R., Moyen, J.-F., Champion, D., 2005. An overview of adakite, tonalite–trondhjemite–granodiorite (TTG), and sanukitoid: relationships and some implications for crustal evolution. Lithos 79, 1–24.

Nakajima, T., Iwano, H., Danhara, T., Yamashita, T., Yanagisawa, Y., Tanimura, Y., Watanabe, M., Sawaki, T., Nakanishi, S., Mituishi, H., Yamashina, O., Imahori, S., 2019. Revised Cenozoic chronostratigraphy and tectonics in the Yatsuo Area, Toyama Prefecture, central Japan. The Journal of the Geological Society of Japan 125, 483–516 (in Japanese with English abstract).

Sawada, H., Isozaki, Y., Sakata, S., Hirata, T., Maruyama, S., 2018. Secular change in lifetime of granitic crust and the continental growth: A new view from detrital zircon ages of sandstones. Geoscience Frontiers 9, 1099–1115.

Shuto, K., Nohara-Imanaka, R., Sato, M., Takahashi, T., Takazawa, E., Kawabata, H., Takanashi, K., Ban, M., Watanabe, N., Fujibayashi, N., 2015. Across-arc variations in geochemistry of Oligocene to Quaternary basalts from the NE Japan arc: Constraints on source composition, mantle melting and slab input composition. Journal of Petrology 56, 2257–2294.

Wolfram, L.C., Weinberg, R.F., Nebel, O., Hamza, K., Hasalová, P., Míková, J., Becchio, R., 2019. A 60-Myr record of continental back-arc differentiation through cyclic melting. Nature Geoscience 12, 215–219.

Yamada, R. and Takahashi, T., 2021. Temporal and spatial changes of magmatism related to the Japan Sea opening in the Hokuriku region, central Japan: stratigraphy, chronology and petrology of Oligocene to middle Miocene volcanic rocks. The Journal of the Geological Society of Japan 127, 507–525 (in Japanese with English abstract).

International Association for Gondwana Research 2023 Convention and
20th International Conference on Gondwana to Asia
Niigata, Japan, October 2023
Abstract Volume

Paleozoic high-pressure schists in the Omi area, Itoigawa city, Niigata

Takumi Yoshida[1,*], M. Satish-Kumar[2]

[1]Graduate School of Science and Technology, Niigata University, Niigata 950-2181, Japan
[2]Department of Geology, Faculty of Science, Niigata University, Niigata 950-2181, Japan
[*]E-mail: trilogite@gmail.com

Introduction

The Omi area located in the westernmost Niigata prefecture is known for its Paleozoic crystalline schists which originated in a subduction zone. Previous studies conducted in the Omi area have reported that this area consists of serpentinite-melange, including LT/HP type crystalline schists and various other rock types such as amphibolite, rodingite and jadetite (Banno, 1958; Matsumoto, 1980). Crystalline schists in this area are named as "Omi schist" (Banno, 1958) and are divided in to three mineral isograds (biotite zone, garnet zone, chlorite zone). An eclogitic glaucophane schist boulder was discovered in the western part of the Omi area (Tsujimori et al, 2000). This discovery led to the demarcation of eclogite unit (EC unit) and non-eclogite unit (N-EC unit) in the Omi area. EC unit is defined as consisting of high-pressure rocks such as garnet-glaucophane schists and eclogite facies rocks. In contrast, N-EC unit is comprised low-pressure rocks and medium temperature rocks (such as greenschist and amphibolite). K-Ar and Ar-Ar ages of schists in the Omi area are 300-380Ma. Various studies conducted in the Omi area

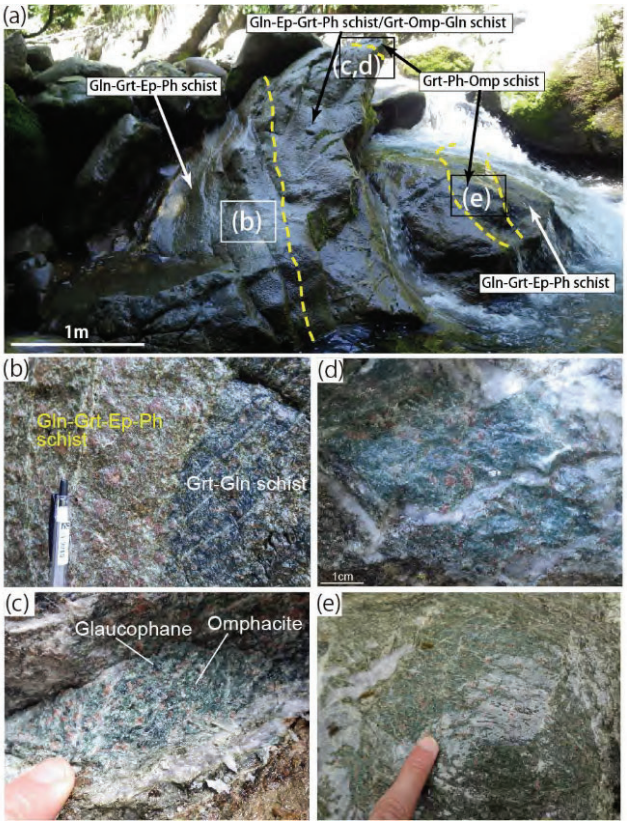

Figure 1: Jolivet, L., Tamaki, K., Fournier, M., 1994. Japan Sea, opening history and mechanism: A synthesis. Journal of Geophysical Research 99, 22237–22259.

Table-1. Representative microprobe analysis of omphacite.

	Kanayamadani eclogite			shinadani eclogite		
wt.%	63	C3-9	C3-22	50	51	31
SiO2	56.66	55.60	55.68	55.66	55.67	55.90
TiO2	0.11	0.10	0.09	0.00	0.00	0.00
Al2O3	11.51	11.60	11.09	11.02	11.09	11.06
Cr2O3	0.00	0.05	0.06	0.04	0.00	0.03
FeO	4.58	5.40	4.66	7.51	7.37	6.76
MnO	0.10	0.01	0.04	0.08	0.10	0.07
MgO	7.96	7.61	8.17	6.56	6.53	6.82
CaO	13.12	13.05	13.42	11.83	11.80	12.05
Na2O	6.00	6.85	6.91	7.54	7.58	7.54
K2O	0.02	0.00	0.00	0.00	0.00	0.00
Total	100.06	100.26	100.11	100.24	100.15	100.21
O=4						
Si	2.027	1.977	1.976	1.986	1.987	1.990
Ti	0.003	0.003	0.002	0.000	0.000	0.000
Al	0.485	0.486	0.464	0.464	0.466	0.464
Cr	0.000	0.001	0.001	0.001	0.000	0.000
Fe	0.137	0.160	0.138	0.224	0.220	0.201
Mn	0.003	0.000	0.001	0.002	0.003	0.002
Mg	0.424	0.404	0.432	0.349	0.348	0.362
Ca	0.503	0.497	0.510	0.452	0.451	0.460
Na	0.416	0.472	0.475	0.522	0.525	0.520
K	0.001	0.000	0.000	0.000	0.000	0.000
Total	4.000	4.000	4.000	4.000	4.000	4.000
XJd	0.54	0.44	0.42	0.44	0.44	0.44
XAe	0.00	0.03	0.05	0.09	0.08	0.08
XAug	0.46	0.53	0.53	0.48	0.48	0.48

reported that this area consists of serpentinite-melange, including high-pressure metamorphic rocks and serpentinite. But detailed tectonics of metamorphic rocks in this area are not clear. So, field investigations in the Omi area were carried out to understand the geological relations and petrologic significance of the EC and N-EC units. In addition, the quantitative analysis of minerals was obtained using a WDS electron micro probe analyzer (JEOL JXA-8600 SX; Table-1). Zircon separation and U-Pb analysis were also performed.

Result

According to the results of this study, I have found out two new eclogite (Kanayamadani eclogite and Shinadani eclogite) locality in the EC unit area (Kanayamadani eclogite shown in Fig-1) Kanayamadani-eclogite occurs as about 1-1.5m wide layer in garnet-glaucophane-phengite schist. Shinadani-eclogite is discovered as boulder of about 2.5m boulder. In addition, I carried out zircon U-Pb dating of two samples (garnet-glaucophane schist and garnet-phengite schist) which records blueschist facies metamorphism. The sample used for analysis is a Grt glaucophanite, occurring as a layer or lenticular form surrounded by politic schists (Grt-Ms schist). It comprises euhedral~subhedral garnet porphyroblast (1-4mm) and large amount of euhedral glaucophane. About 200 zircon grains were hand-picked and U-Pb analysis was carried out using an Agilent 7500a LA-ICPMS at Niigata University. Zircon grains in both samples show core and rim structure and clearly oscillatory zoning in the core. Age distribution shows a strong peak at about 450-460Ma for garnet-glaucophane schist with some of the zircons showing old age (600-1400Ma). Two peaks of about 420-450Ma and 570-600Ma are recognized in garnet-phengite schist and it contains older zircons as well (1000-3200Ma; Yoshida et al., 2020).

Discussion

The Archean to Proterozoic zircons were possibly derived from South China continental crust. In early Paleozoic Japan, proto-Japan located in the continental margin of South China whereby older population of detrital zircons (600-3200Ma) were carried to trench filling sedimentary rocks. In addition, subduction related plutonism (around 400-500Ma) is observed deep below in the proto-Japan. Thus, various zircons were combined and descended to mantle along with oceanic plate and metamorphosed to high-pressure conditions such as eclogite and blueschist.

References

Banno, S., 1958. Glaucophane schists and associatited rocks in the Omi district, Niigata Prefecture, Japan. Japanese Journal of Geology and Geography 29, 29-44

Matsumoto, K.., 1980. Serpentinite mélange of Omi area, Hida-Gaien belt, Synthetic research of Hida-Gaien belt: study report, 1, 1-14.

Tsujimori, T., et al., 2000. Eclogitic glaucophane schist from the Yunotani valley in Omi Town, the Renge metamorphic belt, the Inner Zone of southwestern Japan. Journal of The Geological Society of Japan, Vol. 106, 353-362.

Yoshida, T., Taguchi, T., Ueda, H., Horie, K., Satish-Kumar, M., 2021. Early Carboniferous HP metamorphism in the Hida Gaien Belt, Japan: Implications for the Palaeozoic tecnic history of proto-Japan. Journal of Metamorphic Geology, 39, 77-100.https://doi.org/10.1111/jmg.12564.

International Association for Gondwana Research 2023 Convention and
20th International Conference on Gondwana to Asia
Niigata, Japan, October 2023
Abstract Volume

Application of Raman spectra of carbonaceous material and carbon isotope thermometry in low-medium grade metacarbonate from the Chitradurga Schist Belt, Dharwar Craton

Sasidharan Kiran[1,*], Madhusoodhan Satish-Kumar[2], Yoshihiro Nakamura[3], Tomokasu Hokada[4]

[1]Graduate School of Science and Technology, Niigata University, Japan
[2]Faculty of Science, Niigata University, Japan
[3]Geological Survey of Japan, AIST, Japan
[4]National Institute of Polar Research, Tachikawa, Japan
[*]E-mail: kiransasidharan.s@gmail.com

Structural evolution of carbonaceous material to graphite based on micro-Raman spectrosocpy is widely used as a geothermometer in metapelitic rocks. However, the application of this technique in metacarbonate rocks has not been established yet because of fluorescence of calcite and isotopic exchange between graphite and carbonate minerals. Here, we compare Raman spectroscopy of carbonaceous material thermometry and carbon isotope thermometry in low- to medium-grade metacarbonate rocks from the Archean Chitradurga Schist Belt in the Dharwar Craton, India. The carbonates in the lowermost Bababudan Group have metamorphosed under lower amphibolite facies metamorphic conditions giving consistent estimates for both Raman spectra of carbonaceous material thermometry (460–592 °C) and carbon isotope thermometry (450–560 °C). Nevertheless, in the Vanivilas Formation, the carbonaceous material with very fine flaky morphology in the grain boundary has slightly lower crystallinity, when compared to the coarse-grained ones near the vein boundary. Contrastingly, the carbon isotope thermometry estimated a lower temperature by more than 100 °C compared to Raman spectra of carbonaceous material thermometry. The difference in the temperature estimations might be resulted by the widespread post-metamorphic aqueous hydrothermal fluid infiltration, evidenced by the abundance of quartz veins crisscrossing the carbonates. The oxygen isotope ratio of the carbonates near the vein boundary lowered by 2.3‰, while the carbon isotope ratios without any variation also supports this. Fluid assisted recrystallization and coarsening of the carbonaceous material near the vein boundary is revealed by the enhancement of the crystallinity from the Raman spectra. Furthermore, the negative 13C shift in the carbonaceous material (c. –8.5 to –13‰) could have been attributed to the recrystallization after partial CO2 degassing. The Bababudan Group and the Vanivilas Formation in the Chitradurga Schist Belt have undergone regional metamorphism under lower amphibolite facies conditions, probably as a result of the extensive granitic intrusion at around 2.61 Ga and later being impacted by a hydrothermal event at around 2.5 Ga.

International Association for Gondwana Research 2023 Convention and
20th International Conference on Gondwana to Asia
Niigata, Japan, October 2023
Abstract Volume

Establishment of modern plate tectonic regime and modern Earth system in the late Neoproterozoic- early Cambrian

Yao Jinlong[1,*], Zhao Guochun[2,1], Cawood PA[3], Han Yigui[1], Liu Qian[1]

[1]Department of Geology/State Key Laboratory of Continental Dynamics, Northwest University, Xi'an 710069, China.
[2]Department of Earth Sciences, The University of Hong Kong, Hong Kong, China
[3]School of Earth, Atmosphere & Environment, Monash University, Melbourne, VIC 3800, Australia.
[*]E-mail: yaojinong@nwu.edu.cn

Plate tectonic regime drives the recycle and exchange of elements and energy between lithosphere and Earth surface, therefore sustaining a habitable Planet Earth, but Earth was not born with Plate tectonics. The evolution of plate tectonics is controlled by ambient mantle temperature and sediments in subduction channel. Plate tectonic regime initiated at some time in the Archean and evolved from warm subduction to possible stagnant Earth's middle age, and finally to cold and deep type subduction. Since the Neoproterozoic, low thermobaric ratio (T/P) ultra-high pressure metamorphic rocks occurred, especially in the phanerozoic. Meanwhile, Mariana type subduction initiation ophiolites, formation of which requires high lab strength controlled by mantle temperate, also occurred. These geological evidences indicate transition of tectonic regime into cold and deep subduction at this age range. In the early Cambrian, during final Gondwana assembly stage, a global tectonic re-organization at ca. 530~520 Ma occurred. Moreover, numbers of passive margins, thermobaric ratios, mean zircon Hf-O values reached the highest or lowest values at the same time, suggesting a peak of subduction flux. Therefore, we conclude that modern type plate tectonic regime initiated at sometime in the Neoproterozoic and was established in the early Cambrian, following a short interval of tectonic transition. Establishment of modern plate tectonic regime led to the formation of unprecedently high super-mountains during Gondwana assembly, and thus increased surface erosion rates that supplied massive nutrition to oceans and enhanced organic carbon sequestration, improving ocean photosynthesis productivity and thus responsible for the Neoproterozoic Oxidation Event (NOE). In addition, high subduction flux also increased tectonic degassing rate, which facilitated the NOE as well. Therefore, both orogeny related erosion and carbon cycle in subduction zone contributed to the NOE and a more habitable Earth, eventually leading to the Ediacaran and early Cambrian life explosion events. With Earth's climate and environment gradually analogues to modern Earth and almost all branches of animals occurred on Earth, a multiple cycle closely coupled and life flourished modern Earth system was formed.

Acknowledgement

This research is funded by the NSFC grants (41972238, 41730213, and 42072264), the State Key Laboratory of Continental Dynamics (201212000174) and the Hong Kong Research Grants Council General Research Fund (grants 17307918).

International Association for Gondwana Research 2023 Convention and
20th International Conference on Gondwana to Asia
Niigata, Japan, October 2023
Abstract Volume

Updating the digital paleogeographic maps for East Tethys from Middle Permian to Middle Triassic

Anqing Chen[1,2,*], Mingcai Hou[1,2], Qiang Ren[1,2], Mengxia Tang[1,2], Peng Ti[3], Hanting Zhong[1,2], Zhilin Li[3]

[1]Key Laboratory of Deep-time Geography and Environment Reconstruction and Applications, MNR & Institute of Sedimentary Geology, Chengdu University of Technology, Chengdu 610059, China
[2]State Key Laboratory of Oil and Gas Reservoir Geology and Exploitation, Chengdu University of Technology, Chengdu 610059, China
[3]Faculty of Geosciences and Environmental Engineering and The State-Province Joint Engineering Laboratory of Geospatial Information Technology for High-Speed Railway Safety, Southwest Jiaotong University, Chengdu 611756, China
[*]E-mail: chaq@cdut.edu.cn

Deep-time geographic maps are the setting base of geological research and integrated windows for looking the past earth. Reconstructing paleogeography involves the evolution of the earth's surface tectonic process, the pattern of land and sea, climate, and biology in geological history. To now, an advancing trend is developing digital paleogeographic model to replace the traditional maps. There already have been various global paleogeographic models based on digital softs, but it is still a lack of intelligent or efficient tools for updating these paleogeographic models or creating new maps via integrating tectonic, lithofacies, paleontology, and paleoclimate data. In this study, a case study of the comprehensive paleogeographic reconstruction is carried out for the Middle Permian-Middle Triassic East Tethys, where is highly concerned and rich in geological data accumulation. The digital maps are reconstructed by the combination of automatic mapping with machine learning and manual correction. We use the newly upgraded paleomagnetic, geological and paleontological data to restore the paleoposition of the East Asian blocks at 260, 250 and 240 Ma, which shows the Paleo-Tethys Ocean (PTO) had a wider east-west range than the previous version due to a new paleolongitude of South China at 260 Ma through adopting the method of the Torsvik et al. (2008). Our model shows the multiple microblocks in the PTO were divided into north and south branches, which were semi-closed with several narrow seaways rather than total-closed at 260 Ma. Based on the newly lithofacies paleogeographic atlas of China and marine fossils data, we updated the surface landscape on our new block-pattern by developing a method of automatic mapping paleotopography with manual supervised machine learning.

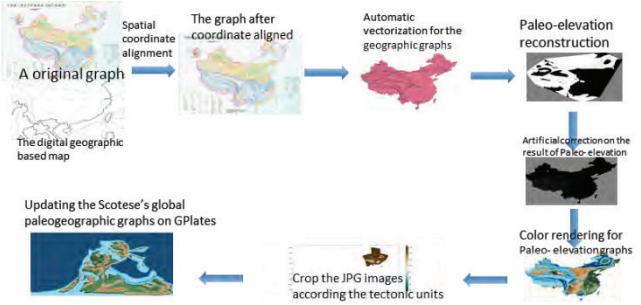

Figure 1: The workflow of landform reconstruction by litho-paleogeographic map using image machine learning technique.

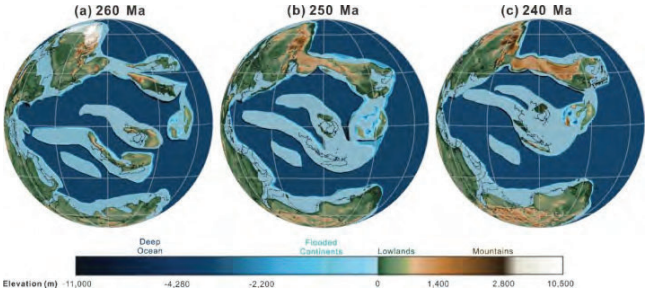

Figure 2: The newly updated paleogeographic graphs of the Eastern Tethyan domain

International Association for Gondwana Research 2023 Convention and
20th International Conference on Gondwana to Asia
Niigata, Japan, October 2023
Abstract Volume

Statistical periodicities of Japan earthquakes detected by Hi-Net seismic network

Jinhai Zhang[1,*], Jinbo Zheng[1]

[1]Engineering Laboratory for Deep Resources Equipment and Technology, Institute of Geology and Geophysics, Chinese Academy of Sciences, Beijing 100029, China
[*]E-mail: zjh@mail.iggcas.ac.cn

Earthquakes, with their potential for significant damage, remain a global concern. However, understanding the physical and chemical changes in earthquake focal areas, stress accumulation, and triggering mechanisms present challenges due to accessibility limitations. Nevertheless, external triggering mechanisms can be explored through seismic event catalogs from ground observation stations. This study investigates earthquake triggering mechanisms as a vital avenue to explore earthquake laws before conducting in-situ studies of the focal area.

The existence of daily cycles in earthquake activity has been a topic of contention, influenced by several factors. Inadequate and inconsistent accumulation of seismic catalogs result in insufficient data to extract weak periodic signals, while the lack of widely accepted processing methods hinders the identification of ultra-faint signals. Additionally, distinguishing between diurnal cycles related to human activities and inherent seismic events poses a challenge. Addressing these obstacles will require advancements in data accumulation and processing techniques.

Japan, with its intense seismic activity and comprehensive seismic network (Hi-Net), presents a promising dataset for studying earthquake periodicity. We utilize time-frequency and stacking methods to analyze Japan's earthquake catalog from the past 15 years. The catalog we analyzed includes constraining the depth range of seismic sources (0-30km), considering events within 30km of Japan's coastline, and avoiding periods with strong human noise (00:00-06:00). Our results revealed a diurnal periodicity, but the expected Moon-associated period remains elusive. The study diligently considered data selection, method validation, and human noise interference, ensuring credible results. Notably, a distinct low valley of nightside earthquakes around 3:30 reflects a pattern in Japan's seismic activity (Fig.1). Contradicting the assumption of a completely random distribution, a local peak during 3:00-4:00 was not observed, suggesting periodic variations in earthquake occurrence from midnight to daybreak. This implies a weak trend of change over time, with fluctuations ranging from -5% to +8% (around the reference of 3500). However, the weak 24-hour period was significant in M1.0+ data but limited in M2.0+ data.

The periodicity appears to be linked to the Sun rather than the Moon, with certain solar factors like the solar wind, temperature variation, and Earth's rotation potentially playing dominant roles. While this work contributes to statistical seismology and offers insights into earthquake periodicity, determining the primary physical factor requires further investigation.

In conclusion, our research indicates periodic variations in earthquake activity, particularly from midnight to daybreak, providing valuable reference for statistical seismology. Notably, the identified periodicity pattern aligns with small earthquakes, which constitute the majority of seismic events. This study contributes to the understanding of earthquake periodicity and triggering mechanisms, offering potential avenues for future research.

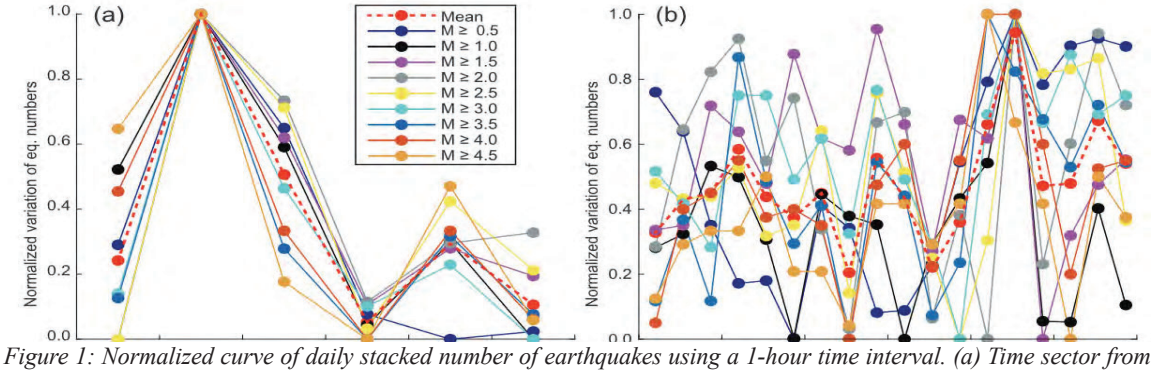

Figure 1: Normalized curve of daily stacked number of earthquakes using a 1-hour time interval. (a) Time sector from 0:00 to 6:00; (b) time sector from 6:00 to 24:00

How deceptive is typology of granitic rocks? Insights from the Triassic Xiangride felsic igneous complex in Kunlun Orogen, North Tibet

Fuhao Xiong[1,*] Changqian Ma[2]

[1]Chengdu University of Technology, Chengdu 610059
[2]China University of Geosciences (Wuhan), Wuhan 430074
[*]E-mail: fhxiong@cdut.edu.cn

The genetic types of granites and their volcanic equivalents are closely controlled by magma sources, evolutionary processes and tectonic settings, and these changeable factors make it difficult to accurately determine their typology, which often leads to ambiguous or deceptive understanding of the genetic types. In this study, a systematic petrological, chronological, elemental geochemical and Sr-Nd-Hf isotopic study was conducted on Triassic felsic igneous rocks in the East Kunlun orogenic belt (EKOB), aiming to reveal their genetic types, petrogenesis and geodynamics settings. Zircon U-Pb dating reveals that the Xiangride syenogranites and rhyolites were formed at ca. 228 and 208 Ma, respectively. Field geological and petrological studies indicate that the ca. 208 Ma rhyolites were deposited by eruption over the ca. 228 Ma syenogranites, suggesting a rapid uplift and erosion occurred between 228 and 208 Ma. Geochemical studies show that the syenogranites are metaluminous to weak peraluminous series, similar to typical of highly fractionated S-type granitic rocks. And these syenogranites have negative εHf(t) values of -8.33 to -1.45, with two-stage Hf model ages (TDM) range from 1588 to 1209 Ma. While the ca. 208 Ma Xiangride alkaline rhyolites display high contents of total alkali and (Zr + Nb + Ce + Y) with high Ga/Al ratios, resembling typical of A1-type granite generated in within-plate settings. However, previous studies have revealed the existence of Late Triassic A2-type granites in EKOB. Therefore, how to explain the coexistence of A1-and A2-type granites is particularly interesting. Geochemical and Sr-Nd-Hf isotopic compositions suggest that the late Triassic rhyolites were likely generated via partial melting of a metasomatized lithospheric mantle followed by prolonged fractional crystallization and minor crustal contamination in post-collisional extentsion setting rather than within-plate setting. This study suggest that a tectonic transition in the EKOB from syn-collision to post-collision extension occurred at between 228 Ma and 208 Ma, and reveals that the fractional crystallization of mantle-derived OIB-type arc magma in orogen is an important mechanism for the generation of A1-type granitic rocks. Therefore, detailed discussion on the genetic mechanism of A1-type granites, rather than simply applying classic models, is the key to accurately determine their geodynamic background.

International Association for Gondwana Research 2023 Convention and
20th International Conference on Gondwana to Asia
Niigata, Japan, October 2023
Abstract Volume

Evidence for breakup of Rodinia supercontinent from mid-Neoproterozoic rocks in the northeastern Yangtze Block, China

Yuan Xiaoyu[1,2,*], Cai Qianru[3]

[1]Frontiers Science Center for Deep Ocean Multispheres and Earth System, Key Lab of Submarine Geosciences and Prospecting Techniques, and College of Marine Geosciences, Ocean University of China, Qingdao 266100, China
[2]Laboratory for Marine Mineral Resources, Laoshan Laboratory, Qingdao 266100, China
[3]Shengli oil field exploration and Development Research Institute, Dongying, 257015, China
[*]E-mail: yuanxiaoyu@ouc.edu.cn

Neoproterozoic geological events related to the Precambrian supercontinental cycle are widely developed around the Yangtze Craton, which are useful in revealing the effects of breakup-convergence process of supercontinent on Yangtze Craton. However, owing to the absence of systematic research on volcanism-magmatism, sedimentation in the Northeast Yangtze Craton during this period, it has become a huge obstacle to our understanding of the early evolution of the Yangtze Craton. In response to this issue, Middle Neoproterozoic magmatic-sedimentary rocks in the Zhangbaling Uplift are selected as the major research objects. Petrographic research and zircon U- Pb dating indicate that the target rocks are composed mainly of two episodic silicic magmatic rocks (807–787 Ma granitic gneiss; 757–740 Ma quartz-keratophyre), with the proximal sedimentary rocks were deposited at about 662 Ma. Granitic gneisses and quartz-keratophyres both exhibit affinity of typical A-type granites with high SiO2, total-alkali contents, HFSEs and FeOT/(FeOT +MgO) ratios, corresponding to an extensional tectonic setting in the research region. Significantly, these two episodic magmatic rocks also show the transform of residual mineral from garnet to plagioclase, which hint a variable depth of their magma sources. Together with their diverse zircon Lu-Hf isotopic components (εHf(t) = -29.9–-11.8; -5.8–2.5), revealing a crustal structure composed of ancient lower crust and juvenile middle-upper crust. The particular crustal structure is obviously different from the adjacent Dabie-Sulu orogenic belt, hinting the Zhangbaling Uplift is an in-situ uplift zone. Thus, the complete process of magma evolution reflected by granitic gneisses and quartz-keratophyres correspond to different stages of continental rifting, which records the change in regional tectonic system from initial extension to mature rifting under the drive of Rodinia supercontinent breakup. In addition, the prominent affinity between low δ18O magmatism and sedimentation in the Yangtze and India Craton speculated that the Yangtze Craton should be located on the margin of the Rodinia supercontinent.

International Association for Gondwana Research 2023 Convention and
20th International Conference on Gondwana to Asia
Niigata, Japan, October 2023
Abstract Volume

Felsic – mafic magmatism in the Madras Block, India: Insights into Neoarchaean tectonics

P. V. Thanooja[1,2,*], K. Sajeev[1], M. Satish-Kumar[3], I. S. Williams[4]

[1]Centre for Earth Sciences, Indian Institute of Science, Bengaluru, India
[2]Hydrology and Climatology Research Group, Centre for Water Resources Development and Management, Calicut, Kerala, India.
[3]Department of Geology, Faculty of Science, Niigata University, 2-8050 Ikarashi, Nishi-ku, Niigata, Japan
[4]Research School of Earth Sciences, Australian National University, Canberra, Australia
[*]E-mail: pvthanooja@gmail.com

Although about 85% of newly formed continental crust was generated during the Neoarchaean period (Hawkesworth et al., 2010 and references therein), well-preserved terranes of that age are relatively rare. The Neoarchaean Madras Block, forming a transition zone between the Dharwar Craton and the Southern Granulite Terrane in southern India, is an exception, providing an opportunity to study crustal petrogenesis during this key period of Earth's early history (Thanooja et al., 2021 and references therein).

The Madras Block consists mainly of charnockite, felsic orthogneiss (e.g., hornblende-biotite gneiss, biotite gneiss, quartzo-feldspathic gneiss) and meta- monzodiorite, with minor amounts of amphibolite and meta-pelitic rocks (e.g., garnet- sillimanite gneiss). Epidote-hornblende gneiss and meta-volcanic rocks are present locally, mostly in the southern and north-western parts of the block. This basement is intruded by granite, gabbro, syenite, and dolerite dykes. The charnockite outcrops are massive, forming rocky hillocks with exposed vertical sections up to tens of meters high. Felsic-orthogneiss, meta-monzodiorite and amphibolite are widespread, the mafic rocks occurring mostly as enclaves, lenses, pods or small outcrops in close association with the felsic-orthogneiss and charnockite.

Zircon U-Pb dating indicates that magmatism and subsequent crustal melting in the Madras Block were initiated at ~ 2.79 Ga with the intrusion of charnockite. The magmatic process reached its peak at ~ 2.54 Ga with the formation of a genetically related coherent group of felsic–mafic rocks: charnockite, felsic-orthogneiss and meta-monzodiorite. The present study of Neoarchaean tectonics focused on that suite of rocks.

The felsic-orthogneiss has a highly fractionated REE profile (La/YbN = ~ 42) that resembles Archaean TTG. The meta-monzodiorite, in contrast, has a weakly fractionated REE pattern (La/Yb)N = ~ 17.6) and higher HREE content (∑HREE = ~ 88 ppm), similar to that of the ~ 2.54 Ga charnockite. The amphibolite that occurs as enclaves has a relatively flat REE pattern, whilst that occurring in larger volumes (outcrop scale) has higher LREE. The similar initial 143Nd/144Nd and low initial 87Sr/86Sr in the rock suite, along with field and geochemical evidence, suggests that the suite formed from the same parental magma (basaltic in affinity) or source. It is likely that magma generation was multi-stage, starting with partial melting of a mantle-derived underplated basaltic source, followed by mixing and homogenisation with small amounts of crustal felsic melt, and different rates of continuous fractionation to form a range of ~ 2.54 Ga felsic to mafic compositions. The whole Neoarchaean terrane in the Madras Block was subjected to high grade regional metamorphism from ~ 2.52 to 2.45 Ga as prolonged upwelling and magmatism raised the temperature of the whole crust.

References

Hawkesworth, C.J., Dhuime, B., Pietranik, A.B., Cawood, P.A., Kemp, A.I.S. and Storey, C.D., 2010. The generation and evolution of the continental crust. The Journal of Geological Society of London, v. 167, p. 229–248.

Thanooja P.V., Williams, I.S., Satish-Kumar, M., Durgalakshmi, Zhai, M.G., Oh, C.W., Windley, B.F. and Sajeev, K., 2021. Were South India, the North China Craton, and Korean Peninsula contiguous in a Neoarchaean supercontinent? New geochemical and isotopic constraints. Lithos, v. 398, p. 106294.

International Association for Gondwana Research 2023 Convention and
20th International Conference on Gondwana to Asia
Niigata, Japan, October 2023
Abstract Volume

Petrological and Geochemical variations of charnockitic rocks in the Wanni Complex, Sri Lanka

Pahan Abewardana[1,2,*], P.L. Dharmapriya[1], S.P.K. Malaviarachchi[1]

[1]Department of Geology, University of Peradeniya, Peradeniya, Sri Lanka
[2]Postgraduate Institute of Science, University of Peradeniya
[*]E-mail: drckpahan@gmail.com

Orthopyroxene bearing granulite facies charnockitic rocks are significant key components to understand the mid to lower continental crustal processes. Charnockitic rocks are spread throughout the Wanni Complex (WC) which is the westward Proterozoic crustal belt of Sri Lanka with the majority of meta-igneous and a minority of meta-sedimentary rocks. We performed petrological observations and major/trace element geochemical (XRF and LA-ICPMS) analyses on a set of charnockitic rocks collected from the Wanni Complex, Sri Lanka. Basically, prograde to retrograde reaction textures and peak metamorphic assemblages were identified during the petrological study by suggesting clock-wise P-T path during metamorphism. From the major element geochemical analysis, WC charnockitic rocks indicate orthogneissic origin with granitic to dioritic composition in their protolith magma. In contrast, calc-alkaline signature of subalkaline magma series predominates in the AFM plot and Haker diagrams provide clues for closed system behavior of fractional crystallization. Volcanic Arc Granite (VAG) to Within Plate Granite (WPG) affinity is obtained for the rocks by the trace element geochemical analysis and indicate the protolith rocks have derived from felsic to intermediate arc magma. Furthermore, subduction related magmatism is dominantly identified for the WC charnockitic rocks within an active continental margin field. Additionally, trace element concentrations of zircons from these rocks also suggest a volcanic arc setting for their origin and the zircon REE patterns provide signs of redox conditions of the source magma.

International Association for Gondwana Research 2023 Convention and
20th International Conference on Gondwana to Asia
Niigata, Japan, October 2023
Abstract Volume

Geologic evolution of the Indian Ocean sector of the Antarctic continent - update of recent two decades

Tomokazu Hokada[1,2,*]

[1]National Institute of Polar Research, Tachikawa, Tokyo 190-8518, Japan
[2]Polar Science Program, Graduate Institute for Advanced Studies, Sokendai, Tachikawa, Tokyo 190-8518, Japan
[*]E-mail: hokada@nipr.ac.jp

The Indian Ocean sector of the Antarctic continent comprises of high-grade metamorphic terranes of late Archaean, Mesoproterozoic and late Neoproterozoic-Cambrian ages. Geologic framework of this part of Antarctica has been established in early 2000's (e.g., Fitzsimons, 2000; Harley, 2003; Jacobs et al., 2003; Shiraishi et al., 2003). The Japanese Antarctic Research Expedition (JARE) has investigated the area of longitude between 10°E and 55°E (eastern Dronning Maud Land and Enderby Land) of the Antarctic continent since 1957. Total 39 sheets of the geological maps have been published. Main part of this area recorded Neoproterozoic-early Cambrian (>600-520 Ma) metamorphic events (central Dronning Maud Land, Sør Rondane Mountains, Yamato-Belgica Complex, Lützow-Holm Complex, Western Rayner Complex). To the east, Archaean-early Paleoproterozoic (>2550-2480 Ma) UHT metamorphic terrane of the Napier Complex, and Meso-Neoproterozoic (1000-900 Ma) granulite terranes of the Rayner Complex and the Cape Hinode Block are distributed (e.g., Shiraishi et al., 2008; Dunkley et al., 2020). This presentation summarizes the current understanding of the geologic framework and crustal evolution of this part of Antarctica, and discuss the future planning of Antarctic field programs expected to start from 2023- seasons.

References

Dunkley, D., Hokada, T., Shiraishi, K., Hiroi. Y., Nogi, Y., Motoyoshi, Y., 2020. Geological subdivision of the Lützow–Holm Complex in East Antarctica: From the Neoarchean to the Neoproterozoic. Polar Sci. 26, 100606.

Fitzsimons, I.C.W., 2000. Grenville-age basement provinces in East Antarctica; evidence for three separate collisional orogens. Geology, 28, 879–882.

Harley, S.L., 2003. Archaean–Cambrian crustal development of East Antarctica: metamorphic characteristics and tectonic implications. In: Yoshida, M., Windley, B.F., Dasugpta, S. (Eds.), Proterozoic East Gondwana: Supercontinent Assembly and Breakup. Geological Society of London, Special Publication 206, 203–230.

Jacobs, J., Fanning, C.M., Bauer, W., 2003. Timing of Grenville-age vs. Pan-African medium- to high-grade metamorphism in western Dronning Maud Land (East Antarctica) and significance for correlations in Rodinia and Gondwana. Precambrian Research, 125, 1–20.

Shiraishi, K., Hokada, T., Fanning, C.M., Misawa, K., Motoyoshi, Y., 2003. Timing of thermal events in the Dronning Maud Land, East Antarctica. Polar Geoscience, 16, 76–99.

Shiraishi, K., Dunkley, D.J., Hokada, T., Fanning, C.M., Kagami, H., Hamamoto, T., 2008. Geochronological constraints on the Late Proterozoic to Cambrian crustal evolution of eastern Dronning Maud Land, East Antarctica: a synthesis of SHRIMP U–Pb age and Nd model age data. In: Satish–Kumar, M., Motoyoshi, Y., Osanai, Y., Hiroi, Y., Shiraishi, K. (Eds.), Geodynamic Evolution of East Antarctica: A Key to the East–West Gondwana Connection. Geological Society of London, Special Publication 308, 21–67.

Lithosphere subduction process of the Molucca Sea microplate

Junjiang Zhu[1,2,*], Ruixue Chen[1,2], Xingquan Chen[1,2], Qianqian Li[1,2], Qinglong Zhu[1,2], Sanzhong Li [1,2]

[1]Frontiers Science Center for Deep Ocean Multispheres and Earth System, Key Lab of Submarine Geosciences and Prospecting Techniques, MOE and College of Marine Geosciences, Ocean University of China, Qingdao 266100, China
[2]Laboratory for Marine Mineral Resources, Qingdao National Laboratory for Marine Science and Technology, Qingdao 266100, China
[*]E-mail: zhujunjiang@ouc.edu.cn

The Molucca Sea microplate is an ideal small plate for studying lithosphere subduction processes in deep in the Sulawesi-Philippines tectonic region. Based on the bathymetric data, seismic data, focal mechanism solutions of subduction-related earthquakes, and regional gravity data, the location, stress state, and boundaries of the Molucca Sea microplate are constrained. According to images from horizontal slices and vertical tomographic cross-sections from the global MIT-P08 tomography model, lithospheric subduction structure of the Molucca Sea microplate in the mantle is clear tracked and outlined. An updated subduction model is constructed according to the P-wave high-velocity anomaly of the Molucca Sea and its surrounding plates setting. Our results show that the Molucca Sea microplate is bounded by the Philippine trench, the Sangihe trench, the Halmahera trench, and the Sorong fault. The Molucca Sea subducted slab shows a compression stress in the deep, and the extension stress is at the depth of 70-350 km. The slab gap along the Sangihe subducting slab (about 300 to 500 km) is likely caused by the southward subduction of the Celebes Sea plate. The high-velocity anomaly of 660-1400km is attributed to the westward subduction of the Pacific plate below the West Sulawesi from 70 to 45Ma and the southwest subduction of the Pacific plate in the eastern Philippines from 45 to 25Ma. The tectonic plate evolution indicates that the subduction of the Molucca Sea microplate began in the west at about 20 Ma and continues to present, while the subduction began in the east at about 10 Ma.

International Association for Gondwana Research 2023 Convention and
20th International Conference on Gondwana to Asia
Niigata, Japan, October 2023
Abstract Volume

Carbon geodynamic cycle in the continental crust

M. Satish-Kumar

Department of Geology, Faculty of Science, Niigata University, 2-8050 Ikarashi, Nishi-ku, Niigata 950-2181, Japan
E-mail: satish@geo.sc.niigata-u.ac.jp

Organic carbon and carbonate carbon are two important reservoirs in the Earth's crust that can act as a source or a sink for carbon during plate subduction and continent building processes. In order to understand the geodynamic cycle of carbon, it is important to understand the movement of carbon through different reservoirs not only in the Earth's surface, but also in deeper levels of Earth's crust. Carbon isotope geochemistry has served as a widely applied tool in deciphering the source of carbon and in this presentation a comprehensive review is carried out on the different forms of carbon, its movement among the various reservoirs and the evolution of carbon isotopes. In particular I focus on orogenic belts where large volumes of carbon can be stored as carbonate rocks and graphite in metamorphic rocks which can serve as a long-term sink of carbon. Examples from the orogenic belts in India, Sri Lanka and Antarctica are used to demonstrate that metamorphism of sediments rich in organic material can preserve graphite as carbon sinks for hundreds of millions of years.

A detailed carbon isotope study of carbonate carbon and graphitic carbon was carried out in continental collisions zones in East Antarctica. Metamorphosed carbonate rocks are present in all orogenic belts and their preservation in orogenic belts indicate that pure carbonate rocks are geochemically and isotopically preserve the pristine sedimentary characteristics (Satish-Kumar et al., 2021). However, organic matter in the sediments undergo a series of processes, which results in the formation of graphite. Based on the mode of occurrence, the graphite occurrences in continental crust were classified into three major types, vein-type, disseminate flakes and coarse aggregates. In addition, graphite concentration was also observed along the contact between metacarbonate rocks and silicate rocks. In order to understand the source of carbon, the carbon isotope fractionation between calcite, graphite and carbon-bearing fluids (CO2 or CH4) during metamorphism was considered. For example, at the Skallevikshalsen locality in the Lützow Holm Complex, East Antarctica, all three forms of carbon-bearing phases were present (Satish-Kumar, 2023). Field evidence suggest that CO2 is being pooled at lithological contacts and deposited as graphite. Carbon isotopic composition of graphite and associated carbonates are consistent with graphite precipitation from CO2 fluids released by decarbonation reactions.

Across the regimes of high-temperature metamorphism and partial melting of graphite-bearing rocks Satish-Kumar (2023) has reported 13C enrichment in leucosomes. Based on field, textural and carbon isotope evidence, from a typical example a migmatite outcrop at Rundvagshetta at LHC, graphite crystallization is recognized. This recrystallization is accompanied with a 13C enrichment, as reported previously in southern India (Satish-Kumar et al., 2011) Thus, carbon is recycled and retained as graphite in the continental crust during high-grade metamorphism and anatexis, although its isotopic composition can be considerably modified. A comprehensive review of carbon isotopic composition of graphite in continental crust is presented in order to understand the role of graphite as "long-term sinks" of carbon.

References

Satish-Kumar, M. (2023) Carbon isotopic composition of graphite in metamorphic rocks from Lützow-Holm Complex, East Antarctica: Implications for carbon geodynamic cycle in continental crust. Journal of Mineralogical and Petrological Sciences (under revision).

Satish-Kumar, M., Yurimoto, H., Itoh, S. and Cesare B. (2011) Carbon isotope anatomy of a single graphite crystal in a metapelitic migmatite revealed by high-spatial resolution SIMS analysis. Contributions to Mineralogy and Petrology, 162, 821–834.

Satish-Kumar, M., Shirakawa, M., Imura, A., Otsuji-Makino, N., et al. (2021) A geochemical and isotopic perspective on tectonic setting and depositional environment of Precambrian meta-carbonate rocks in collisional orogenic belts. Gondwana Research, 96, 163–204.

Author Index